Faculty of Science and Engineering

An Investigation into the Interrelationship between Petrophysical Properties of Potential Gas Shale Reservoirs from Western Australia

Mohammad Mahdi Labani

This thesis is presented for the Degree of

Doctor of Philosophy

Of

Curtin University

June 2014

AN INVESTIGATION INTO THE INTERRELATIONSHIP BETWEEN PETROPHYSICAL PROPERTIES OF POTENTIAL GAS SHALE RESERVOIRS FROM WESTERN AUSTRALIA

MOHAMMAD MAHDI LABANI

B.Sc., Petroleum University of Technology, 2007

M.Sc., Petroleum University of Technology, 2009

M.Sc., IFP School (French Institute of Petroleum), 2009

A THESIS SUBMITTED IN PARTIAL FULFILLMENT OF THE REQUIREMENTS FOR THE DEGREE OF

DOCTOR OF PHILOSOPHY

THE FACULTY OF SCIENCE AND ENGINEERING

Department of Petroleum Engineering

Curtin University

June 2014

Declaration

To the best of my knowledge and belief this thesis contains no material previously published by any other person except where due acknowledgment has been made. This thesis contains no material which has been accepted for the award of any other degree or diploma in any university.

Mohammad Mahdi Labani

ABSTRACT

An investigation into the petrophysical properties of the potential gas shales from the Perth and Canning Basins has been performed to understand the interrelationship between shale composition, geochemical properties and pore structural parameters and analysing their effect on the nano-scale and macro-scale properties of gas shale reservoirs. The following measurements were done on the collected samples from the Perth and Canning Basins to find out more about the nano-scale properties of the investigated gas shales:

- Low pressure nitrogen adsorption and mercury porosimetry technique for determination of the pore structural properties,
- Gas expansion method for determining the effective porosity,
- High pressure methane adsorption for determination of the adsorbed gas capacity.

In this study three different methods of low pressure nitrogen adsorption, mercury porosimetry and gas expansion were used for pore structure characterization of the investigated gas shales. Mercury porosimetry and gas expansion methods have been used for a long time in characterization of conventional reservoirs but low pressure nitrogen has been used recently as a tool for gas shale evaluation. Quantitative analysis of the obtained results clarifies the shape, size and pore volume of the studied gas shale samples. Analysing the results shows that there is not any consistency between similar parameters like effective porosity or pore size distribution (PSD) extracted from these techniques; several explanations have been proposed for justification of this inconsistency. As well as the results of this study make it clear that each of the usual techniques applied for characterization of gas shale pore systems has some deficiencies and cannot be used alone for this purpose. Whereas, by combining the results of these methodologies pore size spectrum of gas shales can be determined in a more accurate way.

Gas in place is often the critical factor for evaluating the economics of a gas shale system and finding the sweet spot of the gas shale layers. In this study adsorbed gas capacity of the shale samples were measured using high pressure volumetric method. A series of high pressure methane adsorption were measured on the collected shale samples at 23^{o}C and 30^{o}C for measuring the adsorbed gas capacity of the shale samples. Classifying the obtained results based on the studied geological formations showed that the Goldwyer Formation has the higher potential for storing the gas (45.9 scf/ton) while the Carynginia Formation from the Perth Basin has the least capacity for storing the gas (33.6 scf/ton). Furthermore it shows that

although the samples from the Canning Basin have a higher adsorbed gas capacity but they have the lower affinity for desorbing the gas compared to the Perth samples due to the higher enthalpy of adsorption. Qualitative analysis of the obtained results determined the effective parameters on the gas storage. As it was expected the pore space characteristics of the studied shale samples have a stronger effect on the gas storage while the quantity and maturity of organic matter are not effective on the gas storage of the analysed samples. A temperature increase from 23^{o}C to 30^{o}C reduces the adsorbed gas capacity significantly. Therefore considering the reservoir temperature for the studied formations adsorbed gas should not playa prominent role for gas production from these formations.

This study also attempted to upscale the petrophysical studies from nano-scale into macro-scale or well log scale. An index was proposed for determining the thermal maturity of the gas shale units using conventional well log data. Different conventional well logs were evaluated and neutron porosity, density and volumetric photoelectric adsorption were found to be the most proper inputs for defining a log derived maturity index (LMI). LMI considers the effects of thermal maturity on the mentioned well logs and applies these effects for modelling thermal maturity changes. Although there are some limitations for applying LMI but generally it can give a good in-situ estimation of thermal maturity for the studied wells.

The effect of the shale composition and geochemical parameters on the rock mechanical properties derived from log data was investigated. It is shown that converse to the conventional wisdom the effect of organic matter quantity and maturity on the rock mechanical properties of the studied gas shales is not prominent, but the composition of the rock appears to have an important effect on the mechanical properties.

Parts of this thesis have been published in the following journals and conference articles:

- Labani, M.M., Rezaee, R., Saeedi, A., Hinai, A.A., 2013. Evaluation of pore size spectrum of gas shale reservoirs using low pressure nitrogen adsorption, gas expansion and mercury porosimetry: A case study from the Perth and Canning Basins, Western Australia. Journal of Petroleum Science and Engineering 112, 7-16.

- Labani, M.M., Rezaee, R., 2012. Thermal maturity estimation of gas shale layers from conventional well log data: A case study from the Kockatea Shale and Carynginia Formation of the Perth Basin, Australia. SPE Asia Pacific Oil and Gas Conference and Exhibition, Perth, Australia. SPE 158864.

- Labani, M.M., Rezaee, R., 2014. The importance of geochemical parameters and shale composition on rock mechanical properties of gas shale reservoirs: A case study from the Kockatea Shale and Carynginia Formation from the Perth Basin, Western Australia. Rock Mechanics and Rock Engineering, 1-9.

TABLE OF CONTENTS

List of Figures

List of Tables

List of Abbreviations, Acronyms and Conversion Factors

List of Acronyms

^{o}C	Degree Celsius
K	Kelvin
m	meter
wt%	weight percent
ΔlogR	Separation between resistivity and sonic, log scale
φ	porosity, decimal fraction
S_w	Total water saturation, pore vol%
T_{max}	Thermal maturation level determined by Rock-Eval pyrolysis

List of Abbreviations

BET	Brunauer Emmett Teller
BJH	Barret Joyner Halenda
DFT	Density Functional Theory
DH	Dollimore Heal
DT	Sonic transit time, microseconds/ft
EIA	Energy Information Administration
HI	Hydrogen Index
HPVA	High Pressure Volumetric Analyser
IUPAC	International Union of Pure and Applied Chemistry
LMI	Log Derived Maturity Index
MICP	Mercury Injection Capillary Pressure
PEF	Photo Electric Factor
ppm	part per million
PSD	Pore Size Distribution
pu	porosity unit

scf	standard cubic feet
SEM	Scanning Electron Microscopy
tcf	trillion cubic feet
TGA	Thermogravimetric analysis
TOC	Total Organic Carbon
U	Volumetric Photo Electric Absorption
XRD	X Ray Diffraction

Metric prefix

Text	Symbol	Factor
Giga	G	1,000,000,000
Mega	M	1,000,000
Kilo	K	1,000
Hecto	H	100
Deca	da	10
None	None	1
deci	d	0.1
centi	c	0.01
milli	m	0.001
micro	µ	0.000,001
nano	n	0.000,000,001

Conversion factors

Pressure

MPa to PSIA	145.0377
PSIA to MPa	0.0069

Adsorption

cm^3/gr to scf/ton	32.0369
scf/ton to cm^3/gr	0.03121

Acknowledgments

Ten years ago when I started my undergraduate studies in Petroleum University of Technology at Abadan[*] I was thinking that Abadan is the farthest city from my hometown, Birjand[†]; they are around 2000 km far from each other. However when I started my PhD in the south hemisphere in Perth I then realised that the world is much bigger than what I was thinkingbefore!

First of all I owe many thanks to my parents and my beloved sisters; Samaneh and Mahdieh, without their positive energy and their emotional support I could not stand in this city for more than 6 months.

I wish to thank my supervisor, Reza Rezaee, for his supervision, guidance and help throughout the PhD study. His critical comments were always helpful and made me more organised toward approaching my final objective. I also should thank him for the great balance of guidance and freedom who gave me during my PhD study. I would like to thank Dr Ali Saeedi for his kind help in the laboratory of Petroleum Engineering Department of Curtin University for setting up the High Pressure Volumetric Analyser (HPVA) and other useful comments for performing the experiments better.

I would like to thank the Curtin University Shale Gas Consortium Sponsors including Western Australia Department of Mines and Petroleum, Buru Energy, Carnarvon Petroleum, Norwest Energy and Woodside for the financial support and permission to publish the results of this study.

Last but not the least, I would like to extend my appreciation to the Curtin University staff in Petroleum Engineering Department and Chemical Engineering Department for their support during this PhD project.

[*] Abadan is a city in the south-west part of Iran, where had one of the biggest oil refineries in the world till 1980.

[†]Birjand is a small city in the easternpart of Iran, close to the border of Iran and Afghanistan.

CHAPTER 1
INTRODUCTION

CHAPTER 1

Introduction

1.1 Introduction

Over the past decade growing demand for gas, and equally important, growing in the oilfield technologies has led to the consideration of gas shale plays as an important source of energy. Gas shale has become an increasingly important source of natural gas in the United States in recent years, and the strong interest on shale gas has been expressed by Canada, Europe, Asia and Australia. In Australia industries show high interests in exploring gas shales and target the gas shale to be the next energy boom.

According to the initial assessment by U.S. Energy Information Administration (EIA) in February 2011, Australia has major gas shale potential in four main assessed basins: Cooper, Maryborough, Perth and Canning Basins. The Western Australia alone was estimated to be holding the fifth largest reserves of gas shales in the world (EIA, 2011). The focus of this research is on the potential gas shales from Western Australia including the Perth and Canning Basins (Fig. 1.1). The Perth Basin is a north-northwest trending, mostly onshore sedimentary basin extending about 1300 km along the southwest margin of Western Australia. It contains two main organic rich shale formations with gas development potential including the Permian Carynginia Formation and the Triassic Kockatea Shale. The Permian Carynginia Formation is a restricted marine deposit over a wide area of the northern part of the Perth Basin. It has been deposited in a shallow marine environment under proglacial conditions. There is a deep water shale member which occurs near the base of the Carynginia Formation including thin interbeds of siltstone, sandstone and limestone (Cadman et al., 1994). The lower Triassic Kockatea Shale is considered to be the major source rock for the petroleum fields in the Perth Basin. In most wells the Kockatea Shale is organically rich at its base named the Hovea member. The organic content of the Hovea member is commonly closed to 2 wt% TOC, well above the overall formation average that is about 0.8 wt% TOC, although in many wells this rich interval may be only around 15 meters thick (Thomas, 1979).

The Canning Basin is a super basin in the northwest of Western Australia. The Middle Ordovician Goldwyer Formation is one of the targets for the gas shale exploration in the Canning Basin. It is a blanket marine shale of Ordovician age and contains black to dark grey shales and claystones with inter-bedded silty intervals. It is a very rich and proven source rock and present over large areas of the Canning Basin, thus potential exists for very large onshore gas shale resources in this region (Sharifzadeh and Mathew, 2011). Foster et al. (1986)divided the Goldwyer Formation into four members named Units 1 to 4, in ascending stratigraphic order. The upper member (Unit 4) contains the richest source rocks and the most prospective gas shales. TOC values range between 0.46 and 6.40 wt% (1.85 wt% in average) in this unit (Cadman et al., 1993). A recent study performed by the U.S. Energy Information Administration (EIA) (2011) estimated that the recoverable gas shale resources would be in excess of 59 trillion cubic feet (tcf) for the Perth Basin including the Kockatea Shale and the Carynginia Formation and around 230 tcf for the Canning Basin, Goldwyer Formation.

Shale comprises clay (less than 0.0039 mm) and silt (between 0.0039 to 0.0625 mm) sized particles that have been consolidated into rock layers of ultra-low permeability. It is characterised by finely laminated and/or fissility approximately parallel to bedding (Serra, 1988). This definition gives the lowest opportunity for shale as a reservoir. However, the right combinations of geological, geochemical, petrophysical and geomechanical properties would result in the potential gas shale producer. Therefore it is necessary to understand about the petrophysical properties of gas shales to find out about the gas storage capacity and mechanism of gas production in these reservoirs. However there are some inhibitions for assessing the potential of gas shales in this region:

- Due to the traditional point of view to the organic rich shales (considering them as source or seal), there is not any core analysis data for the shale layers. The only available data for most of the wells which have been drilled in the Perth and Canning Basins is the conventional well log data including resistivity, sonic, neutron porosity and density.
- There are limited number of wells which have been drilled recently for the target of gas shales in this region therefore only in number of wells there are special core analysis data for the shale layers.
- Although there are some publications for the gas storage mechanism in the gas shales around the world, the heterogeneity of the shale layers will affect on the relative importance of these parameters in different regions. Therefore it is required to do a

comprehensive study on the potential gas shales from Western Australia to determine the importance of shale characteristics for economic gas production. By identifying the importance of shale characteristics on the gas storage capacity mapping the gas shale sweet spots would be more successful.

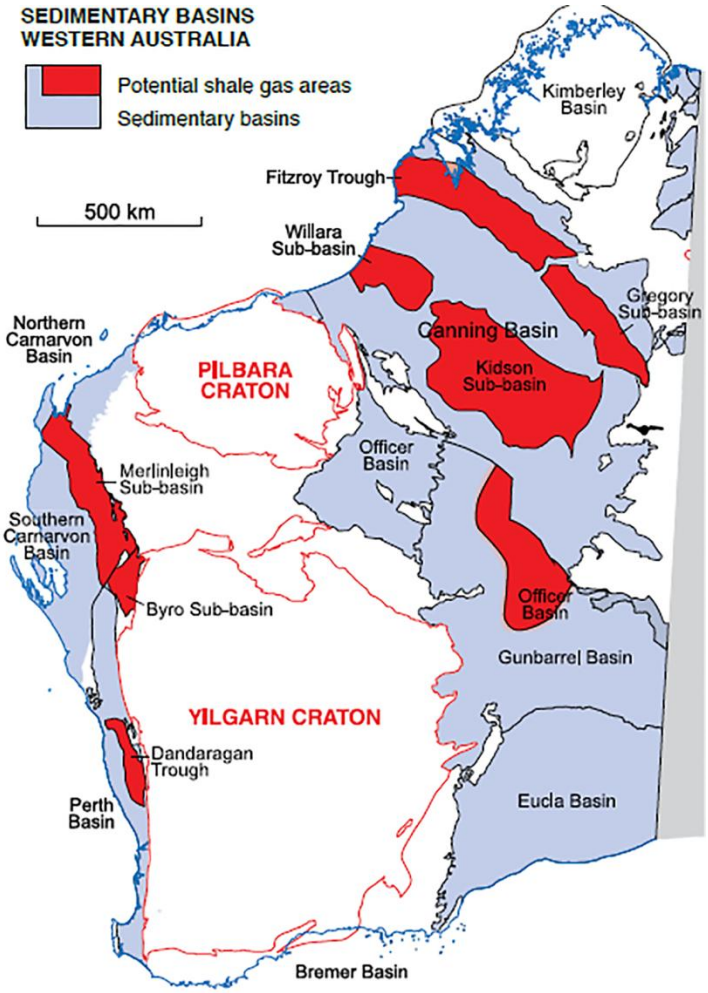

Fig. 1.1: Location map showing the sedimentary basins of Western Australia accompanied with the potential shale gas areas (from DMP, 2014).

1.2 Thesis objectives

This study attempted to investigate the potential of the gas shale reservoirs for gas production through laboratory measurements and log analysis. The following issues will be addressed in this study:

- How much is the gas storage capacity of the studied gas shale samples and based on the laboratory analysis which formation provides the better opportunity for gas shale exploration?

- What are the controlling parameters on the gas storage capacity of the studied gas shales?
- What are the effective parameters on the pore space characteristics of the studied gas shales?
- Considering the different techniques available for evaluation of the gas shale pore structure, what are the strength points and deficiencies of these techniques?
- Are there any similarities between similar pore structure parameters measured from different techniques for the studied gas shales?
- How it is possible to locate the nano and micro properties of gas shale reservoirs to the macro scale or in other word is it possible to calibrate the laboratory data to the log data for evaluation of the gas shale reservoirs?

1.3 Structure of thesis

This thesis covers four main topics through four different chapters for petrophysical evaluation of gas shale reservoirs; laboratory studies on the gas shales (including Chapters 2 and 3) and log analysis of the gas shale layers (Chapters 4 and 5). In the following the content of each chapter has been explained briefly addressing how each chapter contributes for answering the above questions.

Chapter 2 explains how different techniques including low pressure nitrogen adsorption, gas expansion and mercury porosimetry can be used for evaluation of pore size spectrum of gas shale reservoirs. This chapter addresses how each of these techniques can determine the pore structure parameters of the gas shale reservoirs. It will be followed with the experimental results of each technique, discussing about why there is not any consistency between similar parameters like effective porosity or pore size distribution extracted from these techniques and the disadvantages of each technique for pore structure evaluation.

Chapter 3 evaluates the gas storage potential of the studied gas shales using high pressure methane adsorption technique. A series of low pressure and high pressure adsorption measurements was conducted on the collected shale samples to determine the gas storage capacity of the shale layers. Furthermore this chapter considers effect of shale composition, geochemical parameters and temperature on the adsorption capacity of the analysed samples. It tries to explain the importance of adsorption heat in locating the gas shales with high potential for gas production as well.

Chapter 4 introduces a qualitative technique for evaluation of the thermal maturity of the gas shale layers from the conventional well log data including neutron porosity, density and volumetric photoelectric adsorption. It is proposed that thermal maturity can affect on the matrix properties of the gas shales and consequently these effects can be monitored in the conventional well log responses as well. However there are some limitations for using this approach which were explained in detail in chapter 4.

Chapter 5 examines the influence of shale composition and geochemical parameters on the extracted rock mechanical properties from log data. In doing so, the significance of total organic content (TOC), thermal maturity and weight percentages of quartz and clay minerals were investigated on Young's modulus and Poisson's ratio extracted from sonic and density log data.

1.4 References

Serra, O., 1988. Clay, silt, sand, shales: a guide for well-log interpretation of siliciclastic deposits. Schlumberger Limited.

USA Energy Information Administration, 2011. World Shale Gas Resources: An Initial Assessment of 14 Regions Outside the United States.

Western Australia Department of Mines and Petroleum, 2014. Natural gas from shale and tight rocks: An overview of Western Australia's regulatory framework. Access through website: www.dmp.wa.gov.au

CHAPTER 2

EVALUATION OF PORE SIZE SPECTRUM OF GAS SHALE RESERVOIRS USING LOW PRESSURE NITROGEN ADSORPTION, GAS EXPANSION AND MERCURY POROSIMETRY

CHAPTER 2

Evaluation of pore size spectrum of gas shale reservoirs using low pressure nitrogen adsorption, gas expansion and mercury porosimetry

2.1 Introduction

Pore system characterization is an important step for evaluation of gas shale reservoirs. Therefore it is necessary to use new and more effective techniques to understand the pore structure, gas storage mechanisms and the relationship between pore size and gas storage capacity. The gas is stored in the gas shale reservoirs in the form of free gas and adsorbed gas. The adsorbed gas refers to the gas which can be attached to the surface of the clay minerals or organic materials. To have a better understanding about the adsorbed gas capacity of the gas shale reservoirs it is necessary to measure gas adsorption in both high pressure adsorption and low pressure adsorption analyses. The high pressure adsorption measurement is required to determine the adsorbed gas capacity at reservoir pressure and temperature using the Langmuir isotherm curve (Lu et al., 1995; Ross and Bustin, 2007a). The low pressure adsorption measurement is very important for characterization of the gas shale pore system, pore size distribution (PSD) and studying the parameters which control the adsorbed gas capacity such as surface area and microporosity. PSD is required for fluid flow modelling because gas flow in the shale matrix is expected to be a combination of diffusive transport regime in nanopores and conventional Darcy flow models in larger pores (Javadpour et al., 2007). Low pressure adsorption measurement has been used extensively in surface chemistry analysis for characterization of porous materials but it has been used for characterization of the nanopores in the shale samples recently (Ross and Bustin, 2009; Kuila and Prasad, 2011; Chalmers et al., 2012). In addition to the low pressure adsorption measurement technique there are other techniques which can be used for pore system characterization like helium pycnometry and mercury porosimetry (Giesche, 2006; Bustin et al., 2008; Ross and Bustin, 2009; Chalmers et al., 2012). The previous studies have mainly focused on determination of pore structure parameters of the shale samples. Present study uses low pressure nitrogen adsorption, gas expansion and mercury porosimetry to clarify the shape, size and pore volume of the studied gas shale samples. As well as it will provide new insights about the

inconsistency between similar pore structure parameters derived from different techniques and deficiencies in the available techniques for evaluation of gas shale reservoirs.

Generally, in describing the pore size in shales the pores are all considered to fall within the nanopore range (Javadpour et al., 2007; Javadpour, 2009; Loucks et al., 2009) without any further classifications. Recently Loucks et al. (2012) defined a new pore size classification for mudrocks, however, in this study it has been preferred to use the pore size terminology of the International Union of Pure and Applied Chemistry (IUPAC), which was developed by Rouquerol et al. (1994). According to this pore classification pores are subdivided into three categories: micropores which include pores less than 2 nm diameter, mesopores which comprise pores with diameters between 2 and 50 nm, and macropores which include pores with diameters larger than 50 nm.

In the current study two sets of gas shale samples were studied, 17 samples from the Perth Basin (12 samples from the Carynginia Formation and 5 samples from basal member of the Kockatea Shale named Hovea member) and 6 samples from the Goldwyer Formation of the Canning Basin. Table 2.1lists the available results of XRD and geochemical analyses for some studied samples from the Perth Basin. Total organic carbon (TOC) content for the available samples range from 0.23 to 3.03 wt%. T_{max} which could be tied to thermal maturity of the samples varies between 458 to 509 ^{o}C, however as it is clear the samples RB2-S1, RB2-S2 and RB2-S3 have the higher T_{max} values and therefore they are in the higher thermal maturity status compared to AS2 series samples. The XRD results show the large variability in the mineralogical composition. While RB2 series samples are rich in clay content, most of the AS2 samples are rich in quartz content except AS2-S1.

Table 2.1: Geochemical analyses and mineralogical composition of some samples from the Perth Basin.

Sample Name	TOC Content (wt%)	T_{max}* (°C)	Quartz(wt%)	Clay(wt%)	Carbonate(wt%)
AS2-S1	3.03	459	25	56	5
AS2-S2	1.36	466	49	34	5
AS2-S7	0.64	458	53	31	2
AS2-S8	1.82	460	41	41	4
AS2-S9	1.08	465	54	28	4
AS2-S10	0.23	n/a	45	33	6
RB2-S1	2.99	484	18.2	49.6	---
RB2-S2	2.54	481.5	20.2	52.7	9.7
RB2-S3	1.43	509	42	48.1	---

*T_{max} is one of the output parameters of the Rock-Eval pyrolysis and is indicative of thermal maturity of the rock sample.

2.2 Experimental Methodologies

2.2.1 Gas Expansion

Porosity measurement on the shale samples present several challenges. The gas expansion technique is an old fashioned procedure for measuring effective porosity of a rock sample. However to apply this technique on the shale samples it needs some degree of modification. Due to the low porosity of the shale samples (usually less than 5% pu) the equilibration time between the sample cell and reference cell is extremely long. Therefore measuring porosity using core plug is not feasible. Luffel and Guidry (1992) recommended a new evaluation technique for porosity measurement of the shale samples. According to their procedure the shale samples should be crushed in order to increase the surface area and decrease the equilibration time. As a result, in the current study Luffel and Guidry (1992) procedure has been followed. The studied samples were crushed to yield particle sizes between 12 and 60 mesh sizes (1.40 mm and 250 μm). The crushed samples should be heated to remove gas, free water and any other possible hydrocarbons. In order to achieve this, the samples were heated at 110°C for 8 hours. The main concern during heating the shale sample is preserving the organic materials and the clay bound water. Easley et al. (2007) identified and quantified the evaporated components of the Barnett shale samples during heating using thermogravimetric analysis (TGA) in conjunction with a gas chromatograph. Based on their study during heating the shale samples up to 400°C, only water becomes mobilized. Their results showed that at higher temperatures kerogen, carbonate minerals and clay bound water were liberated from the samples. Considering this point the procedure used for heating the shale samples in the

present study is not expected to have any effect on the matrix of the shale samples. It is worth mentioning that in this study helium was used for porosity measurement.

2.2.2 Low pressure nitrogen adsorption

Low pressure nitrogen adsorption (<18.4 psia) can be used to obtain the following information in microporous materials (Gan et al., 1972):

- specific pore volume: total pore volume per mass of the sample expressed as cm^3/gr,
- shape of the pores,
- specific surface area: total surface area per mass of the sample expressed as m^2/gr, and
- pore sizes and their distribution.

The nitrogen adsorption and desorption isotherms were collected at 77K (-196^oC) using a Micromeritics® TriStar II 3020 apparatus. Samples were crushed to <250 μm to be used for low pressure isotherm analysis. Traces of gas and water molecules available in the sample compete with the nitrogen molecules for adsorption sites, therefore, it is required to remove moisture content and degas the samples prior to pore structure analysis (Bustin and Clarkson, 1998; Busch et al., 2007). For drying the shale samples, the samples were oven dried for 8 hours at 110^oC similar to the preparation procedure for gas expansion method.

In the following section there is a brief explanation on the theory behind the extraction of pore volume, pore size, pore shape and surface area based on the results of low pressure adsorption measurement.

2.2.2.1 Analysis of nitrogen adsorption data

The adsorption measurement is used to quantify the amount of gas adsorbed at different relative pressures (P/P_o) where P is the gas vapour pressure in the system and P_o is the saturation pressure of adsorbent. Micromeritics instrument gives the adsorption isotherm point by point by measuring quantity of nitrogen adsorbed and the equilibrium pressure. Desorption isotherm can be obtained by measuring the quantities of gas removed from the sample as the relative pressure is lowered. All adsorption isotherms may be grouped into one of the five types (type I to type V) shown in Fig. 2.1(Brunauer et al., 1940). These adsorption isotherms are not generally reversible and can exhibit the hysteresis. De Boer (1958) identified five types of hysteresis loops and correlated them with various pore shapes (Fig. 2.2). Type A hysteresis is attributed to cylindrical pores; type B is associated with slit shaped

pores; type C and D hysteresis is produced by wedge shaped pores and type E hysteresis has been attributed to bottle neck pores.

The total pore volume is derived from the amount of vapour adsorbed at relative pressure close to unity, by assuming that the pores are then filled with liquid adsorbate. The average pore size could be estimated from the total pore volume determined at maximum pressure by assuming that the pores which would not be filled below a relative pressure of 1 have a negligible contribution to the total pore volume. For example, assuming cylindrical pore geometry, the average pore radius (r_p) can be expressed as:

$$r_p = \frac{2V_{ads.}}{S} \qquad \text{(Eqn. 2.1)}$$

where $V_{ads.}$is the total amount of nitrogen adsorbed and S is the surface area (Quantachrome, 2008).

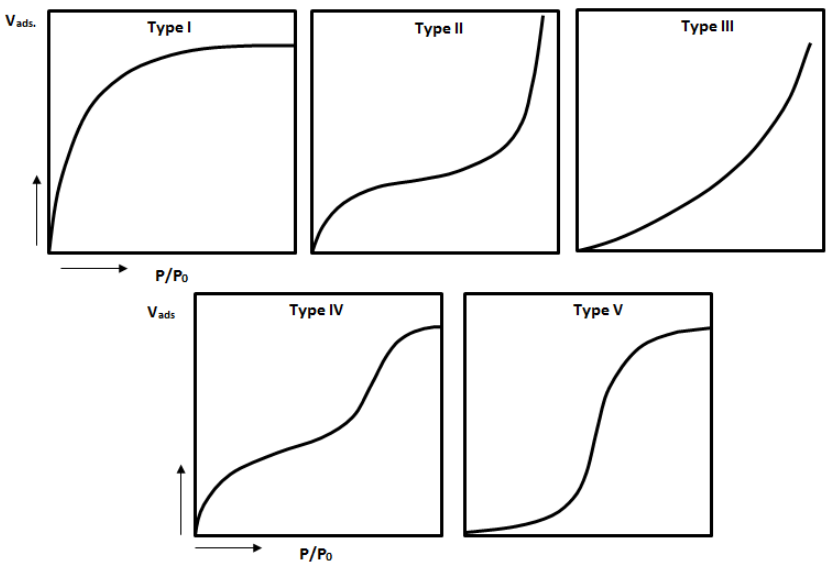

Fig. 2.1: Adsorption isotherm types (modified after Brunauer et al., 1940).

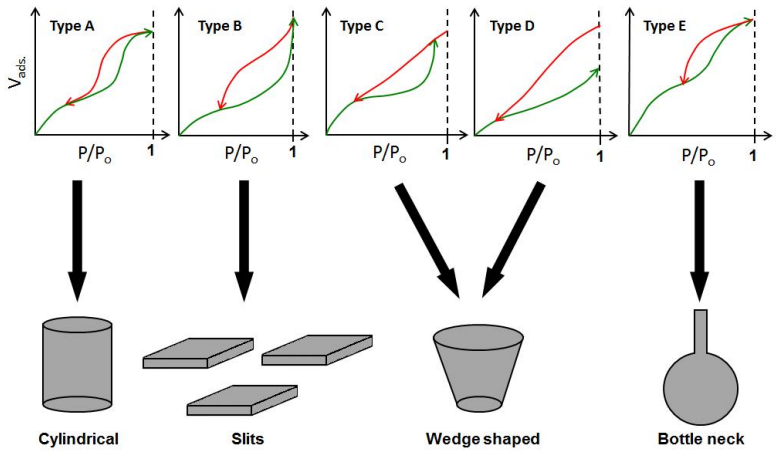

Fig. 2.2: Five types of hysteresis loops and their related pore shapes.

The distribution of pore volume with respect to pore size is called pore size distribution (PSD). There are different methods for calculation of PSD based on the nitrogen adsorption data. Some of them are appropriate for determining the PSD in the mesopore scale such as BJH model (Barret et al., 1951) and DH model (Dollimore and Heal, 1964). Both of these methodologies calculate actual pore size assuming cylindrical shaped pores using the thickness of adsorbed layer and the Kelvin equation (Gregg and Sing, 1991):

$$\ln\left(\frac{P}{P_o}\right) = \frac{2\gamma V_m}{RTr_K}\cos\theta \qquad \text{(Eqn. 2.2)}$$

where:

P is the gas vapour pressure,

P_o is the saturation pressure of adsorbent,

γ is the surface tension of nitrogen at its boiling point (77K) ,

θ is the contact angle between adsorbate (liquid nitrogen) and adsorbent,

V_m is the molar volume of liquid nitrogen,

R is the gas constant,

T is the boiling point of nitrogen (77K), and

r_K is the Kelvin radius of the pore.

However these theories do not give a realistic description of micropore filling and this leads to an underestimation of pore sizes for micropores and even smaller mesopores (Ravikovitch et al., 1998). Density functional theory (DFT) molecular model provides a much more accurate approach for pore size analysis and it can be used for PSD determination in

micropore scale as well as mesopore (Do and Do, 2003). Thus, in this study DFT model was used for PSD determination because micropores have an important role in the pore structure of the shales and BJH and DH models could not determine the pores in this interval accurately. The specific surface area is calculated using the widely accepted BET method (Brunauer et al., 1938) in the P/P_o range of 0.05 to 0.35. The details of different theories for low pressure nitrogen adsorption analysis have been discussed in the mentioned papers; hence they were not explained in this paper.

2.2.3 Mercury porosimetry

Mercury porosimetry provides a wide range of information about a sample, e.g. the pore size distribution, total pore volume or porosity, the skeletal and apparent density and the specific surface area (Giesche, 2006). Similar to low pressure adsorption measurement, the samples should be evacuated under heat treatment for mercury porosimetry before the test to remove moisture and possible gas content of the samples. The mercury intrusion pressure values are converted to the pore size by using the Washburn equation (Washburn, 1921):

$$P=\frac{2\sigma\cos\theta}{r_{pore}} \qquad \text{(Eqn. 2.3)}$$

This equation relates the mercury intrusion pressure to the corresponding pore throat size (r_{pore}) using the surface tension of mercury (σ) and the contact angle (θ) between the sample and mercury. By knowing the intruded volume of mercury and pore radius and assuming cylindrical pore shape, the surface area of the sample could be calculated by rearranging Eqn. 2.1 and considering V as the volume of mercury intruded into the sample:

$$\text{Surface Area}=\frac{2V_{\text{intruded Hg}}}{r_{pore}} \qquad \text{(Eqn. 2.4)}$$

2.3 Experimental results

Fig. 2.3 and Fig. 2.4 illustrate low pressure nitrogen isotherms for the Perth and Canning samples. The shapes of these curves suggest type II isotherms for the analysed samples. Type II isotherms could be interpreted as the micropore filling at low relative pressures, and due to the presence of macropores in the samples the adsorption isotherm rises rapidly near $P/P_o=1$. It is worth mentioning that the amount of adsorbed gas at low relative pressures is correlated with micropore and fine mesopore volume while at high relative pressures it is related to large mesopores and macropores. As it could be seen in Fig. 2.3 and Fig. 2.4, all of the samples show the hysteresis type B. Therefore based on the classification by De Boer (1958),

the pores can be interpreted as the slit-type pores. Table 2.2 and Table 2.3 summarize the collected results from low pressure adsorption measurements including BET surface area, total pore volume measured at maximum relative pressure (P/P_o=1), calculated average pore width and sum of micro and mesopore volume accompanied with the helium porosity derived from gas expansion method for the Perth and Canning samples, respectively. Considering the data in Table 2.2and Table 2.3 and the shape of isotherms, the samples with the higher volume of micro/mesopore show a bigger hysteresis loop compared to others. For example among the Canning samples ML1 has the higher micro/mesopore volume and bigger loop as well while for S2-DD1 which has the lower micro/mesopore volume the desorption branch approximately follows the adsorption branch. Considering the extracted micro, meso and macropore volumes using DFT model and other parameters extracted using low pressure adsorption analysis the following results could be obtained:

- The micro and mesopore volume for the Goldwyer Formation is higher than the Kockatea Shale and the Carynginia Formation (Table 2.4).
- The average surface areas were found to be 13.158 for the Goldwyer Formation, 8.152 for the Kockatea Shale and 6.563 m^2/gr for the Carynginia Formation (Table 2.4).
- All samples showed an increase in micropore volume and decrease in macropore volume with decreasing average pore diameter (Fig. 2.5a, b).
- There is an inverse relationship between pore size and BET surface area (Fig. 2.6a).
- The BET surface area showing an increasing trend with increasing micropore volume (Fig. 2.6b), while there is not any conclusive relationship between macropore volume and BET surface area (Fig. 2.6c).
- Summation of the micro and mesopore volumes for the Perth samples shows a positive correlation with TOC and thermal maturity indicator; i.e. T_{max} (Fig. 2.7a).
- To some extent clay content has a direct relationship with summation of the micro and mesopore volumes for the Perth samples but finding a relationship between quartz content and this summation is difficult (Fig. 2.7b).

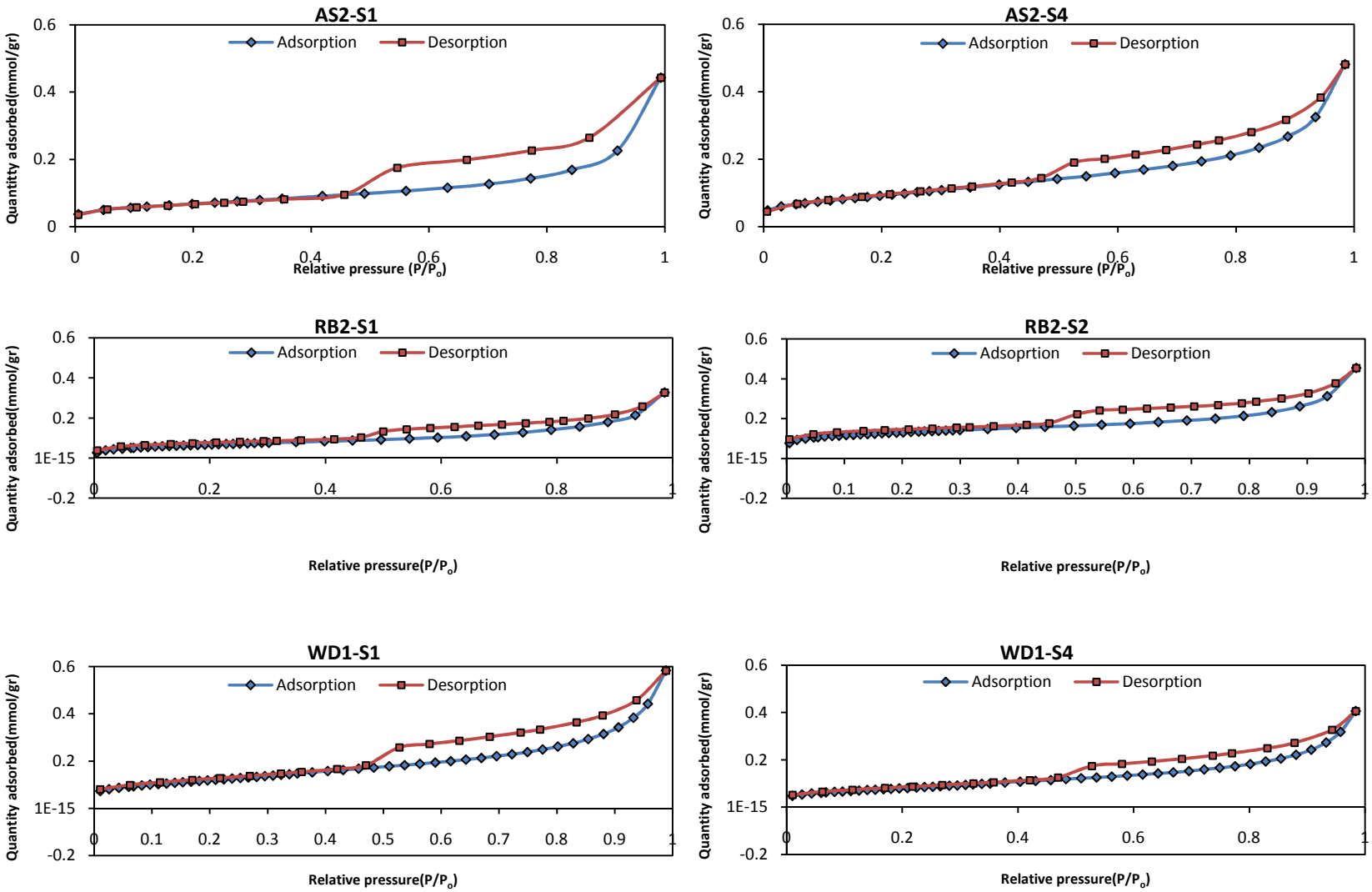

Fig. 2.3: Low pressure N_2 isotherms for numbers of the Perth samples.

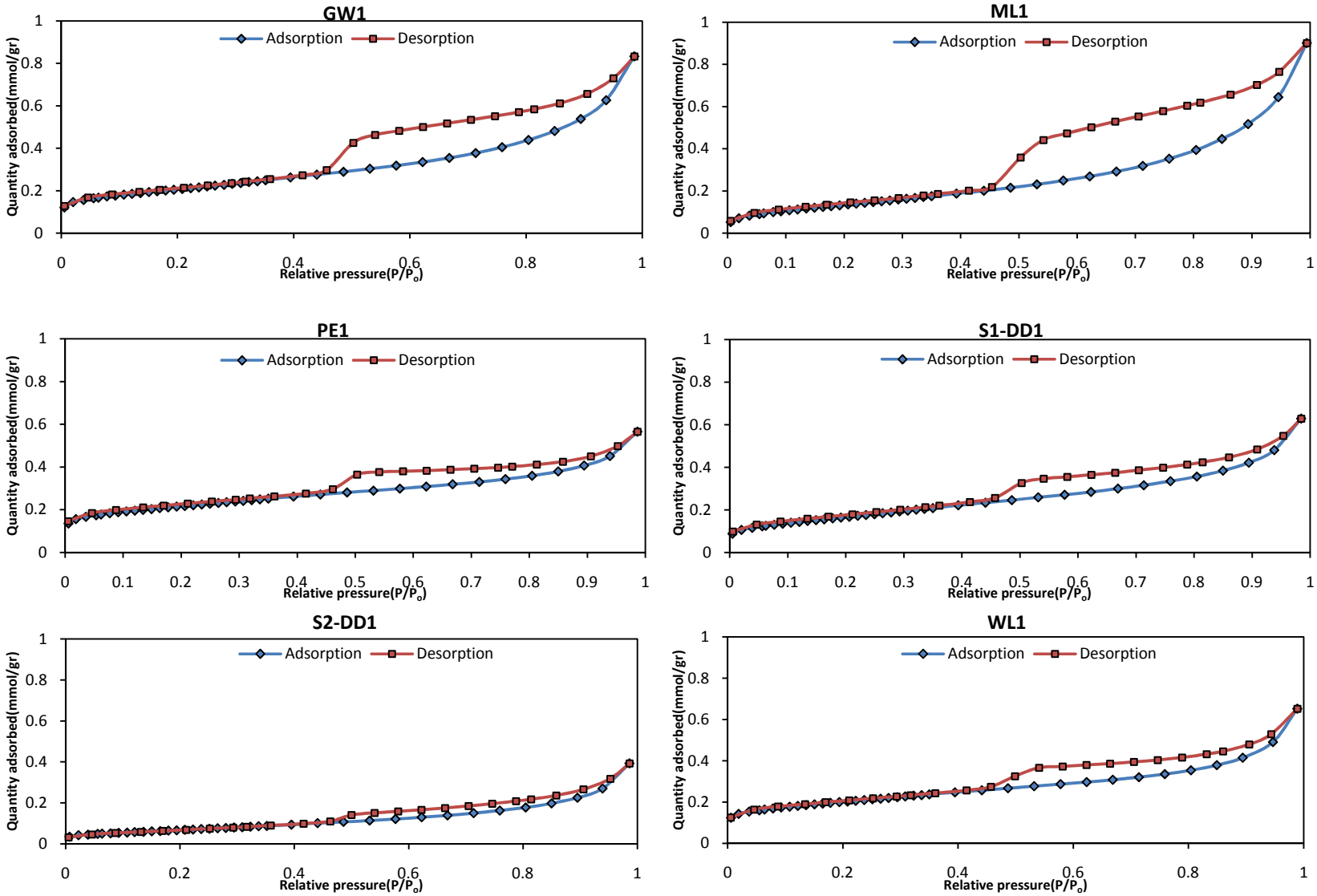

Fig. 2.4: Low pressure N_2 isotherms for the Canning samples.

Table 2.2:Low pressure nitrogen adsorption results accompanied by helium porosity for the Perth samples.

Sample name	Geological Formation	He porosity (%pu)	BET surface area(m^2/gr)	Total pore vol. at maximum pressure(cm^3/100gr)	Adsorption average pore width(nm)	Sum of micro and mesopore vol.(cc/100gr)
AS2-S1	Carynginia	2.783	5.425	1.538	11.324	1.002
AS2-S2	Carynginia	2.894	2.339	0.994	10.997	0.724
AS2-S4	Carynginia	4.150	7.567	1.669	8.824	0.767
AS2-S6	Carynginia	2.920	4.282	1.193	11.142	0.680
AS2-S7	Carynginia	3.111	4.912	1.280	10.424	0.516
AS2-S8	Carynginia	3.225	7.788	1.573	8.081	0.587
AS2-S9	Carynginia	4.233	5.978	1.283	8.584	0.476
AS2-S10	Carynginia	3.663	7.793	1.552	7.968	0.580
RB2-S1	Kockatea	3.075	5.422	1.137	8.390	0.532
RB2-S2	Kockatea	---	9.991	1.574	6.302	0.601
RB2-S3	Kockatea	2.552	12.030	1.880	6.249	1.131
RB2-S4	Kockatea	1.448	7.962	1.314	6.599	0.748
RB2-S5	Kockatea	3.650	5.752	1.091	7.590	0.572
WD1-S1	Carynginia	5.122	9.547	2.021	8.468	0.989
WD1-S2	Carynginia	4.943	9.613	1.949	8.111	0.965
WD1-S3	Carynginia	4.665	7.019	1.488	8.482	0.751
WD1-S4	Carynginia	2.647	6.496	1.408	8.673	0.688

Table 2.3: Low pressure nitrogen adsorption results accompanied by helium porosity for the Canning samples.

Sample name	Geological Formation	He porosity (%pu)	BET surface area(m^2/gr)	Total pore vol. at maximum pressure.(cm^3/100gr)	Adsorption average pore width (nm)	Sum of micro and mesopore vol.(cc/100gr)
GW1	Goldwyer	4.497	16.062	2.890	7.197	1.534
ML1	Goldwyer	5.033	11.660	3.127	10.730	2.220
PE1	Goldwyer	1.102	16.369	1.959	4.789	1.146
S1-DD1	Goldwyer	0.745	13.711	1.193	6.364	1.112
S2-DD1	Goldwyer	5.374	5.767	1.363	9.456	0.941
WL1	Goldwyer	3.598	15.380	2.260	5.879	1.268

Table 2.4: Low pressure nitrogen adsorption results classified by the geological formation.

Geologic Formation	BET surface area(m^2/gr)	Micropore vol. (cc/100gr)	Mesopore vol. (cc/100gr)
Goldwyer	13.158	0.190	1.180
Kockatea (Hovea mb.)	8.152	0.136	0.581
Carynginia	6.563	0.051	0.676

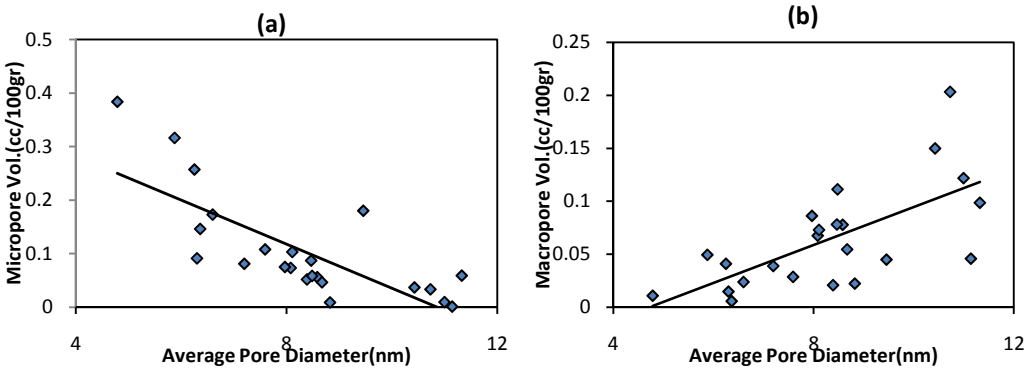

Fig. 2.5: Relationship between average pore diameter and micropore volume (a), and macropore volume (b) for all the measured samples.

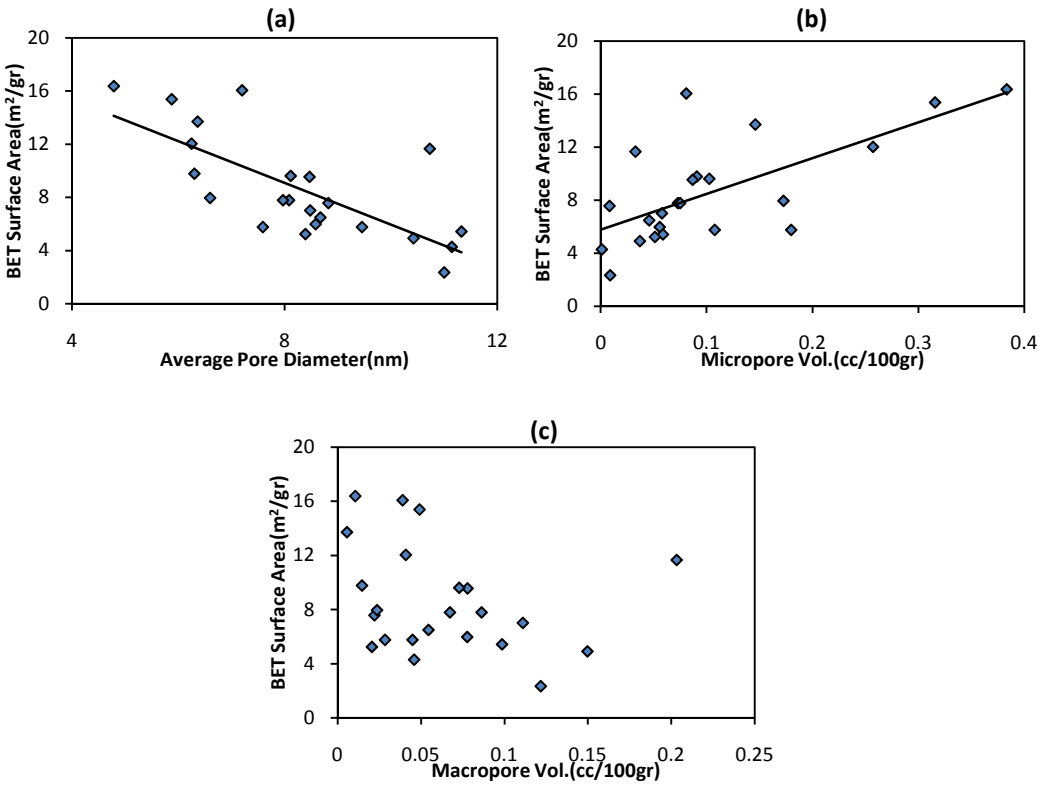

Fig. 2.6: Relationship between BET surface area and (a) average pore diameter, (b) micropore volume, and (c) macropore volume for all the measured samples.

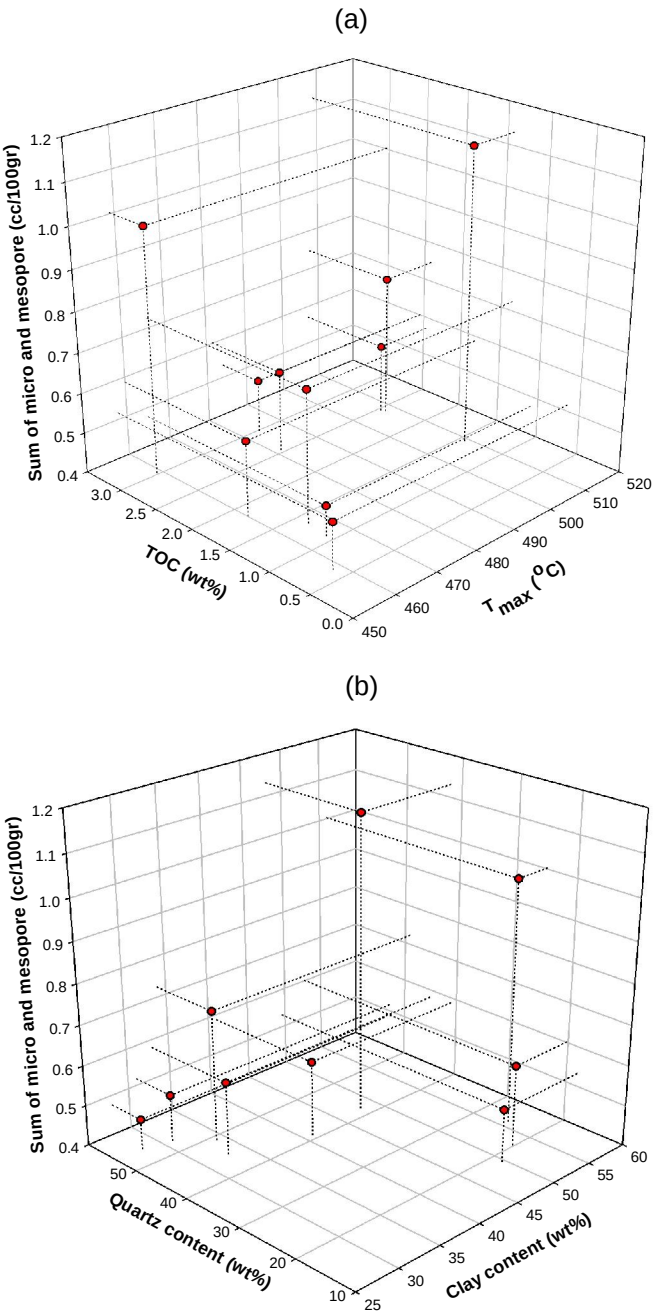

Fig. 2.7: 3D scatter plot showing the relationship between sum of micro and mesopore volume with (a) TOC and T_{max} and (b) quartz and clay content for the Perth samples.

In addition to the aforementioned parameters, PSD could be determined using the gas adsorption analysis.The PSD of the micropores, mesopores and part of macroporesobtained from the gas adsorption analysis using incremental pore volume for the Perth and Canning samples have been shown in Fig. 2.8and Fig. 2.9,respectively. According to these two figures the studied samples show the multimodal pore size distribution. As it could be seen in Fig. 2.8 and Fig. 2.9 two main modes could be detected for the studied samples; the main mode is between 20 nm and 30 nm and the other one is less than 10 nm. Fig. 2.10shows the

overlaying of PSD determined from mercury porosimetry with PSD derived from gas adsorption analysis. According to Fig. 2.10the PSD is between 3 nm and 375 µm based on mercury porosimetry and between 1 nm and 200 nm for gas adsorption analysis.

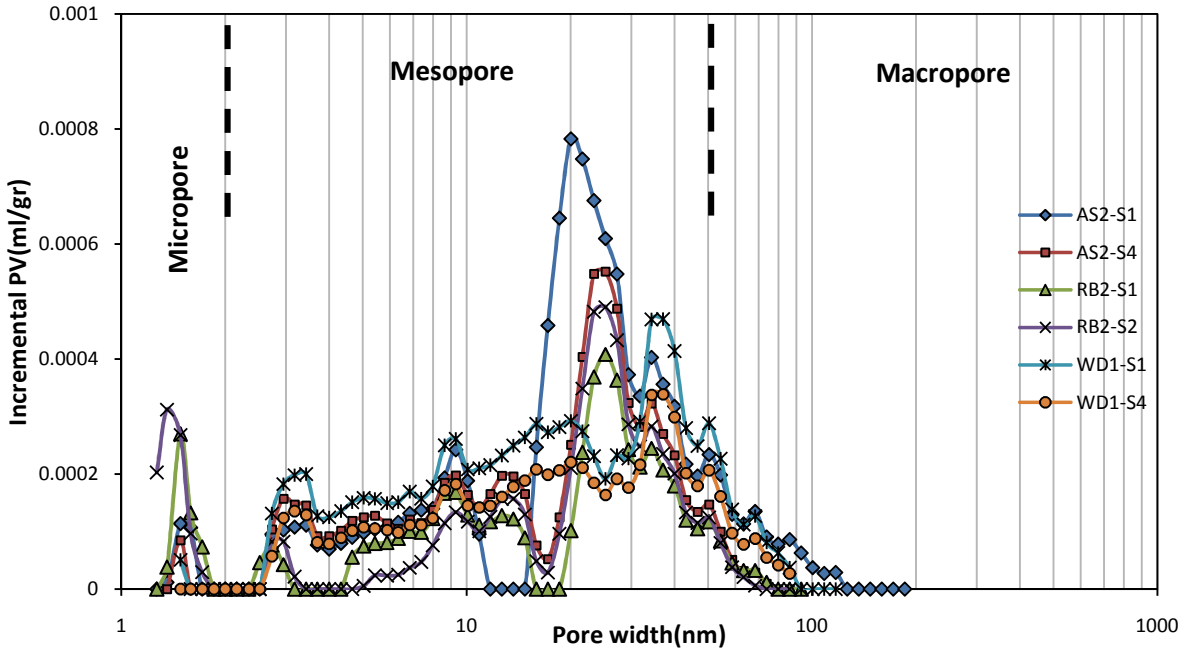

Fig. 2.8: Pore size distribution defined by incremental pore volume using low pressure nitrogen adsorption analyses for six samples from the Perth Basin.

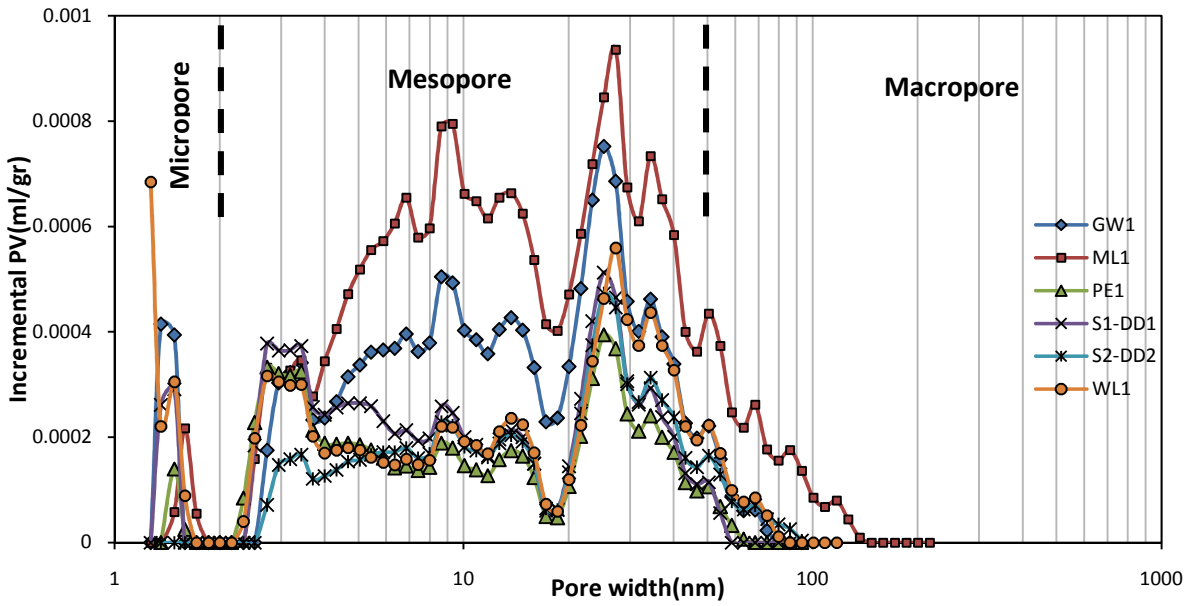

Fig. 2.9: Pore size distribution defined by incremental pore volume using low pressure nitrogen adsorption analyses for the Canning samples.

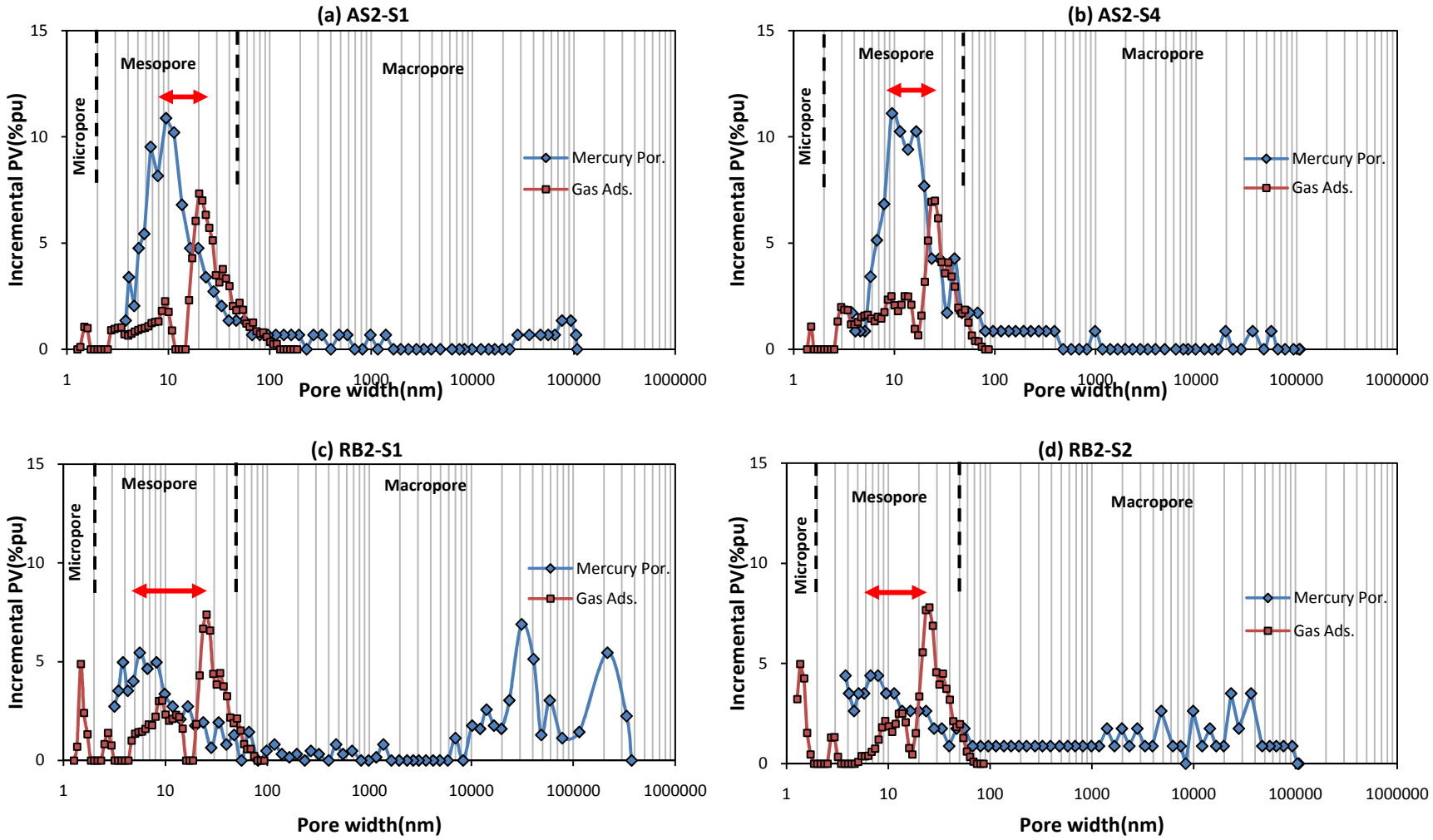

Fig. 2.10: Overlaying PSD defined by incremental pore volume using mercury porosimetry and gas adsorption data for 4 gas shale samples from the Perth Basin (The arrows show the difference between peak positions in the mesopore area).

2.4 Discussion

According to the theory all of the obtained relationships in the results section are meaningful:

- Beliveau (1993) showed that there is an inverse relationship between pore size and surface area.
- Chalmers and Bustin (2007, 2008) showed that the micropores have a greater contribution in surface area.
- Clay content can affect the micropore and mesopore volume because aluminosilicates such as illite have microporosity (Ross and Bustin, 2007b).
- Existing nanopores in the organic matter (Loucks et al., 2009; Passey et al., 2010) and developing microporosity in the organic matter with increasing thermal maturity (Prinz and Littke, 2005; Jarvie et al., 2007; Modica and Lapierre, 2012) could justify the relationship between TOC, T_{max} and summation of the micro and mesopore volumes.

Besides these findings analysing the obtained results shows that there is not any consistency between similar pore structure parameters; i.e. effective porosity or PSD. While gas expansion and nitrogen adsorption techniques both measure effective porosity, it is expected to have a meaningful relationship between measured porosities using these two techniques but this relationship is not obvious (Fig. 2.11). To find a justification for this inconsistency between porosities derived from gas expansion and nitrogen adsorption it is required to convert specific pore volume derived from nitrogen adsorption to porosity unit and calculate the difference between measured porosities using the following formula:

$$\text{Porosity}_{\text{adsorption}}(\%\text{pu}) = \rho_{\text{bulk}}\left(\frac{\text{gr}}{\text{cm}^3}\right) \times \text{Specific pore volume}\left(\frac{\text{cm}^3}{\text{gr}}\right) \times 100 \quad \text{(Eqn. 2.5)}$$

$$\Delta\varphi(\%\text{pu}) = \text{Porosity}_{\text{adsorption}}(\%\text{pu}) - \text{Porosity}_{\text{expansion}}(\%\text{pu}) \quad \text{(Eqn. 2.6)}$$

Where ρ_{bulk} is the bulk density of the shale sample derived from the density log and $\Delta\varphi$ is the difference between measured porosities using nitrogen adsorption and gas expansion. The difference between nitrogen adsorption porosity and helium porosity increases by increasing summation of micro and mesopore volumes (Fig. 2.12), implying that possibly gas expansion method cannot measure the micro and mesopore volume of the shale samples even after crushing the shale samples.

Furthermore, mercury porosimetry and gas adsorption analysis can determine PSD of the shale samples. Fig. 2.10shows the determined PSD using mercury porosimetry for 4 samples

in the Perth Basin overlaid on the PSD derived from nitrogen adsorption. As could be seen in this figure, nitrogen adsorption can give PSD in micro and mesopore ranges while mercury porosimetry can give the PSD in meso and macropore ranges, therefore combining these two techniques yields a full pore size characterization of the shale samples. By comparing the PSD in the overlapped area; i.e. mesopore, it is clear that the position of the peaks does not match precisely (Fig. 2.10). For all four samples, mercury porosimetry suggests a lower mode pore diameter compared to that obtained from nitrogen adsorption. There are two possible explanations for this observed shift:

- Based on the Washburn equation for accessing the smaller pore diameters mercury injection pressure should increase. The experimental results show that the mercury injection pressure for accessing pore diameters around 3 nm is about 60 kpsi. This high pressure as suggested by Giesche (2006) could compress the sample and subsequently decrease the measured pore throat size especially at smaller sizes.
- Mercury porosimetry measures the largest entrance towards a pore, but not the actual inner pore size. It should be noted that the pores in heterogeneous shale matrix are not in uniform shape. Considering the bottle neck shape for the pores (Fig. 2.2); it can be assumed that the pore throat is smaller than the actual inner pore size. Thus, the measured pore size using mercury would be smaller than that obtained from the nitrogen adsorption results.

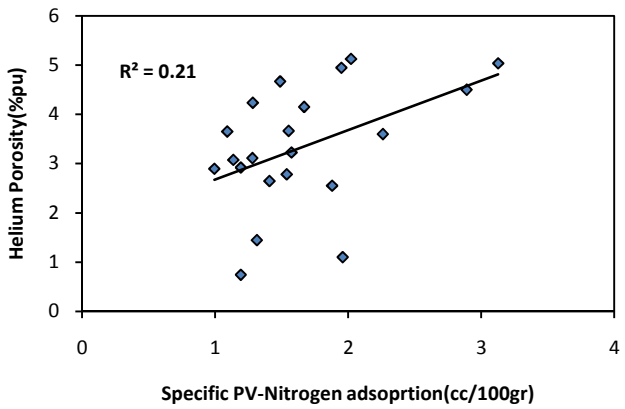

Fig. 2.11: Relationship between specific pore volume derived from nitrogen adsorption and helium porosity for all measured samples.

In addition to the above two possible sources of error in mercury analysis, the size of the samples could be a contributing factor to the observed difference between the two PSDs obtained from mercury porosimetry and gas adsorption analysis. The sample size used for

nitrogen adsorption analysis is less than 250 μm while the samples used for mercury porosimetry are irregular shape of shale chunks (Fig. 2.13). It could be concluded that crushing the shale samples in this scale removes the macro-fabric effect which is possibly present in the sample used for mercury porosimetry and might result in a different PSD.

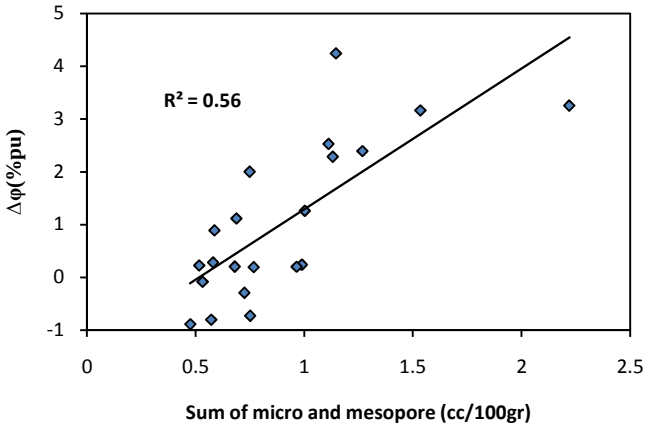

Fig. 2.12: Relationship between sum of micro and mesopore volume with Δφ for all measured samples.

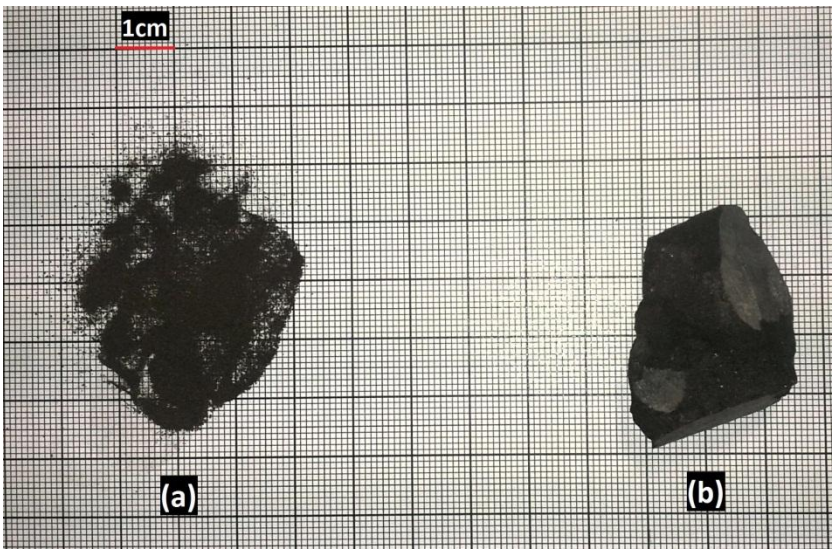

Fig. 2.13: A crushed sample (particles less than 250 μm) used for nitrogen adsorption (a) versus a chunk of shale used for mercury porosimetry (b).

2.5 Conclusion

In this study low pressure nitrogen adsorption, gas expansion and mercury porosimetry techniques have been used for characterization of gas shale pore system. The following conclusions can be drawn based on the results obtained:

a) Mercury porosimetry could not be used for determining the PSD of the shale samples alone due to its limitations in investigating pore spectrum but its combination with

nitrogen adsorption can determine a full spectrum of pore sizes (micropore, mesopore and macropore) in a more accurate way.

b) For most of the shale samples effective porosity determined from gas expansion technique is lower compared to the same parameter determined from low pressure nitrogen adsorption possibly due to the limitation of gas expansion method for measuring micro and mesopore volumes of the shale samples.
c) Overlaying PSD of mercury intrusion and nitrogen adsorption shows the lower peak position for mercury compared to nitrogen in the mesopore area. This might be due to the pore geometry of the analysed sample or compressibility of the sample at high mercury intrusion pressure.
d) Gas adsorption analysis results show that there is an inverse relationship between surface area and pore size. Furthermore, these results suggest that micropores have a higher surface area compared to mesopore and macropore. Due to the importance of surface area for methane adsorption it could be concluded that micropores are very important for gas shale production.
e) There are many parameters which can affect the micro and mesopores. Analysing XRD results and geochemical data showed that increasing TOC, thermal maturity and clay content can increase the summation of the micro and mesopores and subsequently would increase the volume of the adsorbed gas.
f) Comparing the results of case study shows that the Goldwyer Formation has the higher micro/mesopore volume and specific surface area compared to the other two studied formations; i.e. Kockatea Shale and Carynginia Formation (Table 2.4). Therefore considering the effect of surface area and micro/mesopore on adsorbed gas capacity it could be concluded that the Canning samples (samples from the Goldwyer Formation) have the higher potential to be considered as gas shales.

It is worth mentioning that due to the high degree of heterogeneity of the shale layers the results of this study may not be representative of the mentionedgeological formations but they can be used to clarify the complexity of the pore structure in these formations. Further study on the gas shale samples from these two basins includes high pressure methane adsorption in different pressures to build the Langmuir isotherm for finding the Langmuir volume and Langmuir pressure which are required for calculation of adsorbed gas capacity of the gas shale reservoir.

2.6 References

Barret, E.P., Joyner, L.G., Halenda, P.P., 1951. The determination of pore volume and area distribution in porous substances: Computations from nitrogen isotherms. Journal of American Chemical Society 73, 373-380.

Beliveau, D., 1993. Honey, I shrunk the pores! Journal of Canadian Petroleum Technology 32, 15-17.

Brunauer, S., Deming, L.S., Deming, W.S., Teller, E., 1940. On a Theory of the van der Waals Adsorption of Gases. Journal of the American Chemical Society 62, 1723-1732.

Brunauer, S., Emmett, P.H., Teller, E., 1938. Adsorption of gases in multimolecular layers. Journal of the American Chemical Society 60, 309-319.

Busch, A., Gensterblum, Y., Krooss, B.M., Siemons, N., 2007. Investigation of high-pressure selective adsorption/desorption behaviour of CO_2 and CH_4 on coals: an experimental study. International Journal of Coal Geology 66, 53-68.

Bustin, R.M., Bustin, A.M.M., Cui, X., Ross, D., Pathi, V.M., 2008. Impact of shale properties on pore structure and storage characteristics. SPE Shale Gas Production Conference, Fort Worth, Texas, USA. SPE119892.

Bustin, R.M., Clarkson, C.R., 1998. Geological controls on coalbed methane reservoir capacity and gas content. International Journal of Coal Geology 38, 3-26.

Chalmers, G.R., Bustin, R.M., 2007. On the effects of petrographic composition on coalbed methane sorption. International Journal of Coal Geology 69, 288-304.

Chalmers, G.R., Bustin, R.M., 2008. Lower Cretaceous gas shales in northeastern British Columbia, Part I: geological controls on methane sorption capacity. Bulletin of Canadian Petroleum Geology 56, 1-21.

Chalmers, G.R., Bustin, R.M., Power, I.M., 2012. Characterization of gas shale pore systems by porosimetry, pycnometry, surface area, and field emission scanning electron microscopy/transmission electron microscopy image analyses: Examples from the Barnett, Woodford, Haynesville, Marcellus, and Doig units. AAPG Bulletin 96, 1099-1119.

De Boer, J.H., 1958. The structure and properties of porous materials. Proceedings of the tenth symposium of the Colston Research Society held in the University of Bristol, Butterworths, London, 68-94.

Do, D.D., Do, H.D., 2003. Pore characterization of carbonaceous materials by DFT and GCMC simulations: A Review. Adsorption Science and Technology 21, 389-423.

Dollimore, D., Heal, G.R., 1964. An improved method for the calculation of pore-size distribution from adsorption data. Journal of Applied Chemistry 14, 109-114.

Easley, T.G., Sigal, R., Rai, C., 2007. Thermogravimetric analysis of Barnett shale samples. International Symposium of the Society of Core Analysts, Calgary, Alberta, Canada.

Gan, H., Nandie, S.P., Walker Jr., P.L., 1972. Nature of porosity in American coals. Fuel 51, 272-277.

Giesche, H., 2006. Mercury Porosimetry: A General (Practical) Overview. Particle & Particle Systems Characterization 23, 9-19.

Gregg, S.J., Sing, K.S.W., 1991. Adsorption, surface area and porosity. Academic Press: London, 303 pp.

Jarvie, D.M., Hill, R.J., Ruble, T.E., Pollastro, R.M., 2007. Unconventional shale-gas systems: The Mississippian Barnett Shale of north-central Texas as one model for thermogenic shale-gas assessment. AAPG Bulletin 91, 475-499.

Javadpour, F., 2009. Nanopores and apparent permeability of gas flow in mudrocks (Shales and Siltstone). Journal of Canadian Petroleum Technology 48, 16-21.

Javadpour, F., Fisher, D.,Unsworth, M., 2007. Nano-scale gas flow in shale gas sediments. Journal of Canadian Petroleum Technology 46, 55-61.

Kuila, U., Prasad, M., 2011. Surface area and pore-size distribution in clays and shales, SPE Annual Technical Conference and Exhibition, Denver, Colorado, USA. SPE 146869.

Loucks, R.G., Reed, R.M., Ruppel, S.C.,Hammes, U., 2012. Spectrum of pore types and networks in mudrocks and a descriptive classification for matrix-related mudrock pores. AAPG Bulletin 96, 1071-1098.

Loucks, R.G., Reed, R.M., Ruppel, S.C., Jarvie, D.M., 2009. Morphology, genesis, and distribution of nanometer-scale pores in siliceous mudstones of the Mississippian Barnett shale. Journal of Sedimentary Research 79, 848-861.

Lu, X.C., Li, F.C., Watson, A.T., 1995. Adsorption measurements in Devonian shales. Fuel 74, 599-603.

Luffel, D.L., Guidry, F.K., 1992. New core analysis methods for measuring reservoir rock properties of Devonian Shale. SPE Journal of Petroleum Technology 11, 1184-1190.

Modica, C.J., Lapierre, S.G., 2012. Estimation of kerogen porosity in source rocks as a function of thermal transformation: Example from the Mowry Shale in the Powder River Basin of Wyoming. AAPG Bulletin 96, 87-108.

Passey, Q.R., Bohacs, K., Esch, W.L., Klimentidis, R., Sinha, S., 2010. From oil-prone source rock to gas-producing shale reservoir - geologic and petrophysical characterization of unconventional shale gas reservoirs, International Oil and Gas Conference and Exhibition, Beijing, China. SPE131350.

Prinz, D., Littke, R., 2005. Development of the micro- and ultramicroporous structure of coals with rank as deduced from the accessibility to water. Fuel 84, 1645-1652.

Quantachrome, 2008. Autosorb AS-1/ASWin Gas sorption system operation manual. Boynton Beach, Florida, Quantachrome Instruments, 200 pp.

Ravikovitch, P.I., Haller, G.L., Neimark, A.V., 1998. Density functional theory model for calculating pore size distributions: pore structure of nanoporous catalysts. Advances in Colloid and Interface Science 76-77, 203-226.

Ross, D.J.K., Bustin, R.M., 2007a. Impact of mass balance calculations on adsorption capacities in microporous shale gas reservoirs. Fuel 86, 2696-2706.

Ross, D.J.K., Bustin, R.M., 2007b. Shale gas potential of the Lower Jurassic Gordondale Member, northeastern British Columbia, Canada. Bulletin of Canadian Petroleum Geology 55, 51-75.

Ross, D.J.K., Bustin, R.M., 2009. The importance of shale composition and pore structure upon gas storage potential of shale gas reservoirs. Marine and Petroleum Geology 26, 916-927.

Rouquerol, J., Avnir, D., Fairbridge, C.W., Everett, D.H., Haynes, J.H., Pernicone, N., Ramsay, J.D.F., Sing, K.S.W., Unger, K., 1994. Recommendations for the characterization of porous solids. International Union of Pure and Applied Chemistry. Pure and Applied Chemistry 68, 1739-1758.

U.S Energy Information Administration (EIA), 2011. World shale gas resources: an initial assessment of 14 regions outside the United States. 365pp.

Washburn, E.W., 1921. Note on the method of determining the distribution of pore sizes in a porous material. Proceedings of the National Academy of Sciences of the U.S.A 7, 115-116.

CHAPTER 3

DETERMINATION OF GAS STORAGE POTENTIAL OF GAS SHALE RESERVOIRS USING COMBINATION OF HIGH PRESSURE METHANE ADSORPTION AND LOW PRESSURE NITROGEN ADSORPTION

CHAPTER 3

Determination of gas storage potential of gas shale reservoirs using combination of high pressure methane adsorption and low pressure nitrogen adsorption

3.1 Introduction

Gas storage is often the critical factor for evaluating the economics of a gas shale system. Mechanism of gas storage in the shale layers is different with conventional reservoirs. Shale gas can be stored in two main ways (Fig. 3.1) (Lu et al., 1995; Curtis, 2002; Ross, 2007):

- Free gas in pores and fractures,
- Condensed gas in the form of adsorbed gas in organic matter pores and on inorganic minerals, or dissolved gas in liquid hydrocarbons and pore water.

In the laboratory conditions it is difficult to differentiate between adsorbed gas and dissolved gas therefore for convenience the 'adsorbed gas' term is used instead of 'condensed gas'. The physical adhesion of a gas molecule to the surface of solids by pore volume filling or by completion of a monolayer is called adsorption (Gregg and Sing, 1991). There are many different studies tried to determine the major parameters control the gas storage capacity of gas shale layers (Lu et al., 1995; Ross and Bustin, 2009; Zhang et al., 2012; Hao et al., 2013). Based on these studies the importance of each gas storage mode (i.e. free gas and adsorbed gas) is determined by pore space characteristics, organic matter characteristics and mineralogical parameters. Although effective parameters on the gas storage capacity of the shale layers are listed in the previous studies, shale heterogeneity will affect on the relative importance of these parameters in different regions. Therefore it is required to do a comprehensive study on the potential gas shales from Western Australia to determine the importance of shale characteristics for economic gas production. By identifying the importance of shale characteristics on the gas storage capacity mapping the gas shale sweet spots/pay zones would be more successful.

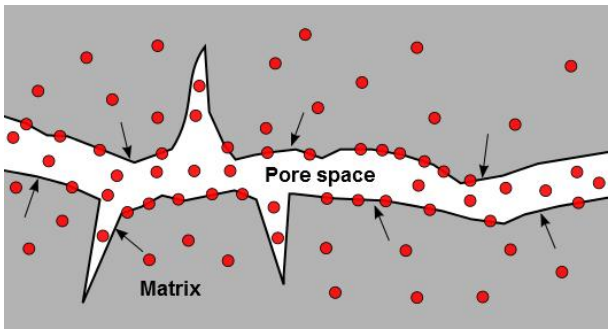

Fig. 3.1: Nano-scale schematic of gas molecule locations in the gas shale reservoirs (modified after Ross, 2007; Javadpour et al., 2009).

Low pressure adsorption measurement is required to know about the pore space characteristics of the gas shales and to determine the free gas capacity of these reservoirs.Pore structure parameters extracted from low pressure nitrogen adsorption can be used for analysing the effect of pore structure parameters on the gas storage capacity of the analysed samples. High pressure methane adsorption is required to make the adsorption isotherm; the relationship between adsorption capacity and pressure at a constant temperature. Once this relationship was established, the adsorbed gas capacity of the shale layer can be determined by knowing the pore pressure of the formation. Combining the results of low pressure and high pressure adsorption can give an insight about the free gas, adsorbed gas and total gas capacity of the gas shale layers and will help in determining the sweet spots for gas production.

3.2 Experimental methods and procedures

3.2.1 Sample preparation

In the current study two sets of gas shale samples were studied, 17 samples from the Perth Basin (12 samples from the Carynginia Formation and 5 samples from the Hovea member of the Kockatea Shale) and 6 samples from the Goldwyer Formation of the Canning Basin. The Perth shales are currently being explored as gas shale reservoirs, however the shale samples from the Canning Basin are from the old wells which have been drilled years ago for the target of conventional reservoirs.

The samples needed to be crushed before sorption analysis. Crushing the shale samples into smaller particles can help in diffusing gas faster to micropore sorption sites and therefore the equilibrium time will be shorter compared to larger particles (Weniger et al., 2010). There is no standard particle size for the samples to be analysed for sorption purposes. However in most of the similar studies performed previously (Ross and Bustin 2009; Chalmers et al.,

2012; Chareonsuppanimit et al., 2012) the shales were pulverised to 250 μm size. Therefore in this study the same particle size was selected for crushing the shale samples to be able to compare the results of this study with other similar studies have been done before.

Between 5 to 6 grams of the shale samples were crushed to yield particle sizes less than 250 μm for high pressure methane adsorption, a part of around 1 gram was used for low pressure nitrogen adsorption. These two techniques are looking for gas adsorption into micro and mesopores (Ross and Bustin, 2007a; Clarkson et al., 2011) therefore crushing the samples in this size range (250 μm) does not affect on the investigated pore structure and the measured gas adsorption capacity. The samples need to be dried before any sorption analysis because the traces of gas and water molecules available in the sample compete with the nitrogen or methane molecules for attaching to the adsorption sites (Bustin and Clarckson, 1998; Busch et al., 2006). Thus it is required to remove the moisture content and degas the samples prior to analysis and the final sorption analysis results were reported on a dry basis. For drying the shale samples, the samples are degassed at evacuated oven at 110^{o}C for 8 to 10 hours prior to analysis.

3.2.2 Low pressure nitrogen adsorption

Low pressure nitrogen isotherms (<18.4 psia) can be used to obtain the following information in microporous[*] materials (Gan et al., 1972):

- Specific pore volume: total pore volume per mass of the sample expressed as cm^3/gr,
- shape of the pores,
- specific surface area: total surface area per mass of the sample expressed as m^2/gr, and
- pore sizes and their distribution.

The nitrogen adsorption and desorption isotherms were collected at 77 K (-196^{o}C) using a Micromeritics® TriStar II 3020 apparatus. The repeatability of the analysis on this apparatus is about ±10%. The BET (Brunauer-Emmett-Teller) method is the most widely used procedure for determination of the surface area of porous samples. Equivalent surface area is calculated using the BET equation (Brunauer et al., 1938). The total pore volume is derived from the amount of vapour adsorbed at the maximum pressure, by assuming that the pores are completely filled with the liquid adsorbate at that pressure. The size of the pores can be

[*] Based on the pore classification proposed by the International Union of Applied and Pure Chemistry (IUPAC) (Rouquerol et al., 1994), micropores are <2 nm in diameter, mesopores 2-50 nm and macropores>50 nm.

determined using different pore size distribution models like BJH (Barret et al., 1951), DH (Dollimore and Heal, 1964) and DFT (Do and Do, 2003). Hence these models are explained by detail in different reviews (Barret et al, 1951; Dollimore and Heal, 1964; Do and Do, 2003); they are not explained herein. In this study the DFT model was used for pore size distribution determination. By using the PSD model it would be possible to determine the micropore, mesopore and macropore volumes separately.

3.2.3 High pressure methane adsorption

Gas storage evaluation of the gas shales is performed through two different measurements. Measuring the free gas component can be done using techniques that measure the pore volume like nitrogen adsorption. However for measuring the adsorbed gas capacity, there are two common methods: volumetric and gravimetric. As their names show the volumetric technique measures the volume of gas adsorbed to the sample while the gravimetric technique measures the change in the weight of adsorbent and correlates it to the adsorbed gas volume.

In this study, High Pressure Volumetric Analyser (HPVA) was used to measure the high pressure methane isothermsthrough the volumetric technique. All adsorption isotherms may be grouped into one of the five types (type I to type IV) shown in Fig. 3.2. Typically type I isotherm (Langmuir) fits and is used for adsorption of methane onto micorporous structure of the shale matrix. According to the Langmuir equation, the adsorbed gas capacity ($V_{ads.}$) can be expressed as follows:

$$V_{ads.} = \frac{V_L P}{P + P_L} \quad \text{(Eqn. 3.1)}$$

where V_L and P_L are the Langmuir volume and pressure respectively and P is the reservoir pressure. By rearranging Eqn. 3.1 the Langmuir parameters can be determined using the below formula with the limited pressure data points:

$$\frac{P}{V_{ads.}} = \frac{P}{V_L} + \frac{P_L}{V_L} \quad \text{(Eqn. 3.2)}$$

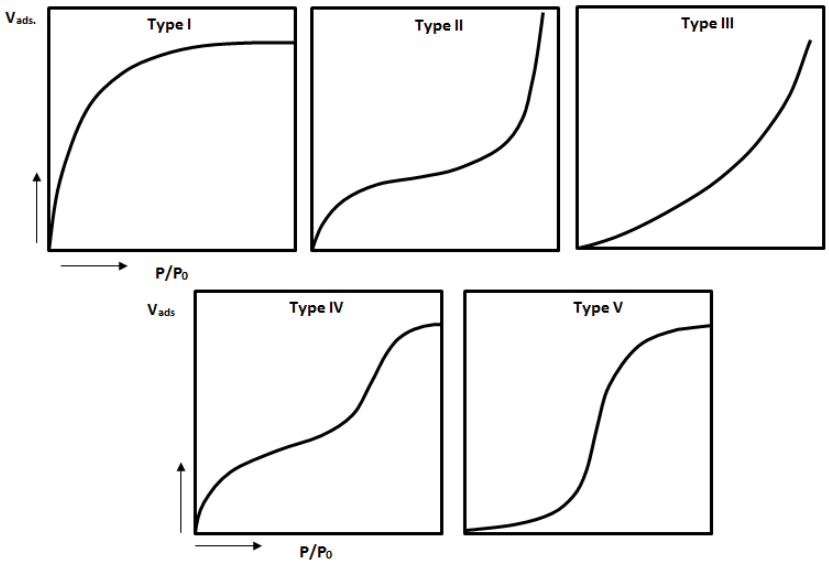

Fig. 3.2: Adsorption isotherm types (modified after Brunauer et al., 1940).

A plot of $P/V_{ads.}$ versusP produces a straight line, the reciprocal of the fitted line slope relates to methane monolayer volume (V_L).The high pressure adsorption behaviour of methane on the provided shale samples was investigated at two different temperatures, 23^{o}C and 30^{o}C. For each sample, the pressure points were collected up to around 870 psi. Using the collected adsorbed gas volume at different pressures and Eqn. 3.2 the V_L and P_L were calculated for each sample.

3.2.3.1 Experimental setup

A scheme depicting the key elements of our volumetric adsorption apparatus is shown in Fig. 3.3. The experimental set up for gas adsorption basically consists of:

- a vacuum pump and gauge,
- a reference cell maintained at constant temperature (typically at 40^{o}C) with two pressure transducers (high pressure transducer and low pressure transducer),
- a sample cell,
- an outgassing furnace with temperature controller for degassing the sample, and
- a thermostat bath for controlling the sample temperature.

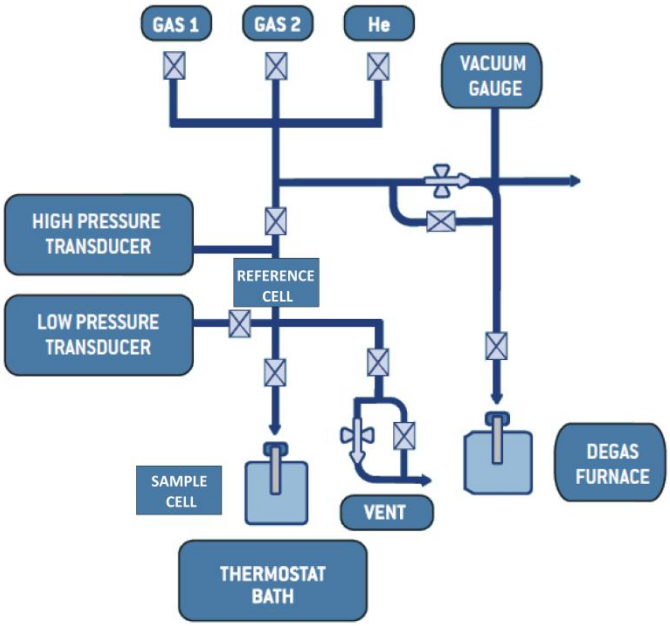

Fig. 3.3: Schematic diagram of adsorption apparatus (modified after Particulate Systems, 2011).

It is worth mentioning that the system has two gas inlets which can be used for measuring the adsorbed gas capacity with mixture of two different gases. The whole system was interfaced with computer, therefore variation of temperature and pressure was recorded accurately. The repeatability of the analysis on this system is about ±8%. Similar to the other volumetric instrument for measuring the adsorbed gas capacity, the apparatus uses the Helium for measuring the void volume in the system. The void volume is defined as the total volume that Helium gas can penetrate when the shale sample is inside the sample cell. It includes free space within the sample cell and porosity within the sample. However due to the dependency of this measurement to temperature it is required to do the void volume measurement before running the experiment in different temperatures. After void volume measurement the system completely evacuated and the methane dosed into the reference cell. As soon as the determined equilibrium criteria were met (pressure variation less than 0.001 bar in one minute or waiting for 20 minutes after dosing the gas into the reference cell) the system injects the methane into the sample cell. By having the pressures, temperatures and volumes of the reference and sample cell before and after dosing the gas and the gas compressibility factor, Z, it would be possible to determine the total amount of gas dosed in the system and the gas occupying the void volume. Gas compressibility factors for pure gas isotherms were determined using the Peng-Robinson equation of state (EOS) (Peng and Robinson, 1976). The amount of adsorbed gas for the analysed sample is determined by the static volumetric method using:

$$n_{ads.}=n_{dosed}-n_{void} \qquad \text{(Eqn. 3.3)}$$

where

$n_{ads.}$ is the amount of moles adsorbed by the sample,

n_{dosed} is the amount of moles doses into the system, and

n_{void} is the amount of moles occupying the void volume.

3.3 Experimental results

3.3.1 Shale composition and geochemical parameters

Table 3.1 shows the available XRD results and geochemical analyses for some of the studied samples from the Perth Basin. These data summarized in the ternary diagram (Fig. 3.4). Considering Table 3.1 and ternary diagram (Fig. 3.4) there is a large variability in the mineralogical composition of the studied samples. While the RB2 series samples and most of the WD1 series samples are rich in clay content, AS2 samples are rich in quartz content except AS2-S1. Total organic carbon (TOC) content for the available samples ranges between 0.23 and 4.42wt%. T_{max} is one of the output parameters of the Rock-Eval pyrolysis and could be tied to thermal maturity of the rock sample; this parameter varies between 458 to 509 ^{o}C. As it is clear the RB2 and WD1 samples have the higher T_{max} values compared to AS2 samples and therefore they are in the higher thermal maturity status compared to other studied samples.

3.3.2 Pore structure parameters of the shale samples

Table 3.2 and Table 3.3summarize the collected results from low pressure adsorption measurements including BET surface area, total pore volume measured at maximum relative pressure ($P/P_o=1$) and sum of micro and mesopore volumes for the Perth and Canning samples. Generally BET surface areas for all the analysed samples increase with increasing micropore volumes (Table 3.2 and Table 3.3); however the strength of this relationship is different in different studied geological formations (Fig. 3.5). Furthermore classifying the nitrogen adsorption results based on the geological formation shows the higher surface area and micro/mesopore volumes for the Goldwyer Formation compared with other two studied formations (Table 3.4).

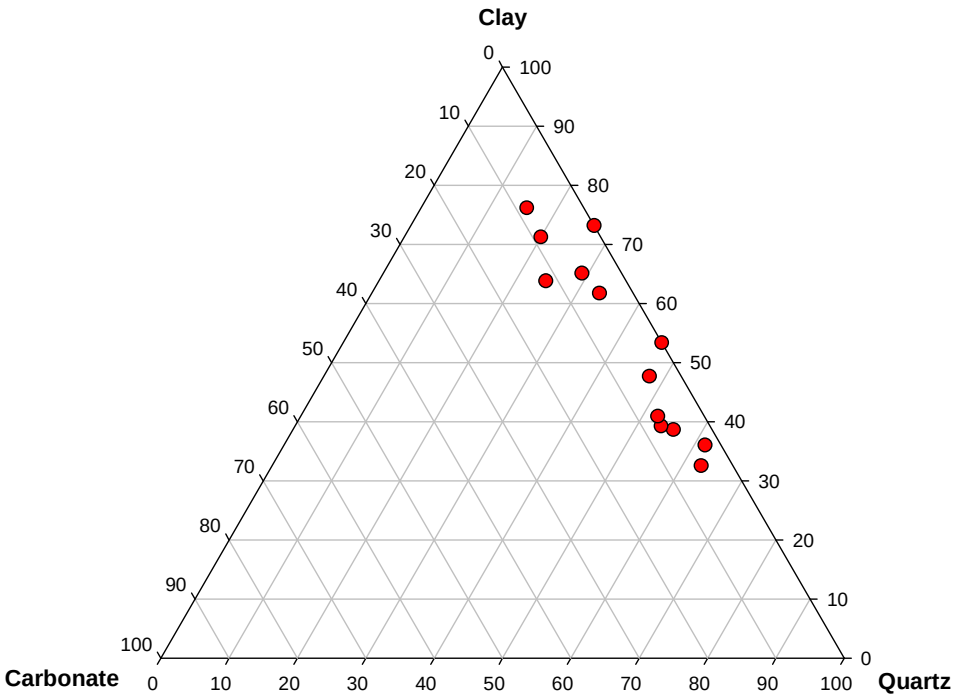

Fig. 3.4:The mineralogical ternary diagram summarizes the composition based on the normalized data from table 1.

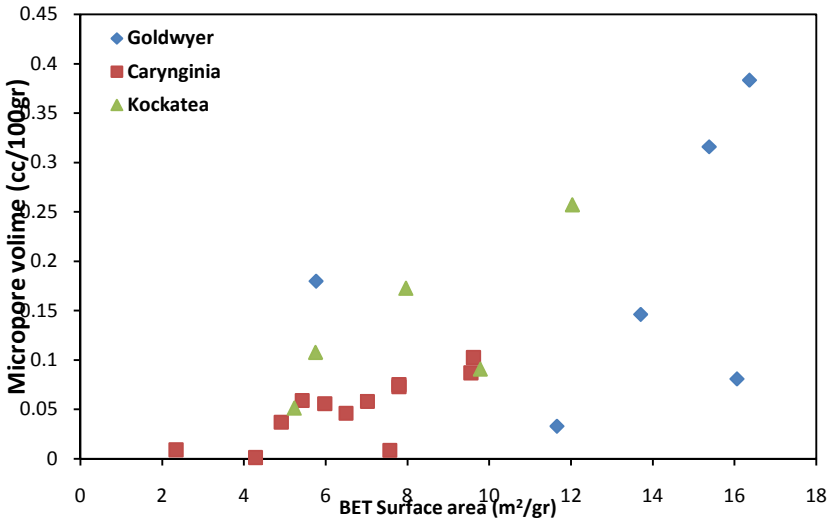

Fig. 3.5: Correlation between micropore volume and BET surface area for the analysed shale samples (Goldwyer Formation r^2=0.10; Carynginia Formation r^2=0.60; Kockatea Shale r^2=0.60).

Table 3.1: Available geochemical analysis and mineralogical composition for the studied samples.

Sample Name	TOC Content (wt%)	T_{max}(^{o}C)	Quartz (wt%)	Clay (wt%)	Carbonate (wt%)
AS2-S1	3.03	459	25	56	5
AS2-S2	1.36	466	49	34	5
AS2-S7	0.64	458	53	31	2
AS2-S8	1.82	460	41	41	4
AS2-S9	1.08	465	54	28	4
AS2-S10	0.23	n/a	45	33	6
RB2-S1	2.99	484	18.2	49.6	0
RB2-S2	2.54	481.5	20.2	52.7	9.7
RB2-S3	1.43	509	42	48.1	0
RB2-S4	2.415	507.5	n/a	n/a	n/a
RB2-S5	2.46	507	n/a	n/a	n/a
WD1-S1	2.61	481	16	57	7
WD1-S2	4.42	476	13	64	7
WD1-S3	2.1	486	27	50	4
WD1-S4	1.04	500	46	36	6

Table 3.2: Pore structure parameters derived from low pressure nitrogen adsorption for the Perth samples.

Sample name	Geological Formation	BET surface area(m^2/gr)	Total pore vol. at maximum pressure(cm^3/100gr)	Sum of micro and mesopore vol.(cc/100gr)
AS2-S1	Carynginia	5.425	1.538	1.002
AS2-S2	Carynginia	2.339	0.994	0.724
AS2-S4	Carynginia	7.567	1.669	0.767
AS2-S6	Carynginia	4.282	1.193	0.680
AS2-S7	Carynginia	4.912	1.280	0.516
AS2-S8	Carynginia	7.788	1.573	0.587
AS2-S9	Carynginia	5.978	1.283	0.476
AS2-S10	Carynginia	7.793	1.552	0.580
RB2-S1	Kockatea	5.422	1.137	0.532
RB2-S2	Kockatea	9.991	1.574	0.601
RB2-S3	Kockatea	12.030	1.880	1.131
RB2-S4	Kockatea	7.962	1.314	0.748
RB2-S5	Kockatea	5.752	1.091	0.572
WD1-S1	Carynginia	9.547	2.021	0.989
WD1-S2	Carynginia	9.613	1.949	0.965
WD1-S3	Carynginia	7.019	1.488	0.751
WD1-S4	Carynginia	6.496	1.408	0.688

Table 3.3: Pore structure parameters derived from low pressure nitrogen adsorption for the Canning samples.

Sample name	Geological Formation	BET surface area(m^2/gr)	Total pore vol. at maximum pressure.(cc/100gr)	Sum of micro and mesopore vol.(cc/100gr)
GW1	Goldwyer	16.062	2.890	1.534
ML1	Goldwyer	11.660	3.127	2.220
PE1	Goldwyer	16.369	1.959	1.146
S1-DD1	Goldwyer	13.711	1.193	1.112
S2-DD1	Goldwyer	5.767	1.363	0.941
WL1	Goldwyer	15.380	2.260	1.268

Table 3.4: Low pressure nitrogen adsorption results classified by the geological formation.

Geologic Formation	BET surface area(m^2/gr)	Micropore vol. (cc/100gr)	Mesopore vol. (cc/100gr)
Goldwyer	13.158	0.190	1.180
Kockatea (Hovea mb.)	8.152	0.136	0.581
Carynginia	6.563	0.051	0.676

3.3.3 Gas contents

3.3.3.1 Adsorbed gas measurements

Table 3.5 and Table 3.6 show the measured adsorbed gas capacity and total gas capacity for the analysed samples from the Perth and Canning Basins, respectively. The values for the adsorbed gas capacity are reported at two different temperatures,23^{o}C and 30^{o}C, and at the reservoir pressure. It is worth mentioning that the reservoir pressure was estimated based on the hydrostatic assumption (i.e. pressure gradient=0.43 psi/ft). Measured methane adsorption isotherms at different temperatures can be well fitted by the Langmuir equation (Fig. 3.6). As it was expected the adsorption capacity of the shale samples decreases as the temperature increases due to the exothermic nature of gas adsorption on the solid surfaces. Similar to the low pressure nitrogen adsorption, classifying the gas contents results based on the geological formation shows the lowest adsorbed gas capacity for the Carynginia Formation while approximately the adsorbed gas capacities for the Goldwyer Formation and the Hovea member of the Kockatea Shale are the same (Table 3.7).

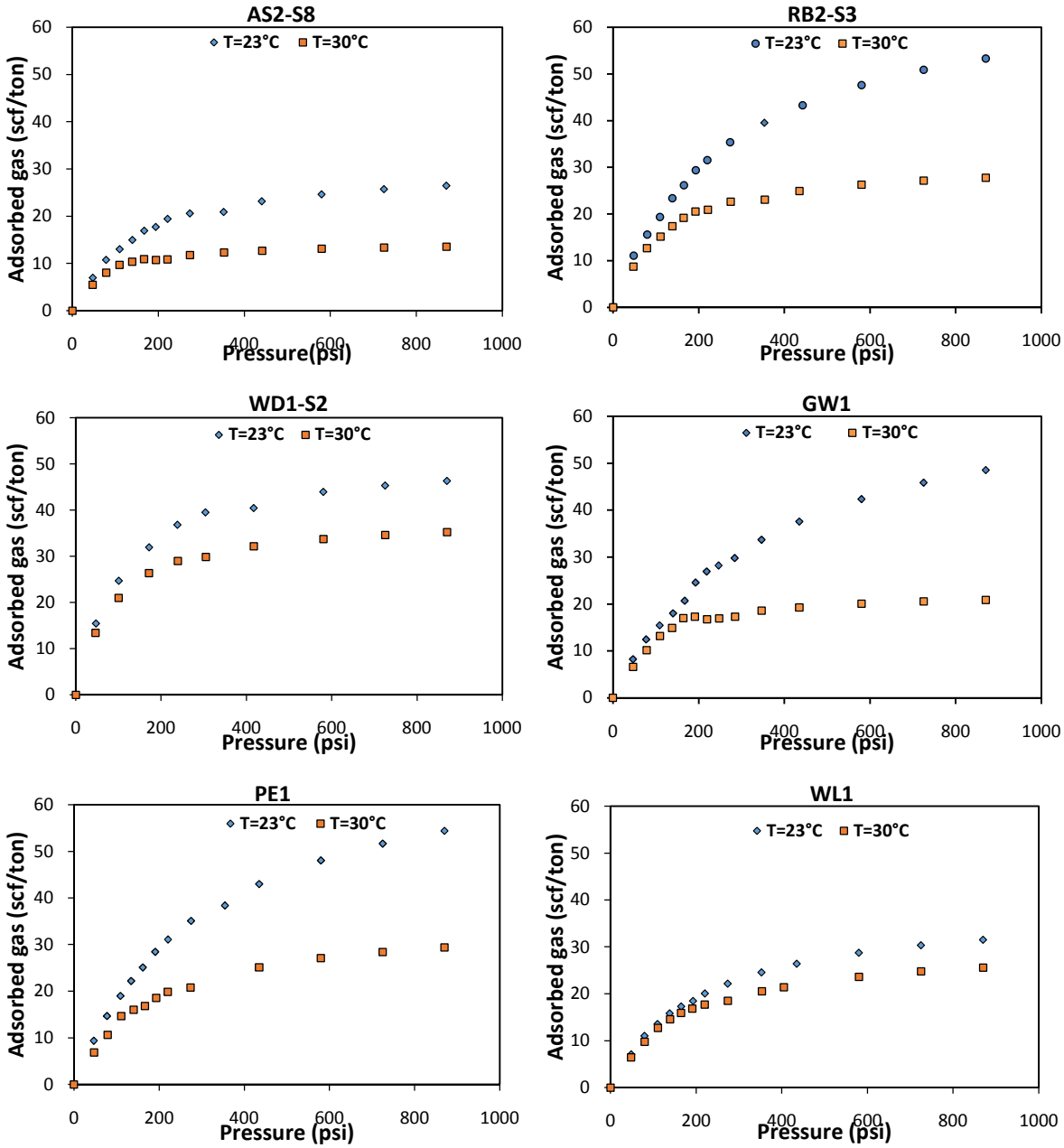

Fig. 3.6: Adsorbed gas isotherms for six selected samples from the Perth and Canning Basins at two different temperatures; T=23^{o}C and T=30^{o}C.

3.3.3.2 Total gas calculations

Although adsorbed gas capacity plays an important role in the gas storage of the gas shale reservoirs but a significant proportion of the total gas in place of these reservoirs is free gas (Montgomery et al., 2005). Thus, measuring the total porosity is important for estimation of the free gas. Due to the limitation of the gas expansion method for measuring micro and mesopore volumes of the shale samples (Labani et al., 2013), total pore volume was determined using low pressure nitrogen adsorption. By having the total pore volume, free gas molar volume can be calculated at each pressure step using the appropriate equation of state:

$$n=\frac{PV}{zRT} \qquad \text{(Eqn. 3.4)}$$

where:

P is the absolute gas pressure, Pascal,

V is the free space volume determined from low pressure nitrogen adsorption, m^3/ton

T is the gas temperature, Kelvin,

z is the gas deviation factor or compressibility,

R is the universal gas constant (8.3145), $J.mol^{-1}.K^{-1}$, and

n is the number of gas moles in the free space.

The free gas isotherm can then be obtained by repeating this procedure at each pressure step until the highest desired gas pressure is achieved (Fig. 3.7). In this study, free gas was estimated using two different assumptions for water saturation; S_w=25% and S_w=50%.

3.3.4 Adsorption affinity of the shale samples

Methane adsorption on the surface of the organic materials and clays is a reversible reaction. It means that it increases with increasing burial depth and pore pressure however after drilling a well and reducing the pore pressure the adsorbed methane can desorb from the gas shales and produce through the natural or hydraulic fractures. Therefore it would be important to determine the adsorption affinity of the studied gas shales due to its effect on gas desorption rate, a shale sample with the higher adsorption affinity will produce in a lower rate. The enthalpy/heat of adsorption is necessary for assessing the adsorption affinity of the gas shales.

Table 3.5: Total gas and adsorbed gas capacity of the analysed samples from the Perth Basin.

Sample ID	Depth(m)	Predicted reservoir pressure (psi)	Adsorbed gas capacity at reservoir pressure (scf/ton)		Total gas capacity at reservoir pressure and T=30°C (scf/ton)	
			T=23°C	T=30°C	S_w=25%	S_w=50%
AS2-S1	2780.26	3922.28	43.953	12.848	119.170	83.729
AS2-S2	2816.71	3973.71	19.611	9.440	78.792	55.675
AS2-S4	2781.64	3924.23	40.894	14.679	130.553	91.929
AS2-S6	2825.35	3985.89	23.333	9.406	144.780	99.655
AS2-S7	2794.47	3942.33	29.101	10.422	99.558	69.846
AS2-S8	2806.42	3959.19	29.838	14.343	123.886	87.372
AS2-S9	2812.55	3967.84	31.227	12.030	101.755	71.846
AS2-S10	2831.34	3994.34	30.756	9.195	118.207	81.870
RB2-S1	3798.84	5359.26	39.327	21.294	117.134	85.187
RB2-S2	3792.52	5350.35	35.256	18.405	150.953	106.770
RB2-S3	3819.34	5388.18	66.575	30.703	189.148	136.333
RB2-S4	3832.77	5407.13	34.352	17.663	129.000	91.888
RB2-S5	3834.52	5409.60	32.112	18.532	110.695	79.974
WD1-S1	2275.70	3210.48	35.394	18.619	141.010	100.213
WD1-S2	2282.03	3219.40	50.396	37.633	155.551	116.245
WD1-S3	2379.27	3356.60	36.137	13.812	106.492	75.599
WD1-S4	2467.27	3480.74	32.992	12.079	102.264	72.202

Table 3.6: Total gas and adsorbed gas capacity of the analysed samples from the Canning Basin.

Sample ID	Depth(m)	Predicted reservoir pressure (psi)	Adsorbed gas capacity at reservoir pressure (scf/ton)		Total gas capacity at reservoir pressure and T=30°C (scf/ton)	
			T=23°C	T=30°C	S_w=25%	S_w=50%
GW1	982.370	1385.89	54.404	9.440	78.792	55.675
ML1	2008.33	2833.27	46.947	22.778	144.759	104.099
PE1	2065.60	2914.07	66.868	33.402	143.805	107.004
S1-DD1	1542.39	2175.95	55.136	21.393	70.881	54.385
S2-DD1	1548.46	2184.51	15.310	3.737	60.501	41.579
WL1	2378.35	3355.29	36.776	29.312	169.979	123.090

Table 3.7: High pressure methane adsorption results classified by the geological formation.

Geologic Formation	Adsorbed gas capacity* (scf/ton)	Adsorbed gas capacity† (scf/ton)
Goldwyer	45.906	20.010
Kockatea (Hovea mb.)	41.524	21.319
Carynginia	33.636	14.542

* Denoted at T=23^{o}C and the reservoir pressure.

† Denoted at T=30^{o}C and the reservoir pressure.

Enthalpy of adsorption can vary with the temperature in accordance with the van't Hoff equation (Konstas et al., 2012):

$$\Delta H = RT\ln\frac{P_0}{P_L} \qquad \text{(Eqn. 3.5)}$$

where:

ΔH is the enthalpy of adsorption, J.mol^{-1},

T is the temperature, Kelvin

P_0 is 14.7 psi as the standard atmospheric pressure,

P_L is the Langmuir pressure, psi

R is the universal gas constant (8.3145), J.mol^{-1}.K^{-1}

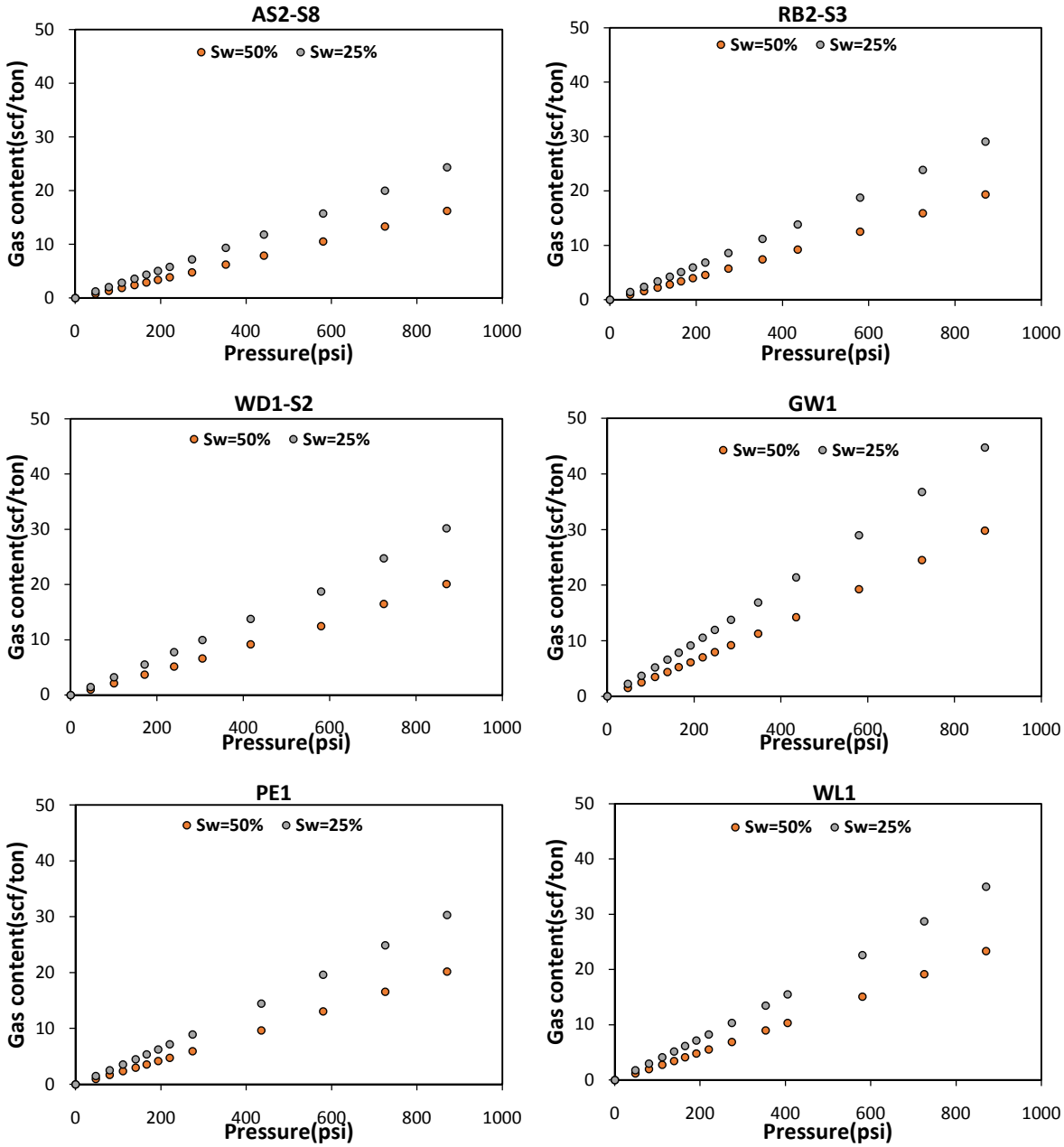

Fig. 3.7: Free gas isotherm (at T=30°C) for six selected samples from the Perth and Canning Basins using two different assumptions for water saturation; S_w=25% and S_w=50%.

Table 3.8 and Table 3.9 show the calculated enthalpy of adsorption for the studied samples from the Perth and Canning Basins, respectively. The reported values for the enthalpy of adsorption are the negative values showing the methane adsorption on the shale samples is an exothermic process. By increasing the analysing temperature from 23°C to 30°C the amount of adsorption decreases therefore as it could be seen in Table 3.8 and Table 3.9 its related produced heat decreases as well. Among the studied samples the Canning samples have the higher enthalpy of adsorption compared to the Perth samples showing their higher affinity for methane adsorption.

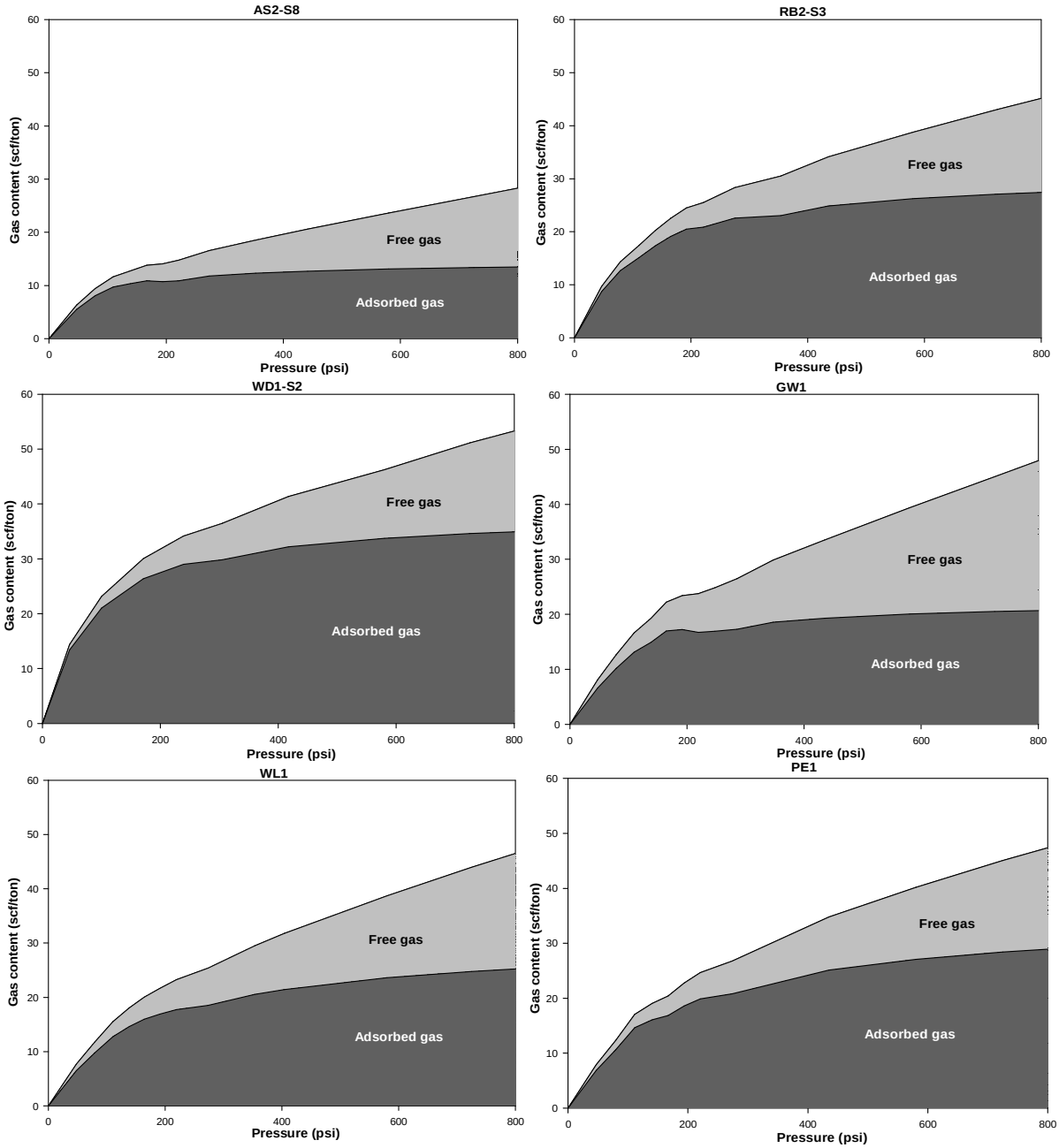

Fig. 3.8: Total gas isotherm accompanied with the adsorbed gas isotherm for six selected samples from the Perth and Canning Basins, assuming S_w=50% and T=30^{o}C.

Table 3.8: Enthalpy of adsorption for the studied samples from the Perth Basin at the analysed temperatures.

Sample ID	ΔH at T=23°C	ΔH at T=30°C
AS2-S1	-6.550	-2.663
AS2-S2	-5.636	-3.301
AS2-S4	-6.152	-3.812
AS2-S6	-5.467	-2.354
AS2-S7	-5.614	-2.706
AS2-S8	-5.714	-3.734
AS2-S9	-5.844	-3.210
AS2-S10	-6.193	-3.887
RB2-S1	-5.686	-2.869
RB2-S2	-6.525	-4.466
RB2-S3	-7.181	-5.144
RB2-S4	-6.223	-3.942
RB2-S5	-5.048	-2.904
WD1-S1	-6.488	-4.404
WD1-S2	-4.911	-4.380
WD1-S3	-5.257	-2.357
WD1-S4	-5.949	-3.423

Table 3.9: Enthalpy of adsorption for the studied samples from the Canning Basin at the analysed temperatures.

Sample ID	ΔH at T=23°C	ΔH at T=30°C
GW1	-7.904	-4.186
ML1	-6.803	-4.913
PE1	-7.550	-6.308
S1-DD1	-7.367	-5.400
S2-DD1	-6.498	-2.159
WL1	-6.558	-6.281

3.4 Discussion

3.4.1 Effective parameters on the gas storage capacity

Theoretically the relative importance of free gas and adsorbed gas is determined by (Allen et al., 2009; Ross, 2007):

- Organic matter characteristics including quantity (TOC) and maturity of organic matter,

- The composition of matrix minerals, and
- Pore space characteristics.

Fig. 3.9 shows the 3D scatter plot relating the mentioned parameters with the adsorbed gas capacity measured at T=30^{o}C. As it was expected the presence of clay minerals increases the gas storage capacity but the quartz minerals reduce the adsorbed gas capacity (Fig. 3.9a). Increasing the adsorbed gas capacity with clay content is due to its effect on the pore space characteristics. Clay content can affect on the micropore volume because aluminosilicates such as illite have microporosity (Ross and Bustin, 2007b).

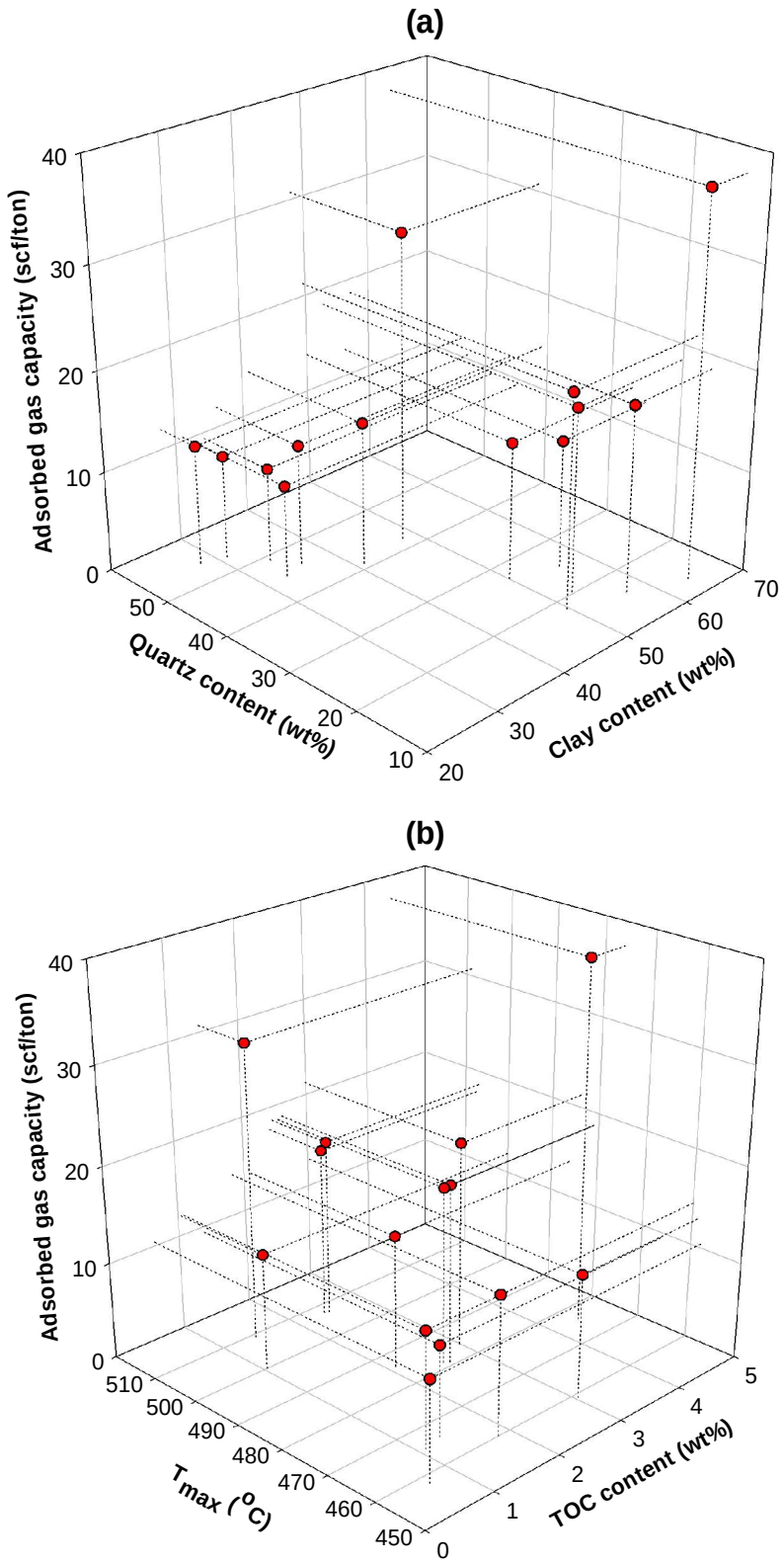

Fig. 3.9: 3D scatter plot showing the relationship between (a) shale composition, (b) geochemical parameters and (c) pore structural parameters with adsorbed gas capacity at T=30^{o}C.

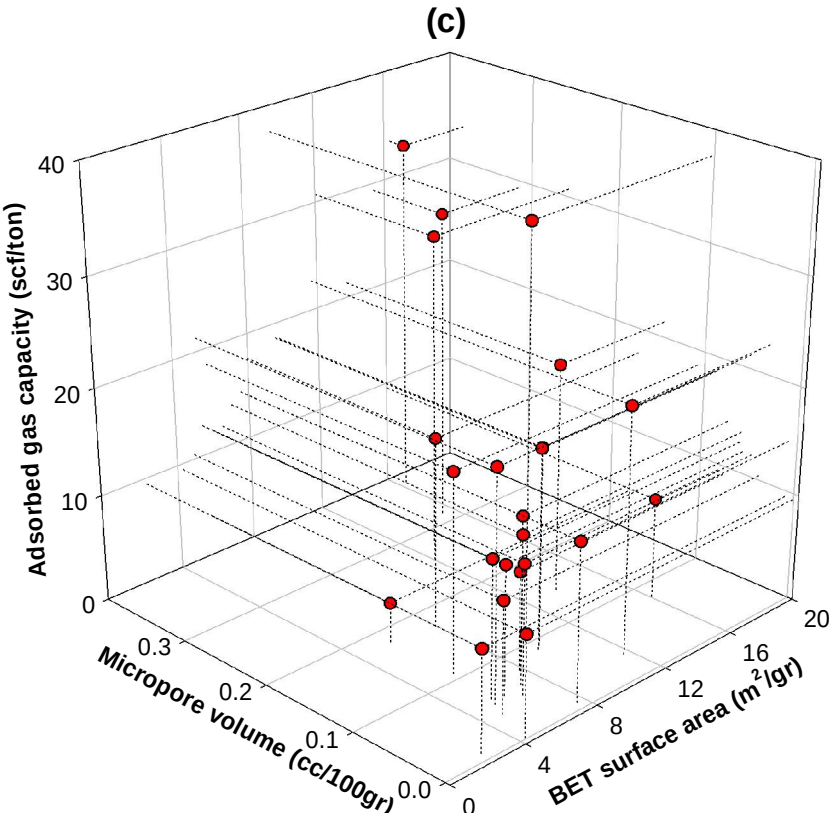

Fig. 3.9: Continued.

Theoretically it is believed that existing nanopores in the organic matter (Loucks et al., 2009; Passey et al., 2010) can increase the micropore volume and consequently adsorbed gas capacity. Most of these nanopores are formed during thermal decomposition of organic matter to hydrocarbon (Prinz and Littke, 2005; Jarvie et al., 2007; Modica and Lapierre, 2012). However, converse to the common idea effect of geochemical parameters especially thermally maturity on the adsorbed gas capacity of the studied samples is not evident (Fig. 3.9b). This might be due to the least effect of these parameters on micropore volume and surface area (Fig. 3.10).

Presence of micropore volume is the most important controlling factor on the gas storage capacity of the gas shale reservoirs and each parameter which could be effective on micropore volume can be considered as the controlling parameter on the gas storage capacity as well. Due to this point, the micropore volume and surface area have the higher dependency with the adsorbed gas capacity (Fig. 3.9c). As it is mentioned clay content and organic content are effective on the adsorbed gas capacity due to their effect on the pore structure properties like micropore volume.

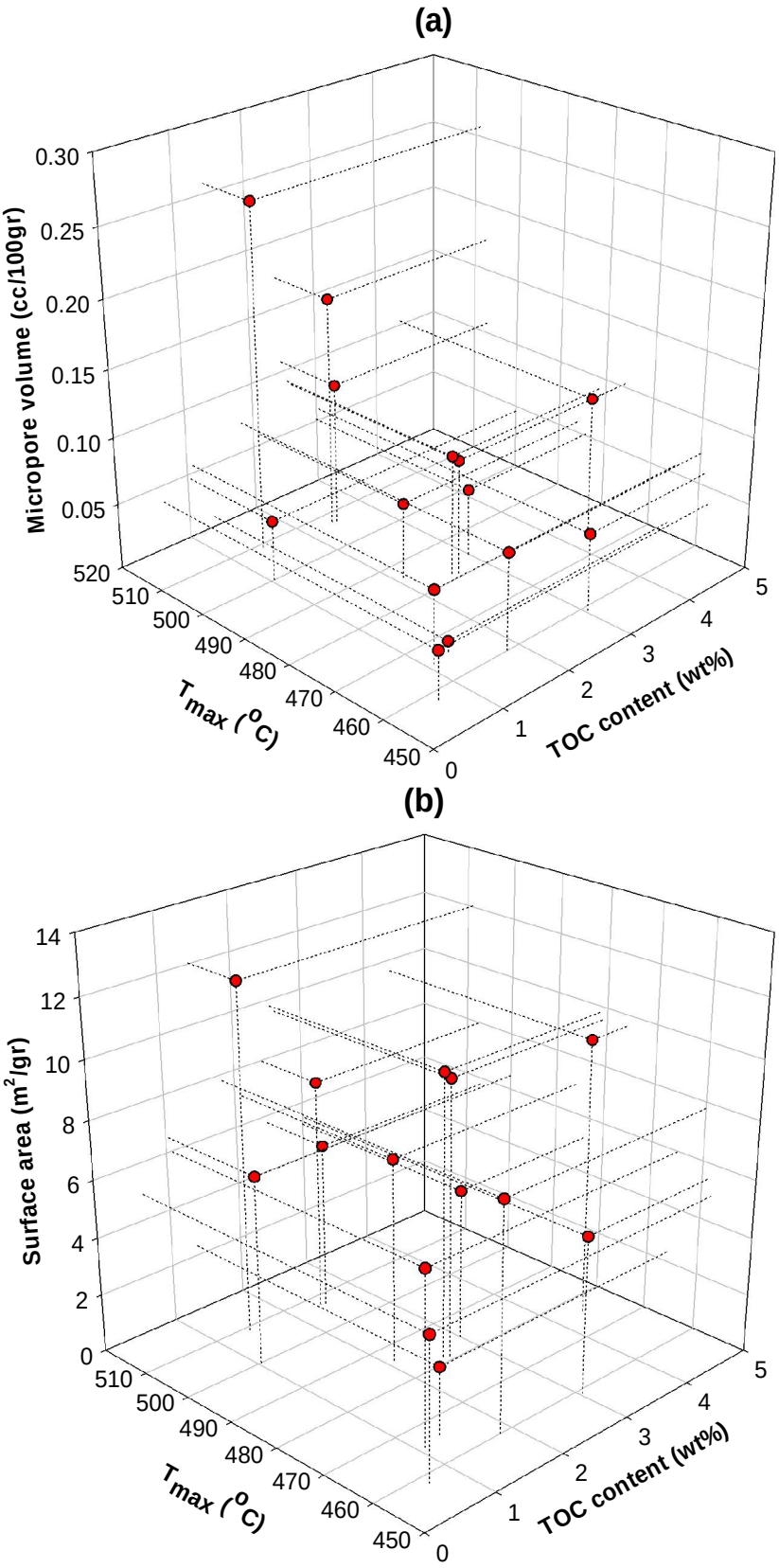

Fig. 3.10: 3D scatter plot showing the relationship between (a) micropore volume and (b) surface area with geochemical parameters.

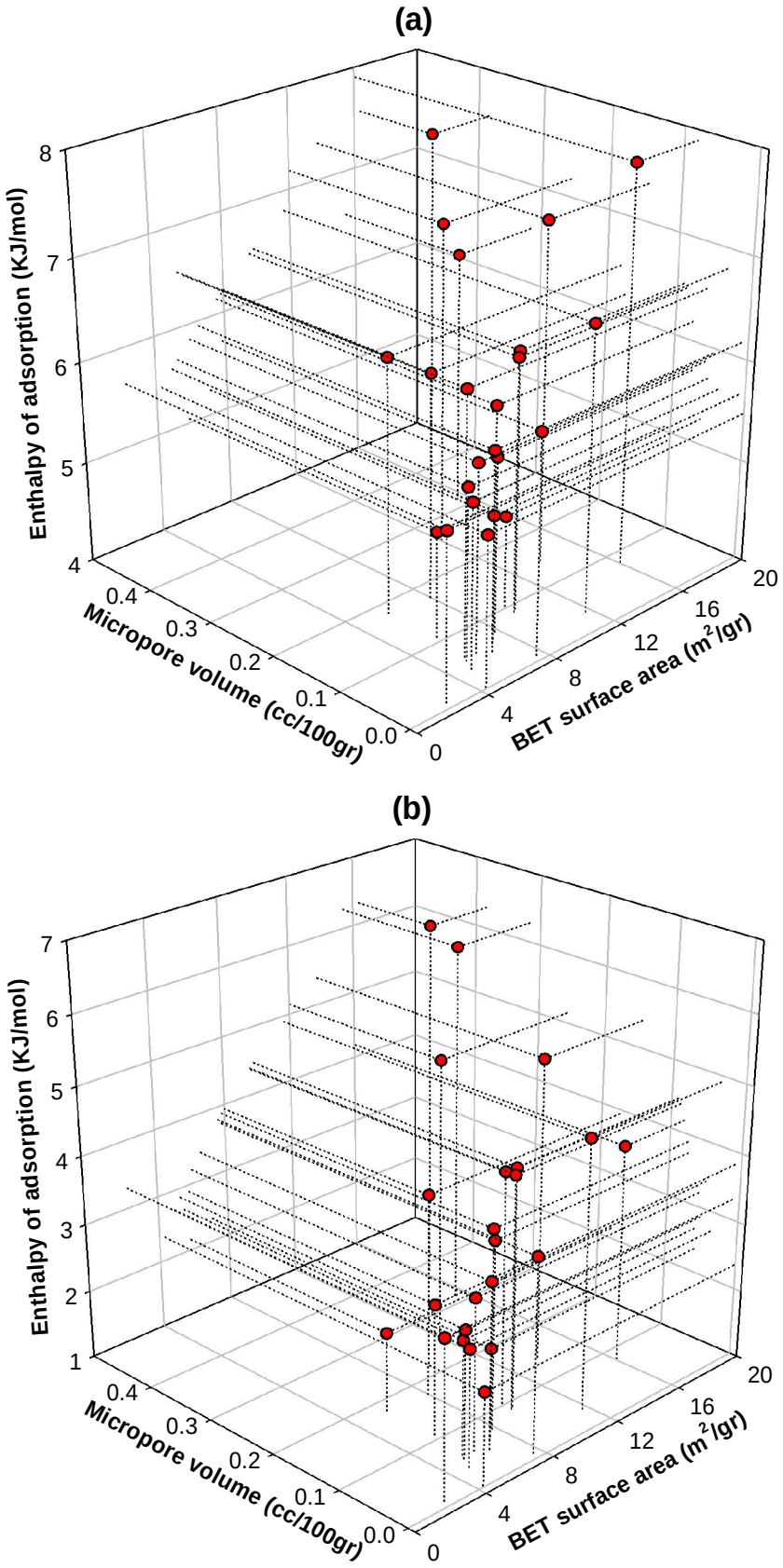

Fig. 3.11: 3D scatter plot showing the relationship between pore structure parameters with enthalpy of adsorption at (a) T=23^{o}C and (b) T=30^{o}C (The negative sign of enthalpy has been ignored in the plot display).

As well as analysing the obtained results shows that in the laboratory conditions, the adsorbed gas capacity of the analysed samples decreases significantly with increasing temperature from 23^{o}C to 30^{o}C (Table 3.5 and Table 3.6). Considering the recorded geothermal gradient for the Perth and Canning Basins which ranges from 2 to 5.5^{o}C/100 m (Ghori, 2008); approximately the average reservoir temperature for the analysed samples should be more than 100^{o}C. Therefore at this reservoir temperature the adsorbed gas capacity of the analysed samples is quite low. As a result, adsorption alone cannot be sufficient source of gas production for the studied gas shales from the Perth and Canning Basins and the role of free gas becomes more significant for these shales.

3.4.2 Effective parameters on the adsorption affinity

Due to the importance of adsorption affinity and enthalpy of adsorption on the gas desorption rate, a potential gas shale layer should have an optimised enthalpy of adsorption, a value which is not so high or low, as well as other parameters mentioned in the literature like specific surface area. Enthalpy of adsorption depends on the adsorbate (methane) and the pore structure properties of the adsorbent (shale sample). Analysing the relationships between enthalpy of adsorption and pore structure parameters showed that as it was expected they are related with each other, increasing the surface area and micropore volume will be resulted in increasing the adsorption capacity and enthalpy of adsorption (Fig. 3.11). Based on the data set in this study finding a relationship between shale composition and geochemical parameters with enthalpy of adsorption is inconclusive and no conclusions can be drawn. It might be due to their least effect on the pore structure parameters (e.g. Fig. 3.10).

3.5 Conclusion

A high pressure methane adsorption and low pressure nitrogen adsorption were used with together for determination of gas storage capacity of the potential gas shales from Western Australia. The following conclusions can be reached:

a) The pore space characteristics of the gas shale layers are the most important controlling parameters on the adsorbed gas capacity. Effect of other parameters like quantity and maturity of organic matter or shale composition depends on how much these parameters can affect on the pore space characteristics. For example for the studied shale samples due to the low amounts of TOC content (2 wt% in average) the effect of geochemical parameters is not significant on the adsorption capacity.

b) The obtained results showed that the parameters which are effective on the enthalpy of adsorption are the pore space characteristics; micropore volume and surface area. However finding a relationship between shale composition and geochemical parameters with enthalpy of adsorption is difficult. More investigations are required at more temperatures to determine the effective parameters on the enthalpy of methane adsorption on the shale layers.
c) The adsorption capacity of the studied shales decreases significantly with increasing temperature, proposing that at the high reservoir temperature the amount of adsorbed gas is not enough for gas production from these shales. Therefore at the reservoir condition the gas content of these shales are mostly controlled by the free gas.
d) Classifying the low pressure and high pressure adsorption results based on the studied geological formations showed that the Goldwyer Formation has the higher potential for gas storage and the Carynginia Formation from the Perth Basin has the least capacity for storing the gas (Table 3.4 and Table 3.7). However the enthalpy of adsorption for the Canning samples is higher than the Perth samples showing their lower affinity for desorbing the gas compared to the Perth samples and consequently the lower rate of gas desorption/production.

It is worth mentioning that for successful exploitation of gas from the studied gas shales it is required to upscale these measured values from nano-scale to macro-scale (core scale) and finally mega-scale (reservoir scale). However considering the high heterogeneity of the gas shales locating these properties from pore scale to reservoir scale is complex. As well as further research will be required on more shale samples with different physical properties to determine effect of shale composition and geochemical parameters on the gas storage capacity of the potential gas shales from Western Australia.

3.6 References

Allen, N., Aplin, A., Thomas, M., 2009. Introduction to shale gas storage. Internal presentation. University of Calgary.

Barret, E.P., Joyner, L.G., Halenda, P.P., 1951. The determination of pore volume and area distribution in porous substances: Computations from nitrogen isotherms. Journal of American Chemical Society 73, 373-380.

Brunauer, S., Deming, L.S., Deming, W.S., Teller, E., 1940. On a Theory of the van der Waals Adsorption of Gases. Journal of the American Chemical Society 62, 1723-1732.

Brunauer, S., Emmett, P.H., Teller, E., 1938. Adsorption of gases in multimolecular layers. Journal of the American Chemical Society 60, 309-319.

Busch, A., Gensterblum, Y., Krooss, B.M., Siemons, N., 2006. Investigation of high-pressure selective adsorption/desorption behaviour of CO_2 and CH_4 on coals: an experimental study. International Journal of Coal Geology 66, 53-68.

Bustin, R.M., Clarkson, C.R., 1998. Geological controls on coal-bed methane reservoir capacity and gas content. International Journal of Coal Geology 38, 3-26.

Cadman, S.J., Pain, L., Vuckovic, V., 1994. Australian Petroleum Accumulations Report 10: Perth Basin, WesternAustralia. Bureau of resource sciences, Canberra. 116 pp.

Cadman, S.J., Pain, L., Vuckovic, V., Le Poidevin, S.R., 1993. Australian petroleum accumulation report 9: Canning Basin, Western Australia. Bureau of resource sciences, Canberra. 88pp.

Chalmers, G.R., Bustin, R.M., Power, I.M., 2012. Characterization of gas shale pore systems by porosimetry, pycnometry, surface area, and field emission scanning electron microscopy/transmission electron microscopy image analyses: Examples from the Barnett, Woodford, Haynesville, Marcellus, and Doig units. AAPG Bulletin 96, 1099-1119.

Chareonsuppanimit, P., Mohammad, S.A., Robinson Jr, R.L., Gasem, K.A.M., 2012. High-pressure adsorption of gases on shales: Measurements and modeling. International Journal of Coal Geology 95, 34-46.

Clarkson, C.R., Jensen, J.L., Blasingame, T., 2011. Reservoir engineering for Unconventional Reservoirs: What do we have to consider? North American Unconventional Gas Conference and Exhibition, The Woodlands, Texas, USA. SPE145080.

Curtis, J.B., 2002. Fractured Shale-Gas Systems. AAPG Bulletin 86, 1921-1938.

Do, D.D., Do, H.D., 2003. Pore characterization of carbonaceous materials by DFT and GCMC simulations: A Review. Adsorption Science and Technology 21, 389-423.

Dollimore, D., Heal, G.R., 1964. An improved method for the calculation of pore-size distribution from adsorption data. Journal of Applied Chemistry 14, 109-114.

Foster, C.B., O'Brien, G.W., Watson, S.T., 1986. Hydrocarbon source potential of the Goldwyer Formation, BarbwireTerrace, Canning Basin, Western Australia. APEA Journal, vol. 26, p. 142–155.

Gan, H., Nandie, S.P., Walker Jr., P.L., 1972. Nature of porosity in American coals. Fuel 51, 272-277.

Ghori, K.A., 2008. Western Australia's geothermal resources. AAPG Annual Convention and Exhibition, San Antonio, Texas, USA.

Gregg, S.J., Sing, K.S.W., 1991. Adsorption, surface area and porosity. Academic Press: London, 303 pp.

Hao, F., Zou, H., Lu, Y., 2013. Mechanisms of shale gas storage: Implications for shale gas exploration in China. AAPG Bulletin 97, 1325-1346.

Jarvie, D.M., Hill, R.J., Ruble, T.E., Pollastro, R.M., 2007. Unconventional shale-gas systems: The Mississippian Barnett Shale of north-central Texas as one model for thermogenic shale-gas assessment. AAPG Bulletin 91, 475-499.

Javadpour, F., 2009. Nanopores and apparent permeability of gas flow in mudrocks (Shales and Siltstone). Journal of Canadian Petroleum Technology 48, 16-21.

Konstas, K., Osl, T., Yang, Y., Batten, M., Burke, N., Hill, A.J., Hill, M.R., 2012. Methane storage in metal organic frameworks. Journal of Materials Chemistry 22, 16698-16708.

Labani, M.M., Rezaee, R., Saeedi, A., Hinai, A.A., 2013. Evaluation of pore size spectrum of gas shale reservoirs using low pressure nitrogen adsorption, gas expansion and

mercury porosimetry: A case study from the Perth and Canning Basins, Western Australia. Journal of Petroleum Science and Engineering 112, 7-16.

Loucks, R.G., Reed, R.M., Ruppel, S.C., Jarvie, D.M., 2009. Morphology, Genesis, and Distribution of Nanometer-Scale Pores in Siliceous Mudstones of the Mississippian Barnett Shale. Journal of Sedimentary Research 79, 848-861.

Lu, X.C., Li, F.C., Watson, A.T., 1995. Adsorption measurements in Devonian shales. Fuel 74, 599-603.

Modica, C.J., Lapierre, S.G., 2012. Estimation of kerogen porosity in source rocks as a function of thermal transformation: Example from the Mowry Shale in the Powder River Basin of Wyoming. AAPG Bulletin 96, 87-108.

Montgomery, S.L., Jarvie, D.M., Bowker, K.A., Pollastro, R.M., 2005. Mississippian Barnett Shale, Fort Worth Basin, north central Texas: Gas shale play with multi-trillion cubic foot potential. AAPG Bulletin 89, 155-175.

Particulate Systems, 2011. HPVA series: High pressure volumetric analyser operator's manual. Particulate Systems. USA.

Passey, Q.R., Bohacs, K., Esch, W.L., Klimentidis, R., Sinha, S., 2010. From oil-prone source rock to gas-producing shale reservoir - geologic and petrophysical characterization of unconventional shale gas reservoirs. International Oil and Gas Conference and Exhibition in China, Beijing, China. SPE131350.

Pemg, D.Y., Robinson, D.B., 1976. A new two-constant equation of state. Industrial and Engineering Chemistry: Fundamentals 15:59-64.

Prinz, D.,Littke, R., 2005. Development of the micro- and ultramicroporous structure of coals with rank as deduced from the accessibility to water. Fuel 84, 1645-1652.

Ross, D.J.K., 2007. Investigation into the importance of geochemical and pore structure heterogeneities for shale gas reservoir evaluation. PhD Thesis, University of British Columbia, Canada, 373pp.

Ross, D.J.K., Bustin, R.M., 2007a. Impact of mass balance calculations on adsorption capacities in microporous shale gas reservoirs. Fuel 86, 2696-2706.

Ross, D.J.K.,Bustin, R.M., 2007b. Shale gas potential of the Lower Jurassic Gordondale Member, northeastern British Columbia, Canada. Bulletin of Canadian Petroleum Geology 55, 51-75.

Ross, D.J.K., Bustin, R.M., 2009. The importance of shale composition and pore structure upon gas storage potential of shale gas reservoirs. Marine and Petroleum Geology 26, 916-927.

Rouquerol, J., Avnir, D., Fairbridge, C.W., Everett, D.H., Haynes, J.H., Pernicone, N., Ramsay, J.D.F., Sing, K.S.W., Unger, K., 1994. Recommendations for the characterization of porous solids. International Union of Pure and Applied Chemistry. Pure and Applied Chemistry 68, 1739-1758.

Sharifzadeh, A., Mathew, N., 2011. Shale gas in Western Australia. Petroleum in Western Australia 4, 32-37.

Thomas, B.M., 1979. Geochemical analysis of hydrocarbon occurrences in northern Perth Basin, Australia. AAPG Bulletin 63, 1092-1107.

U.S. Energy Information Administration (EIA), 2011. World Shale Gas Resources: An Initial Assessment of 14 Regions Outside the United States. 365pp.

Weniger, P., Kalkreuth, W., Busch, A., Krooss, B.M., 2010. High-pressure methane and carbon dioxide sorption on coal and shale samples from the Paraná Basin, Brazil. International Journal of Coal Geology 84, 190-205.

Zhang, T., Ellis, G.S., Ruppel, S.C., Milliken, K., Yang, R., 2012. Effect of organic-matter type and thermal maturity on methane adsorption in shale-gas systems. Organic Geochemistry 47, 120-131.

CHAPTER 4

THERMAL MATURITY ESTIMATION OF GAS SHALE LAYERS FROM CONVENTIONAL WELL LOG DATA

CHAPTER 4

Thermal maturity estimation of gas shale layers from conventional well log data

4.1 Introduction

Thermal maturity and total organic carbon (TOC) are very important geochemical factors for evaluation of the gas shale reservoirs. There is a common hypothesis that gas shale layers with the higher potential for gas production (i.e. sweet spots) are located at the higher thermal maturity. Thermal maturity is an indicatorfor determining maximum temperature that a formation reached during different stages of hydrocarbon generation.

Thermal maturity could be estimated through different geochemical methods. The most common method is using the light reflectance from surface of macerals which are abundant in the rock (e.g. vitrinite, exinite or inertinite). Rock-Eval pyrolysis is another method for determining thermal maturity of the shale samples. In Rock-Eval method the pulverised rock sample is heated in controlled stages through a pyrolysis test. By recording the amount of hydrocarbons which are released from the organic matters during different stages and the temperature it is possible to determine quantity, maturity and type of organic matter (Boyer et al., 2006). The details of the Rock-Eval pyrolysis have been discussed in number of papers and books (Tissot and Welte, 1984;Peters, 1986); hence they are not explained in this paper. T_{max} is one of the output parameters of Rock-Eval pyrolysis which could be tied to thermal maturation of the organic material. In this study $T_{max}$and inertinite reflectance data were used as the thermal maturity indicators.

Considering the importance of the thermal maturity for evaluation of the gas shale reservoirs it would be necessary to develop a methodology for estimation of this parameter directly from well log data. Most of the researches that estimate geochemical parameters from well log data have been focused on the TOC evaluation (Schmoker, 1981; Schmoker and Hester,

1983; Fertl and Chilinger, 1988; Passey et al., 1990; Huang and Williamson, 1996; Rezaee et al., 2007; Kadkhodaie et al., 2009). Mallick and Raju (1995) used sonic log and seismic velocity for determining thermal maturity in the Upper Assam basin, India. They used this simple assumption that vitrinite reflectance typically increases with depth of burial as a function of time and temperature and it is accompanied by a decrease in log derived interval transit time. Zhao et al. (2007) defined a maturity index using three types of open hole logs: neutron porosity, deep resistivity, and density porosity. They showed that this index could be correlated well with initial gas/oil ratios (GOR) from well production data. However this maturity index is not based on the well log data alone, it needs to know about crushed sample porosity and whole core porosity of the shale samples. This study will focus on determination of thermal maturity directly from conventional log data to estimate this parameter in the absence of geochemical data.

4.2 Effect of thermal maturity on the gas shale layers

Thermal evolution of the shale layers, during diagenesis, catagenesis and metagenesis, changes many physical or chemical properties of the organic matter (Tissot and Welte, 1984), as well as the shale matrix. In this section these changes are discussed into two groups as physical changes and chemical ones.

4.2.1 Physical changes

As it could be seen in Fig. 4.1, petrophysical model of the gas shale is composed of three main components: organic matter, inorganic minerals and pore space. Total pore space in the gas shale is occupied by hydrocarbons; mobile and capillary bound water and clay bound water. The nature of the pore space in gas shale is one of the challenging discussions which has been studied in number of papers (Jarvie et al., 2007; Loucks et al., 2009, 2012; Modica and Lapierre, 2012). Based on the studies of Loucks et al. (2012) pore types in organic rich mudrocks include interparticle (interP), intraparticle (intraP) mineral pores, and intraP organic grain pores. SEM image studies of the Barnett shale showed that most nanopores are associated with grains of organic matter and the other types of pores are not so common (Loucks et al., 2009). IntraP organic matter pores evolve with the thermal transformation of organic matter and it has not any relation with the interP or intraP mineral pores.

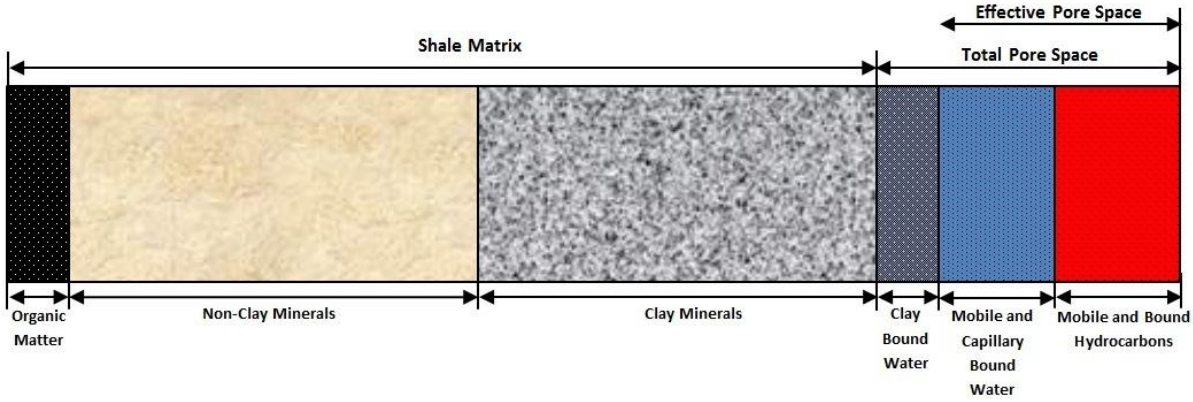

Fig. 4.1: Petrophysical model conceptually showing the volumetric constituents of shale matrix and pore space (modified after Passey et al.(2010)).

As well as the role of thermal maturity on the evolution of organic matter porosity, it has a prominent role in the water saturation of the shale layers. During progressive hydrocarbon generation with increasing thermal maturity the free water and capillary bound water could be replaced by generated hydrocarbons (usually gas at the higher levels of thermal maturity) and this process would result in decreasing total water saturation.

4.2.2 Chemical changes

Smectite to illite conversion is an important mineralogical reaction that occurs during burial diagenesis as well as in geothermal alteration. Mineralogical structure of smectite had a large capacity to retain interlayer water; therefore it is logical to expect that the transformation of smectite to illite results in the release of water molecules. Water release by smectite in a shale of relatively low permeability may cause overpressuring (Colten-Bradley, 1987).

By increasing thermal maturity the longer chains of carbon in the organic matter become shorter; and the heavier components of generated hydrocarbons convert to the lighter ones. The progressive increase in thermal maturity will result in generating the methane which has the simplest structure among the hydrocarbons and the lowest level of hydrogen content per mole.

4.3 Thermal maturity evaluation from log analysis

In this study seven wells (Fig. 4.2) were selected on the basis of availability of appropriate well logs and geochemical data for the analysis of Kockatea shale and Carynginia formation. Table 4.1 summarises the main geochemical information of these wells including kerogen type, average amount of TOC (wt %), average value of T_{max} (^{o}C) and the maturity state of the data points. Sample type refers to the type of the samples for geochemical analysis which are

in three types: ditch cuttings, side wall core (SWC) samples and conventional core (CC) samples. Among the studied wells only in well G the inertinite reflectance has been used as the thermal maturity indicator with the average maceral reflectance equal to 1.75% but for the other wells the T_{max} is the thermal maturity indicator. It is worth mentioning that the interested shale intervals in wells A, B and G are in the postmature state and have the higher potential for gas production.

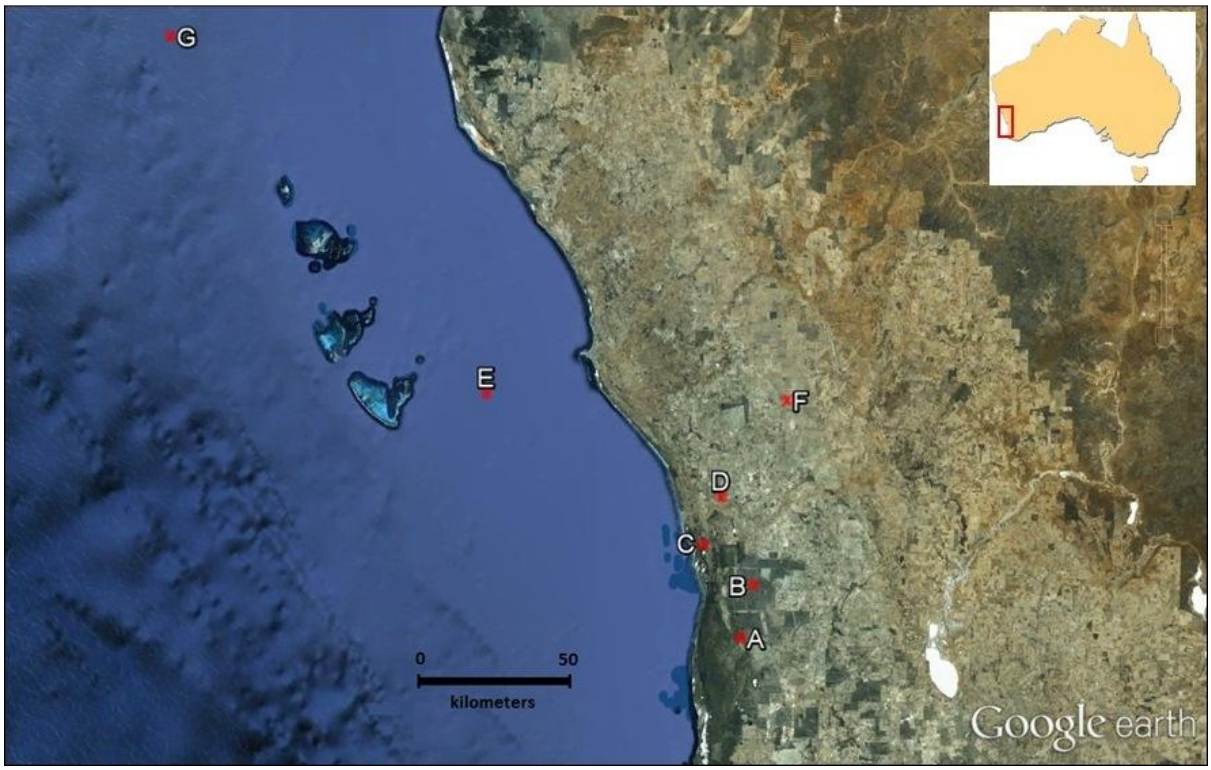

Fig. 4.2: Location of the studied wells in the Perth Basin, Western Australia (Photo courtesy of Google™ Earth, 2012).

Different well logging tools are sensitive to different physical properties of the rock intervals. Neutron porosity, density, sonic transit time and volumetric photoelectric adsorption were used for analysing the thermal maturity of the shale layers. In the following it is tried to correlate thermal maturity changes of the potential gas shale layers with the responses of mentioned well logs and find a reasonable explanation for the existing relationships between corresponding thermal maturity indicator and conventional well log data.

Table 4.1: Main geochemical information of the studied wells.

Well symbol	Number of data points	Sample type	Kerogen type	Average TOC (wt%)	Average T_{max} (^{o}C)	State of maturity
A	10	SWC&CC	Mix. II&III	1.45	461	Postmature
B	37	CC	III	2.42	493	Postmature
C	10	SWC	Mix. II&III	1.11	454.4	Mature
D	10	DC&SWC	Mix. II&III	0.65	438.4	Mature
E	11	SWC	Mix II&III	1.15	443	Mature
F	10	SWC	Mix. II&III	1.49	425.3	Mature
G*	10	SWC	---	---	---	Postmature

* Well G has only maceral reflectance data and it has not any Rock-Eval pyrolysis data.

4.3.1 Sonic transit time (DT)

There are many effective parameters on the sonic transit time. Wang (2001) classified these parameters into three groups; parameters which are related to environment, fluid and rock. Effect of thermal maturity on the sonic transit time for the gas shale reservoirs is complex. There is a simple hypothesis that thermal maturity increases with depth of burial. During burial sediments gradually compact due to the increasing weight of overlying layers and this phenomenon reduces interval sonic transit time. Considering the relations between depth of burial and thermal maturity and between depth of burial and sonic transit time, it is possible correlate sonic transit time with thermal maturity as well. This approach is only valid when there is not any structural complexity in the basin (no differential uplift or erosion) or variance in geothermal gradient (Modica and Lapierre, 2012). On the other hand changes in the gas shale matrix due to thermal maturity like porosity evolution in the organic matter or increasing the pore pressure due to the mineral transformation and hydrocarbon generation could increase the sonic transit time. Thus, sonic transit time can experience a decreasing trend by increasing thermal maturity (considering effect of burial depth) and at the same time number of thermal maturity effects can increase sonic transit time. Because of that the correlation coefficient between sonic transit time and thermal maturity indicator; either T_{max} or inertinite reflectance is not so high (Table 4.2). Due to the opposite effects of thermal maturity on the sonic log it is not possible to consider it as a reliable input for thermal maturity estimation.

Table 4.2: Results of cross plot analysis between thermal maturity indicator with depth, sonic transit time (DT), volumetric photoelectric absorption (U), density (RHOB) and neutron porosity (NPHI).The positive sign refers to the direct relationship and negative sign refers to the indirect relationship.

Well Name	Correlation Coefficient (R^2) with thermal maturity indicator				
	DT(μsec/ft)	U(barns/cm^3)	RHOB(gr/cm^3)	NPHI(pu)	Depth(m)
A	0.29 (-)	0.36 (-)	0.15 (-)	0.31 (-)	0.11 (+)
B	0.41 (-)	0.76 (-)	0.38 (-)	0.47 (-)	0.56 (+)
C	0.05 (-)	0.65 (-)	0.67 (-)	0.54 (-)	0.40 (+)
D	0.32 (-)	0.47 (-)	0.33 (-)	0.17 (-)	0.11 (+)
E	0	---	0.30 (-)	0.45 (-)	0.81 (+)
F	0.12 (-)	---	0.22 (-)	0.22 (-)	0.11 (+)
G	0	0.62 (-)	0.63 (-)	0.39 (-)	0.87 (+)

4.3.2 Volumetric photoelectric absorption (U)

The photoelectric factor (or PEF) log is a continuous record of the photoelectric absorption index or P_e of a formation. The photoelectric absorption index is used principally for lithological determination, either alone or, especially when cross-multiplied with the corresponding density log to produce the value U, which is called volumetric photoelectric absorption index. This log is mainly controlled by mean atomic number of the formation. However, porosity and fluid saturations of rock also are effective on the measured PEF values but their effect on PEF log response is not so prominent therefore it is used for lithological determination (Rider, 1996).

In this study variations of volumetric photoelectric absorption index (U) were observed on the Kockatea Shale and Carynginia Formation. Fig. 4.3is a ternary plot showing the mineralogical distribution of 22 samples from the studied formations. Although the compositional variations are too high but generally the studied shale intervals have high amount of quartz and clay content and less amount of carbonate. Thus, in these shales it would be possible to highlight effect of porosity and fluid saturation changes on the volumetric photoelectric absorption. It should be noted that the lithological variation still has an important role in PEF log response.

Table 4.3 shows the photoelectric factors and related values of shale and common fluids in the gas shale reservoirs. Considering that the water saturation of the shale layers decreases by increasing thermal maturity and meanwhile gas saturation increases and based on the reported values for salt water, oil and methane the indirect relationship between thermal maturity and volumetric photoelectric absorption could be justified. As well as evolution of porosity in the

organic matter due to the thermal maturity could be other reason for decreasing the U values with increasing thermal maturity. The mentioned parameters caused the relatively high indirect relationships between thermal maturity indicator and volumetric photoelectric absorption in the studied wells (Table 4.2).

Table 4.3: Photoelectric factors and related values of the shale and common fluids in the shale gas reservoirs (modified after Rider, 1996).

Name	Formula	P_e(barns/electron)	U(barns/cm^3)	Atomic Number (Z)
Gas	CH_4	0.095	$0.119\times\rho_{gas}$	5.21
Oil	$(CH_2)_n$	0.119	0.12	5.53
Salt water	120,000 ppm NaCl	0.807	0.850	0.807
Pure water	H_2O	0.358	0.398	0.358
Shale(avg.)	---	3.42	9.046	14.07

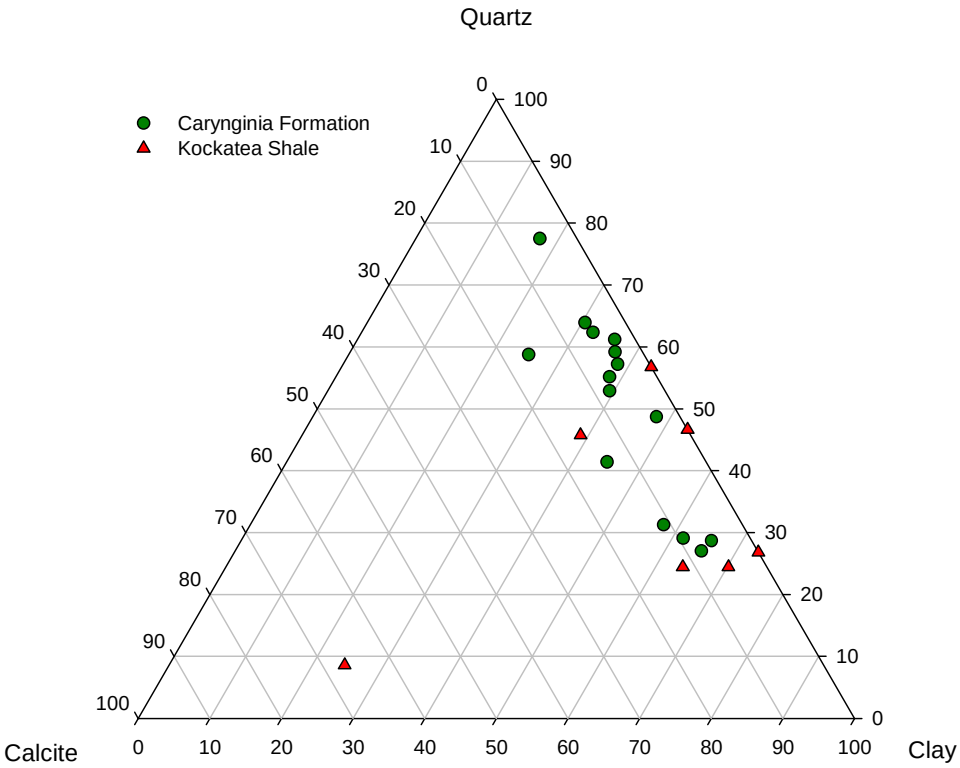

Fig. 4.3: Mineralogical distribution of quartz, calcite, and clay in the Kockatea shale and the Carynginia Formation.

4.3.3 Neutron porosity (NPHI)

The neutron porosity log measures the hydrogen index (HI) which is the ratio of hydrogen atoms per unit volume in the material, to that of the pure water at surface conditions. Therefore the parameters which can affect on the HI of the formation are effective on this log as well. As it could be seen in Table 4.2, there is an indirect relationship between thermal

maturity indicator and NPHI log response in the Kockatea Shale and Carynginia Formation. Regarding the reported neutron porosity values in Table 4.4; the following explanations can justify this relationship:

- HI of generated hydrocarbon in the final stages of thermal maturity (i.e. gas window) is lower than the oil window products for example HI of dry gas is less than wet gas,
- HI of transformed illite is lower than smectite, and,
- Reducing the water saturationat high thermal maturity levels caused the lower HI value for the shale layers.

Table 4.4: Neutron log values of some common fluids and clay minerals in the shale gas reservoirs (modified after Rider, 1996).

Name	Hydrogen Index	Neutron Porosity(pu)
Methane	0.49	20 to 50
Salt water	0.9	60+
Pure water	1	100
Smectite	0.17	44
Kaolinite	0.37	37
Chlorite	0.32	52
Illite	0.09	30

It should be noted that the free water and capillary bound water could be detected as porosity by both the density and the neutron tools but interlayer water will only be detected by the neutron log (Rider, 1996). Therefore the effect of smectite transformation could not follow on the density log. When there is a good relationship between thermal maturity and depth like well B, the NPHI log response could also be correlated to depth. Fig. 4.4 shows the histograms of NPHI log responses for Kockatea Shale in well B for two equal thickness intervals which are located in different depths. According to the Fig. 4.5 while the distribution of the NPHI values has a mean value about 31 pu for the shallow interval; the mean value gradually shifted to the lower values for the deep interval.

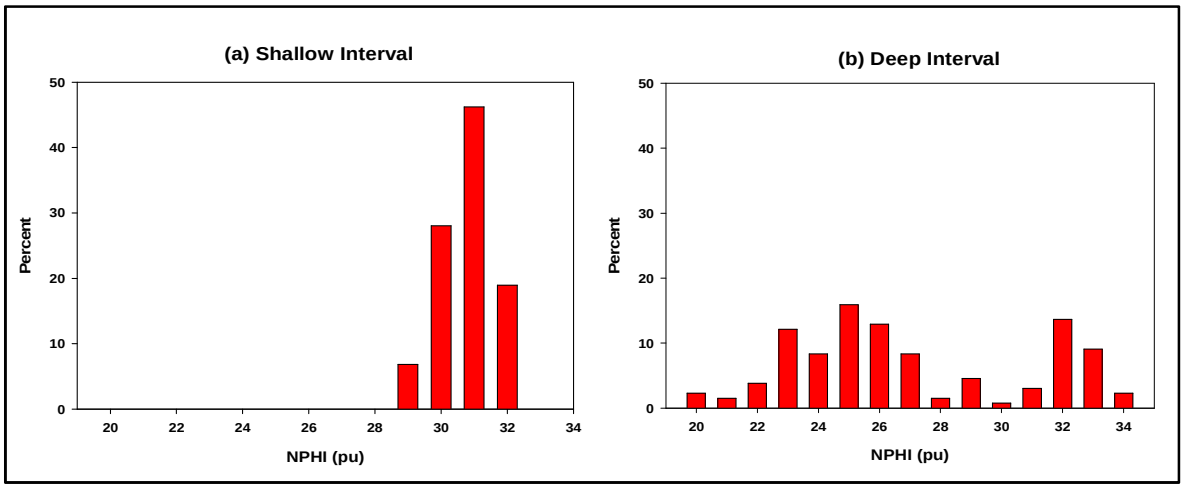

Fig. 4.4: Histograms showing neutron porosity distribution in the Kockatea Shale of well B for (a) a shallow and (b) a deep interval.

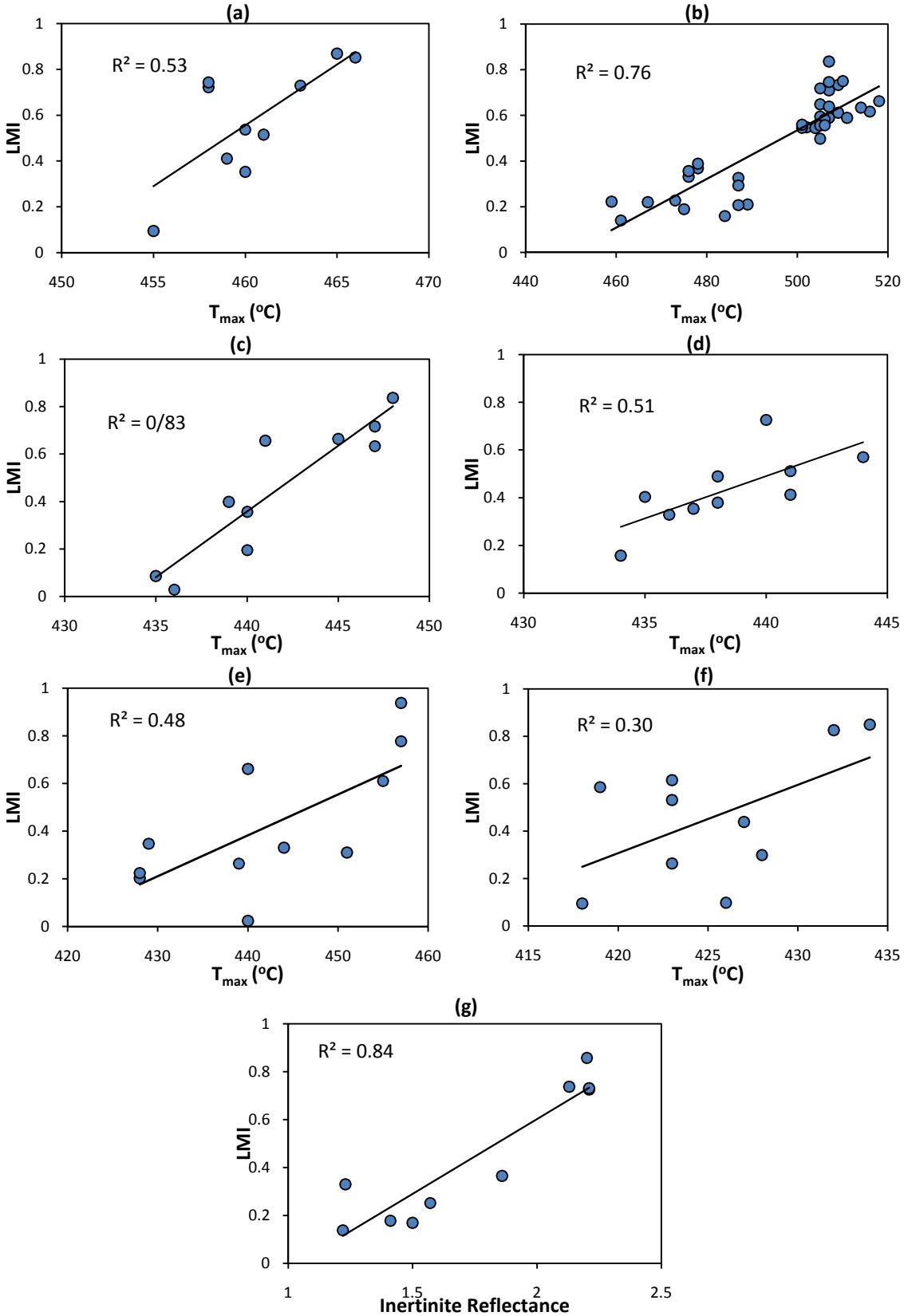

Fig. 4.5: Crossplots showing the relationships between log derived maturity index (LMI) and thermal maturity indicator in the studied wells A (a), B (b), C (c), D (d), E (e), F (f), G (G).

4.3.4 Density (RHOB)

Density log measures the bulk density of a formation. Usually it is used for porosity determination but also it can be a useful lithology indicator. Like the other studied well logs, with increasing thermal maturity there is a decreasing trend for density log responses in the gas shale intervals (Table 4.2). To some extent the effective parameters for decreasing the density log are similar to the parameters which are effective on the volumetric photoelectric absorption index. Briefly these parameters are:

- Changing in the type of saturated fluid from water to gas,
- Changing the heavier components of hydrocarbon to the lighter ones and finally methane,
- Generating porosity in the organic matter due to the thermal transformation, and,
- Increasing pore pressure due to mineral transformation and hydrocarbon generation.

All of these transformations would be resulted in decreasing density of the formation with increasing thermal maturity.

4.3.5 Log derived maturity index (LMI)

According to the finding relationships between conventional well log data and thermal maturity, neutron porosity, density and volumetric photoelectric absorption are considered as the proper inputs for thermal maturity estimation.Maturity index derived from the mentioned well logs using the following procedure:

1. Regarding the indirect relationship between well logs and thermal maturity; the neutron porosity, density and volumetric photoelectric absorption normalized using the Eqn. 4.1 to Eqn. 4.3 to remove the effects of different ranges:

$$MI_{NPHI}=\frac{NPHI-NPHI_{max.}}{NPHI_{min.}-NPHI_{max.}} \qquad \text{(Eqn. 4.1)}$$

$$MI_{RHOB}=\frac{RHOB-RHOB_{max.}}{RHOB_{min.}-RHOB_{max.}} \qquad \text{(Eqn. 4.2)}$$

$$MI_{U}=\frac{U-U_{max.}}{U_{min.}-U_{max.}} \qquad \text{(Eqn. 4.3)}$$

2. Taking simple average and determining the log derived maturity index (LMI):

$$LMI=\frac{MI_{NPHI}+MI_{RHOB}+MI_{U}}{3} \qquad \text{(Eqn. 4.4)}$$

LMI is a number which varies between 0 and 1, obviously when it becomes larger it shows the higher value for thermal maturity of the corresponding shale layer. Fig. 4.5 shows the cross plot analysis between thermal maturity and LMI in the studied wells. As it is clear, LMI performs better for thermal maturity estimation than individual well logs because it has a higher correlation coefficient with thermal maturity indicators in the studied wells.

4.4 Discussions

Developing a methodology for estimation of gas shale parameters using the well log data is a challenging task. In this study thermal maturity considered as an independent variable and responses of the well log data as the dependent variables and only effects of thermal maturity were studied. There are many parameters in the gas shale matrix which can have opposite effects on the well log responses. For example traces of pyrite minerals which are abundant in the marine organic matters could increase the density and volumetric photoelectric absorption and hide the decreasing effect of the thermal maturity. Authors recognized that conventional logs can only be used for thermal maturity estimation if the lithology of the formation does not vary significantly over the interval of interest otherwise changing in lithology can affect on well log responses especially on the responses of volumetric photoelectric adsorption.

Type of the geochemical samples could also be effective on the proposed relationships. There is a resolution difference between samples which are coming from different sources and well log data and sometimes it causes mismatching between data. For example in well D seven samples are from cuttings with a sampling rate equal to 10 meters for the studied interval. Considering the log resolution which is 0.15 m, the resolution difference between log data and geochemical data is very high and this results in relatively lower correlation coefficients in this well.

4.5 Conclusions

In this chapter, a log derived maturity index (LMI) was introduced for thermal maturity estimation of gas shale layers. LMI uses three conventional logs including neutron porosity, bulk density and volumetric photoelectric adsorption for modelling thermal maturity changes along the formation. These well logs have meaningful relationships with $T_{max}$and inertinite reflectance therefore they could be tied to the thermal maturity of the gas shale intervals. It is worth mentioning that this methodology works better in compare to the individual well logs which are used for developing LMI. As well as its performance increases with increasing thermal maturity of the shale intervals. As it is shown in Fig. 4.6, with increasing average

T_{max} of the studied intervals the obtained r-squared between T_{max} and LMI increases which means that LMI could recognize the patterns in the T_{max}data better.

The LMI could be combined with the ΔlogR method (Passey et al., 1990) for determining TOC content of the rock. In the ΔlogR method it is required to know about the level of organic metamorphism (LOM) for TOC estimation using well logs and this is a deficiency for this methodology because it is not based on the log data completely. Furthermore, this methodology is a kind of in-situ measurement and it does not require any sample for thermal maturity determination. Thus it is fast and cost effective compared to conventional geochemical methods.

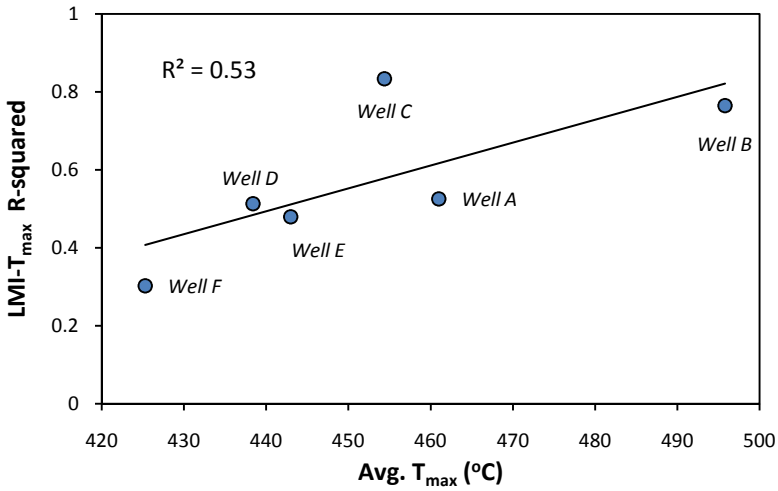

Fig. 4.6: Crossplot showing the relationship between averageT_{max} of the studied wells and obtained r-squared between LMI&T_{max}.

4.6 References

Boyer, C., Kieschnick, J., Suarez-Rivera, R., Lewis, R., Waters, G. Producing Gas from its Source. Oilfield Review, Autumn 2006, 36-49.

Cadman, S.J., Pain, L., Vuckovic, V., 1994. Australian Petroleum Accumulations Report 10: Perth Basin, WesternAustralia. 116 pp.

Coulten-Bradley, V.A., 1987. Role of pressure in smectite dehydration - effect on geopressure and smectite to illite transformation. AAPG Bulletin 71, 1414-1427.

Fertl, W.H., Chilingar, G.V., 1988. Total organic carbon content determined from well logs, SPE Annual Technical Conference and Exhibition, New Orleans, Louisiana, 5-8 October. SPE 15612.

Huang, Z., Williamson, M.A., 1996. Artificial neural network modelling as an aid to source rock characterization. Marine and Petroleum Geology 13, 227-290.

KadkhodaieIlkhchi, A., Rahimpour-Bonab, H., Rezaee, M.R., 2009.A committee machine with intelligent systems for estimation of total organic carbon content from petrophysical data: An example from Kangan and Dalan reservoirs in South Pars Gas Field, Iran, Computers & Geosciences 35, 459-474.

Mallik, R.K., Raju, S.V., 1995. Thermal maturity evaluation by sonic log and seismic velocity analysis in parts of Upper Assam basin, India. Organic Geochemistry 23, 871-879.

Jarvie, D.M., Hill, R.J., Ruble, T.E., Pollastro, R.M., 2007. Unconventional shale-gas systems: The Mississippian Barnett Shale of north-central Texas as one model for thermogenic shale-gas assessment. AAPG Bulletin 91, 475-499.

Loucks, R. G., Reed, R.M., Ruppel, S.C., Hammes., U., 2012. Spectrum of pore types and networks in mudrocks and a descriptive classification for matrix-related mudrock pores. AAPG Bulletin 96, 1071-1098.

Loucks, R.G., Reed, R.M., Ruppel, S.C., Jarvie, D.M., 2009. Morphology, genesis, and distribution of nanometer-scale pores in siliceous mudstones of the Mississippian Barnett Shale. Journal of Sedimentary Research 79, 848-861.

Modica, C.J., Lapierre, S.G., 2012. Estimation of kerogen porosity in source rocks as a function of thermal transformation: example from the Mowry Shale in the Powder River Basin of Wyoming. AAPG Bulletin 96, 87-108.

Passey, Q.R., Bohacs, K., Esch, W.L., Klimentidis, R., Sinha, S., 2010. From Oil-Prone Source Rock to Gas-Producing Shale Reservoir - Geologic and Petrophysical Characterization of Unconventional Shale Gas Reservoirs, International Oil and Gas Conference and Exhibition in China, Beijing, China. SPE131350

Passey, Q.R., Creaney, S., Kulla, J.B., Moretti, F.J. and Stroud, J.D., 1990. A practical model for organic richness from porosity and resistivity logs. AAPG Bulletin 74, 1777-1794.

Peters, K.E., 1986. Guidelines for evaluating petroleum source rock using programmed pyrolysis. AAPG Bulletin 70, 318-329.

Rezaee, M.R., Slatt, R.M., and Sigal, R.F., 2007. Shale gas rock properties prediction using artificial neural network technique and multi regression analysis, an example from a North American shale gas reservoir. Australian Society of Exploration Geophysicists, November 2007, Perth.

Rider, M.H., 1996.The geological interpretation of well logs. Whittles Publishing, 280 pp.

Schmoker, J.W., 1981. Determination of organic matter content of Appalachian Devonian shales from gamma ray logs. AAPG Bulletin 65, 1285-1298.

Schmoker, J.W., Hester, T.C., 1983, Organic carbon in Bakken Formation.United States portion of Williston basin. AAPG Bulletin 67, 2165-2174.

Tissot, B.P., Welte, D.H., 1984. Petroleum formation and occurrence. New York, Springer-Verlag. 699pp.

Thomas, B. M., 1979. Geochemical analysis of hydrocarbon occurrences in northern Perth Basin, Australia. AAPG Bulletin 63,1092-1107.

Wang, Z., 2001. Fundamentals of seismic rock physics. Geophysics 66, 398-412.

Zhao, H., Givens, N.B. and Curtis, B., 2007. Thermal maturity of the Barnett Shale determined from well-log analysis. AAPG Bulletin 91, 535-549.

CHAPTER 5

THE IMPORTANCE OF GEOCHEMICAL PARAMETERS AND SHALE COMPOSITION ON ROCK MECHANICAL PROPERTIES OF GAS SHALE RESERVOIRS

CHAPTER 5

The importance of geochemical parameters and shale composition on rock mechanical properties of gas shale reservoirs

5.1 Introduction

In recent years development and production of unconventional gas resources especially gas shale reservoirs have been increased. Production from gas shale layers requires stimulation by hydraulic fracturing due to the extremely low permeability of the shale layers. Under this situation, it is required to know about the rock mechanical properties as well as petrophysical and geochemical parameters of the gas shale layers to precisely locate the shale layers that are brittle. Brittle shales are more likely to be naturally fractured and will also be more likely to respond well to hydraulic fracturing treatments.

Characterizing organic rich gas shales can be challenging as these rocks change quite significantly (Passey et al., 2010). Due to the complex nature of the organic rich rocks, there are limited studies on physical properties affecting seismic and well log responses of this kind of rock (Vernik and Nur, 1992; Vernik and Liu, 1997, Vernik and Milovac, 2011). The studies have been done by Vernik and his colleagues on a variety of shales with different clay mineralogy, and porosity at a wide range of effective pressure showed that the main controls on elastic properties of organic shales are kerogen content, porosity, clay content, and effective stress. As well as they proposed that a high level of velocity anisotropy is due to the lenticular distribution of organic material and clay minerals parallel to the bedding plane. Hornby et al. (1994) concluded a similar result regarding the distribution effect of clay platelets on the mechanical anisotropy of the shales. Clay content and organic richness are not the only parameters which can affect on the mechanical anisotropy of the shale layers. Vanorio et al. (2008) proposed that there is a relationship between maturity of the shales, expressed in terms of vitrinite reflectance and the anisotropic parameters. Based on their findings although anisotropy in organic-rich shales is a complex function of maturity but generally anisotropy increases from the immature to the early mature stages.

Although there are some studies which attempt to extract the Young's modulus and Poisson's ratio of gas shale reservoirs from sequence stratigraphy (Slatt and Abousleiman, 2011), from rock physics modelling (Zhu et al., 2011) or from true triaxial testing (Josh et al., 2012); however still there is a shortage of analysis for determining effective parameters on the brittleness of the gas shale reservoirs. Theoretically gas shale brittleness, a measure of the rock ability to fracture, is a complex function of lithology, mineral composition, amount of total organic carbon (TOC), effective stress, reservoir temperature, diagenesis, thermal maturity, porosity and type of fluid (Wang and Gale, 2009). There is a common notion that gas shale sweet spots are at higher level of organic content and thermal maturity. On the other hand a gas shale sweet spot should have a high potential for hydraulic fracturing. As it is known organic matter quantity and maturity are the nano scale properties and the potential of the rock for hydraulic fracturing is a macro or mega scale issue (i.e. core scale or reservoir scale). The main objective of this study is to find out whether these two concepts; highly mature and rich in organic matter with high potential for hydraulic fracturing, can be gathered together or not or in other word is it possible to locate the nano and micro issues into macro scale in the gas shale evaluation. To meet this objective firstly it would be tried to determine Young's modulus and Poisson's ratio of the potential gas shale layers from dipole sonic well log data and then investigating the importance of shale composition and geochemical parameters on these two parameters which are effective on brittleness of the shale layers. For some of the studied wells the shear wave velocity was not available therefore as a first step for determination of rock mechanical properties, it was required to estimate shear velocity directly from compressional velocity.

5.2 Case Study

The data set of this study is coming from 5 different wells (Fig. 5.1) that have been drilled in the onshore part of the Perth Basin. These wells are selected based on the availability of geochemical and compositional data along the mentioned gas shale formations. Table 5.1 shows the summary of compositional and geochemical data for the studied wells. However, due to the limitation of gas shale data points with geochemical data, Passey et al. (1990) data base was used for the validation of TOC effect on rock mechanical properties as well.

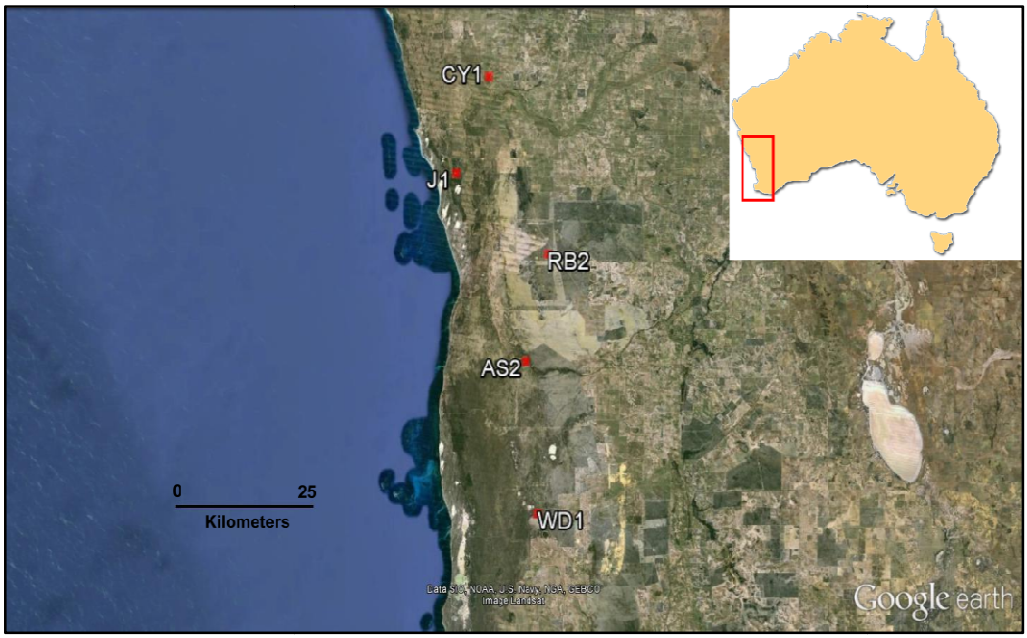

Fig. 5.1: Location of studied wells in the Perth Basin, Western Australia (Photo courtesy of Google earth ™, 2013).

Table 5.1: Average of compositional and geochemical data for the studied wells.

Well	TOC (wt%)	T_{max} (°C)	Quartz content (wt%)	Clay content (wt%)	Carbonate content (wt%)
AS2	1.453	461	43.06	35.73	6.13
CY1	0.57	437	---	---	---
RB2	2.76	473.7	47.13	32.6	2.43
J1	1.24	449.3	---	---	---
WD1	---	---	27.82	10.51	1.13

5.3 Rock mechanical properties from sonic log data

The starting point for doing hydraulic fracturing is determination of rock mechanical properties. There are two different ways for determining rock mechanical properties: static and dynamic. The static method measures these properties using analysis of the rock in the laboratory and the dynamic method calculates the mechanical behaviour of the rock using sonic wave propagation through the rock. The sonic velocities depend on elastic moduli and material density, however intrinsically these parameters are related to environment properties like stress history and temperature, fluid properties like viscosity and density and rock properties like clay content and porosity (Wang, 2001). Due to the mechanical nature of sonic wave, it is used for determination of rock mechanical properties. According to the log-derived mechanical properties shale reservoirs are characterized as brittle versus ductile. The

brittle intervals are considered to be easily fractured while ductile shales behave more plastically and more difficult to fracture.

Rickman et al. (2008) and Grieser and Bray (2007) defined the degree of brittleness (Brittleness Index) based on the combination of Young's modulus (E) and Poisson's ratio (ν). Young's modulus is the ratio of stress to strain and Poisson's ratio is defined as the negative ratio of transverse (or lateral) to axial (or longitudinal) strain. These two components are combined to reflect the rock strength to fail under stress (Poisson's ratio) and maintain a fracture (Young's modulus) once the rock fractures (Rickman et al., 2008). Therefore brittle shales should have low Poisson's ratio and high Young's modulus (Fig. 5.2). It is worth mentioning that the range of variation of these two parameters depends on every single parameter which can affect on the compressional and shear wave velocities and it is hard to determine a specific range for them to consider the gas shale as brittle shale. For example as it could be seen in Fig. 5.2which has been extracted for the Barnett Shale, the brittle shales are shales with Young's modulus higher than around 4 GPa and Poisson's ratio less than 0.25, however this figure doesn't show a global range for the brittleness of the shale layers which could be used for other case studies as well.

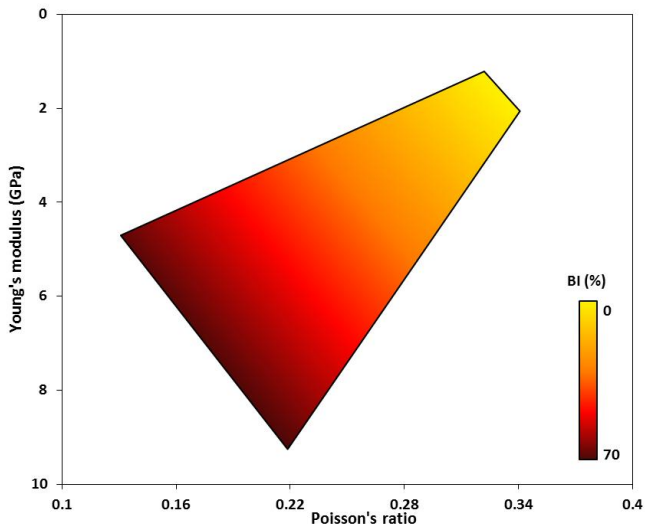

Fig. 5.2: Cross plot of Young's modulus vs. Poisson's ratio showing change in brittleness index for the Barnett Shale (Modified after Wang and Gale, 2009).

The dynamic Young's modulus and Poisson's ratio are calculated from compressional and shear wave velocities using the below formulas:

$$E=\frac{\rho V_s^2(3V_p^2-4V_s^2)}{V_p^2-V_s^2} \qquad \text{(Eqn. 5.1)}$$

$$\nu=\frac{V_p^2-2V_s^2}{2(V_p^2-V_s^2)} \qquad \text{(Eqn. 5.2)}$$

where ρ is the bulk density and V_p and V_s are compressional and shear wave velocities respectively. As it is clear this analysis requires full wave-form sonic data, including shear velocity and compressional velocity. In some cases the shear velocity data is not available in the data set; therefore the shear wave velocity should be estimated from the compressional velocity data.

There are some relationships between V_p and V_s for the siltstones and shale layers in the literature. Table 5.2 shows the popular equations developed for the mudrocks. However as it is clear none of these equations is specifically for the gas shale layers.

Table 5.3 compares the performance of available models for estimation of the shear wave velocity in the studied formations: Kockatea Shale and Carynginia Formation. As it could be seen in different wells and formations the performance of models are different. Gas shales are clearly different from the brine saturated inorganic shales used to establish the known shale empirical equations; therefore these models could not estimate the shear velocity in the gas shale layers accurately. Due to this issue it was preferred to extract the relationship between V_p and V_s for the gas shale data points that have shear velocity data (wells AS2, RB2 and WD1) and using this linear regression for the other wells that V_s data is not available (i.e. wells J1 and CY1). The data points from wells AS2 and WD1 were selected to be used for extracting the relationship between shear and compressional wave velocity. Fig. 5.3 shows the crossplot analysis between shear and compressional wave velocity for the gas shale data points in wells AS2 and WD1. The extracted formula for the selected data points is:

$$V_s=0.71\times V_p-0.62 \qquad \text{(Eqn. 5.3)}$$

Table 5.2: Empirical known equations for shear wave velocity versus compressional wave velocity in the shale layers.

Equation	Reference	Remarks
$V_s=0.862 \times V_p-1.172$	Castagna et al. (1985)	Mudrocks
$V_s=0.769 \times V_p-0.867$	Castagna et al. (1993)	Mudrocks
$V_s=0.70 \times V_p-0.67$	Vernik et al. (2002)	Organic rich shales

Table 5.3: Comparisons of RMSE for estimating shear wave velocity in the gas shale layers from three different wells (AS2, RB2 and WD1) in the Perth Basin.

Equation	RMSE (km/s)	Rank
AS2-Carynginia		
$V_s=0.862 \times V_p-1.172$	0.098	2
$V_s=0.769 \times V_p-0.867$	0.059	1
$V_s=0.70 \times V_p-0.67$	0.105	3
RB2-Kockatea		
$V_s=0.862 \times V_p-1.172$	0.091	2
$V_s=0.769 \times V_p-0.867$	0.057	1
$V_s=0.70 \times V_p-0.67$	0.092	3
RB2-Carynginia		
$V_s=0.862 \times V_p-1.172$	0.171	3
$V_s=0.769 \times V_p-0.867$	0.113	2
$V_s=0.70 \times V_p-0.67$	0.103	1
WD1-Carynginia		
$V_s=0.862 \times V_p-1.172$	0.064	1
$V_s=0.769 \times V_p-0.867$	0.071	2
$V_s=0.70 \times V_p-0.67$	0.143	3

The regression coefficients for the extracted formula are closer to the Vernik model parameters. As it is mentioned before in Table 5.2; Vernik equation has been extracted for the organic rich shale layers which are similar to the matrix of the gas shales. The data points from well RB2 were used for blind testing of the extracted model. Fig. 5.4 shows the comparison between real and predicted V_s using the obtained model (Eqn. 5.3) for the Kockatea Shale and Carynginia Formation versus depth in well RB2. As it could be seen in this figure there is a good agreement between measured and predicted V_s in well RB2 which confirms the validity of extracted formula.

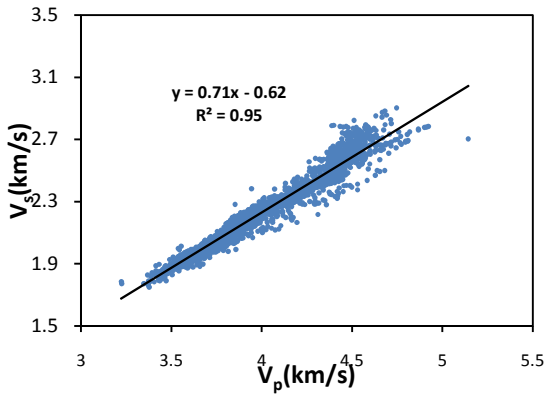

Fig. 5.3:Crossplot analysis between V_p and V_s for the gas shale data points from wells AS2 and WD1.

5.4 Effective parameters on brittleness of the gas shale layers

As it is mentioned before the brittleness of the gas shale layers could be correlated to the combination of Young's modulus and Poisson's ratio. Based on the Eqns. 5.1 and 5.2 the dynamic Young's modulus and Poisson's ratio are functions of formation bulk density, shear velocity and compressional velocity, therefore each effective parameter on these three could be effective on the brittleness of the gas shale layers as well. Among all the possible parameters effective on sonic velocity and bulk density, effect of geochemical parameters (including quantity and maturity of organic matter) and shale composition on the rock potential for hydraulic fracturing have been studied in the followings.

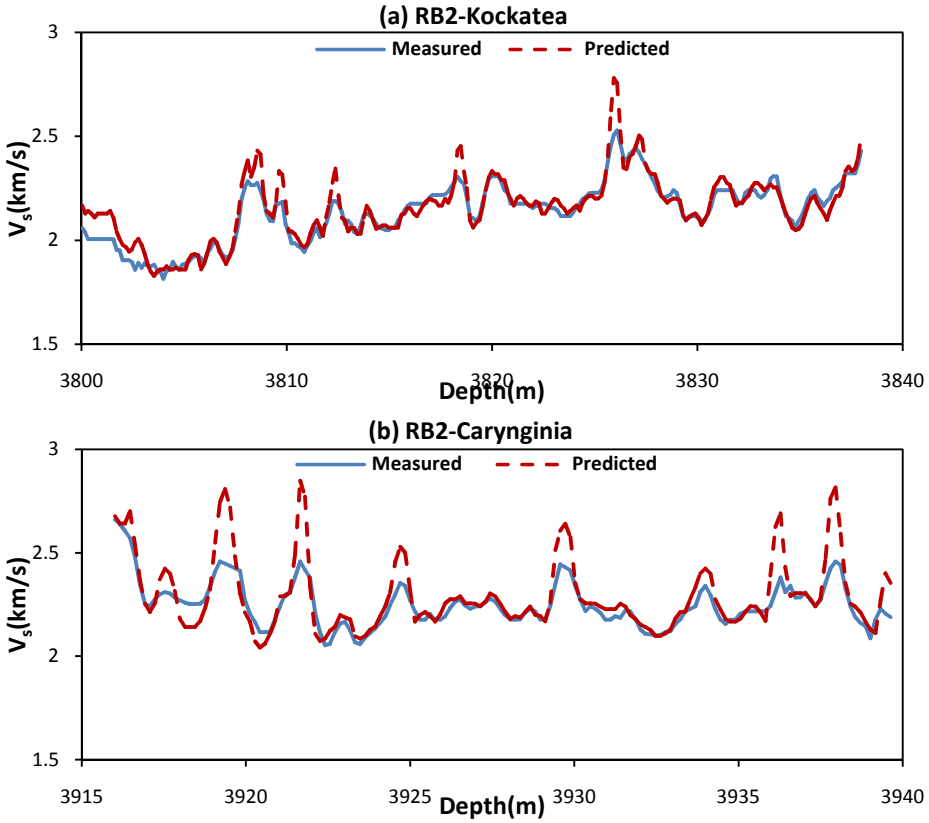

Fig. 5.4: A comparison between measured and predicted V_s using obtained formula versus depth in (a) RB2-Kockatea and (b) RB2-Carynginia.

5.4.1 Geochemical parameters

Organic matter quantity and organic matter maturity are the determining parameters on gas production from gas shale layers. Organic materials have a low density (typically 1.1 to 1.4 gr/cc) (Passey et al., 2010) therefore increasing the organic material would be resulted in decreasing formation bulk density and decreasing sonic velocity (either compressional or shear wave velocity). The final result of this decreasing trend in density and sonic velocity is decreasing the obtained dynamic Young's modulus. As well as considering Eqn. 5.2, this decreasing in sonic velocity could be effective on Poisson's ratio extracted from full wave form sonic data. Fig. 5.5 shows the cross plot of Young's modulus vs. Poisson's ratio for the gas shale data points from the Perth Basin. Although it is hard to find a trend but generally can conclude that by increasing TOC content of the rock samples the Young's modulus decreases while the Poisson's ratio increases. Classifying the data points based on the geological formation shows the effect of TOC on rock mechanical properties better especially in the Carynginia Formation (Fig. 5.6).

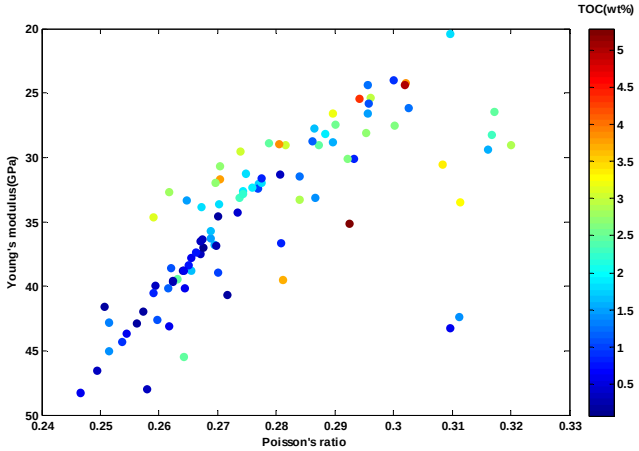

Fig. 5.5:Crossplot of Young's modulus vs. Poisson's ratio (color coded with TOC) for gas shale data points from the Perth Basin.

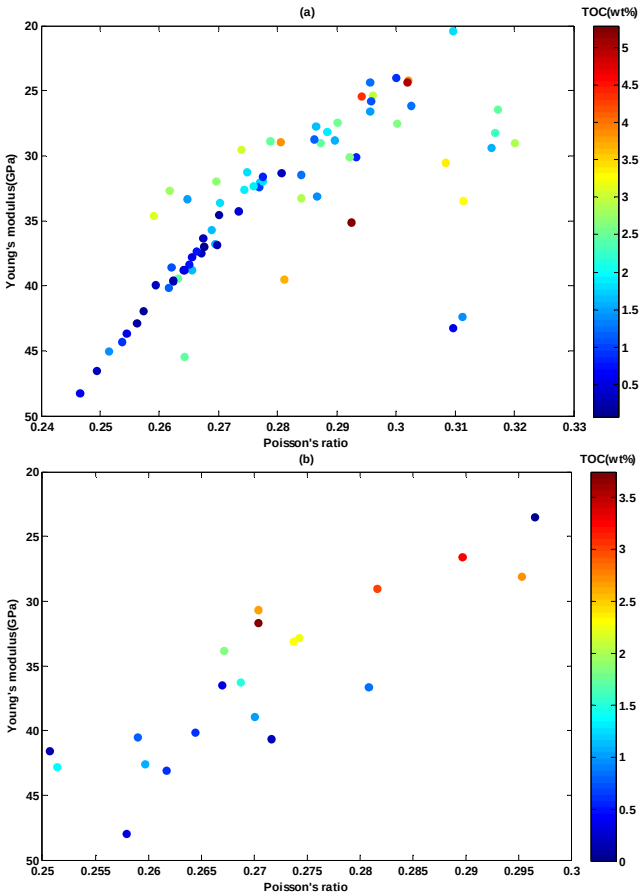

Fig. 5.6: Crossplot of Young's modulus vs. Poisson's ratio (color coded with TOC) for (a) Kockatea Shale and (b) Carynginia Formation.

Effect of TOC on the rock mechanical properties is not limited to the gas shale layers. Analysing effect of TOC content on the Young's modulus and Poisson's ratio of the organic rich source rocks which are similar to the gas shale layers shows the same trend (Fig. 5.7). It is obvious that effect of TOC content for the organic rich source rocks (data points from the Passey data base) is more typical compared to the gas shale data points, due to the higher

TOC content of organic rich source rocks.Fig. 5.8 shows the cross plot of Young's modulus versus TOC and Poisson's ratio versus TOC for the studied gas shale data points. As it could be seen in this figure while qualitatively effect of TOC is obvious on decreasing Young's modulus and increasing Poisson's ratio the quantitative effect of TOC on rock mechanical properties are not so much prominent; the correlation coefficient is not high. Comparing the gas shale data points with the data points published by Passey et al. (1990) shows that for the organic rich shales effect of TOC is more highlighted compared to the studied gas shale data points which are relatively lower in the TOC content (Fig. 5.9).

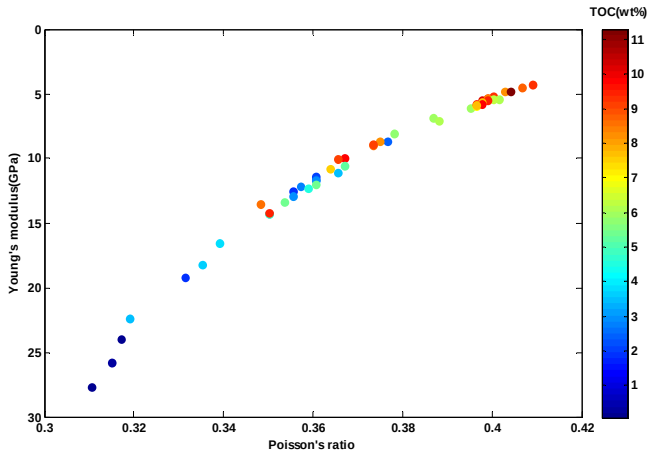

Fig. 5.7: Crossplot of Young's modulus vs. Poisson's ratio (color coded with TOC) for organic rich source rocks, data points sourced from the Passey et al. (1990).

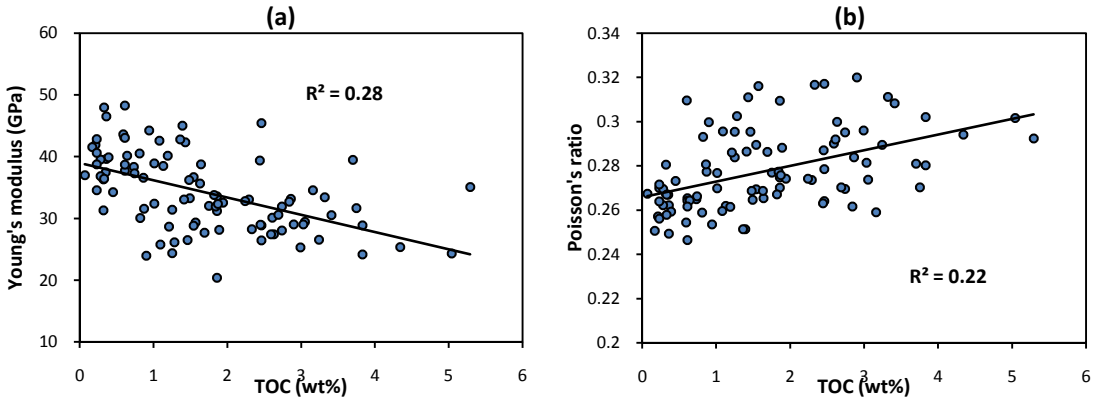

Fig. 5.8: Crossplot analysis between TOC content and (a) Young's modulus and (b) Poisson's ratio for the studied gas shale data points.

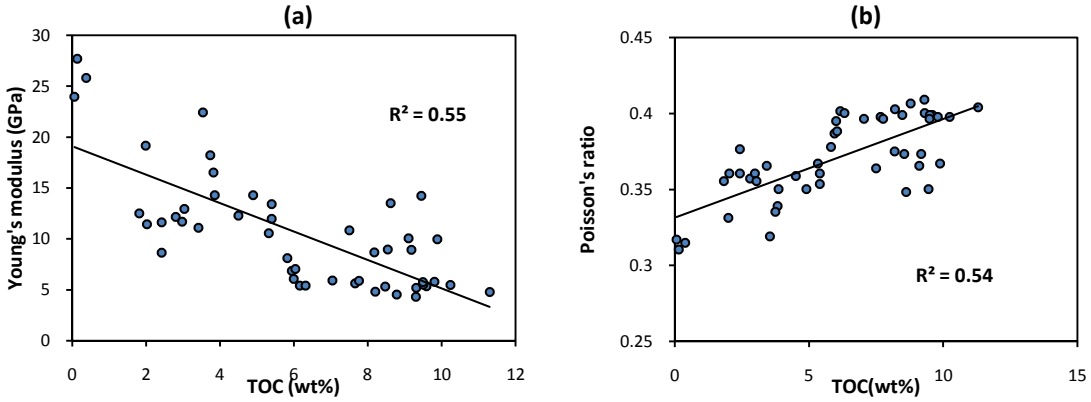

Fig. 5.9: Crossplot analysis between TOC content and (a) Young's modulus and (b) Poisson's ratio for the data points coming from the Passey et al. (1990).

Thermal maturity is another geochemical parameter which could be effective on brittleness of the gas shale layers. However due to the complex nature of the gas shale matrix analysing its effect is not known completely. Thermal maturity can cause these changes in the gas shale matrix (Labani and Rezaee, 2012):

- Porosity evolution in the organic grains due to the thermal transformation of organic matter to hydrocarbon,
- Decreasing total water saturation; at the higher levels of thermal maturity free water and capillary bound water could be replaced by generated hydrocarbon,
- Smectite to illite conversion may cause over-pressuring by water release in a shale which has relativelylow permeability.

All of these changes can be translated to decreasing sonic velocity and bulk density which would be resulted in decreasing dynamic Young's modulus in theory, similar to the TOC effect. Fig. 5.10 shows the crossplot of Young's modulus vs. Poisson's ratio for all the gas shale data points color coded with T_{max} data. T_{max} is one of the output parameters of Rock-Eval pyrolysis which could be tied to thermal maturity of the rock sample. As it could be seen in this figure, similar to the TOC content finding a typical trend for the thermal maturity effect is difficult. Fig. 5.11shows the effect of thermal maturity in the Kockatea Shale and Carynginia Formation separately. Although after classifying data points based on the geological formations there is a better trend for the Kockatea Shale (decreasing rock strength with increasing thermal maturity), still there is not a meaningful one for the Carynginia Formation.

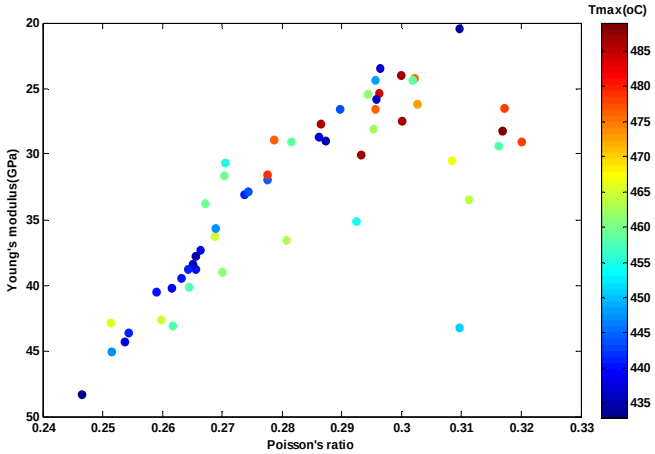

Fig. 5.10: Crossplot of Young's modulus vs. Poisson's ratio (color coded with T_{max}) for gas shale data points from the Perth Basin.

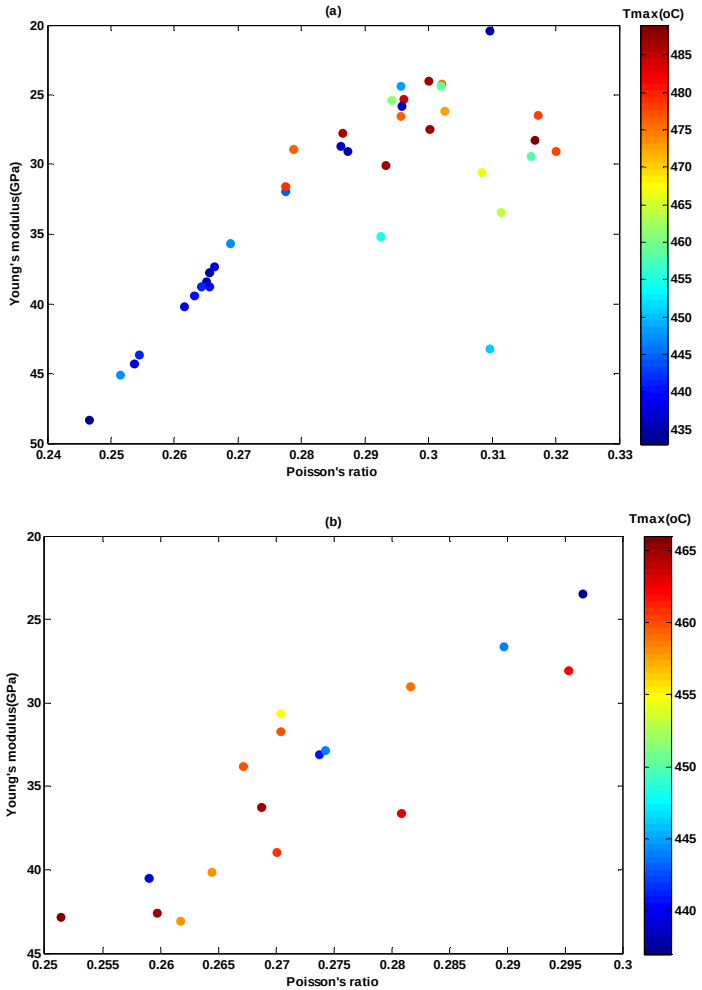

Fig. 5.11: Crossplot of Young's modulus vs. Poisson's ratio (color coded with T_{max}) for (a) Kockatea Shale and (b) Carynginia Formation.

5.4.2 Shale composition

Evaluation of gas shale reservoirs is complex due to the variable mineral composition. Clay, quartz and carbonate minerals are the main minerals forming the shale layers. Mineralogy plays a significant role in controlling shale properties. The non-clay minerals especially quartz content is an important parameter on rock mechanical properties of the shale layers. Table 5.4 shows the sonic velocity and bulk density of the common components in the matrix of gas shale reservoirs. However as it could be seen in this table the sonic velocity of clay minerals (i.e. smectite and kaolinite) are not well constrained due to their fine grained nature. Considering the reported sonic velocity for common components in the shale matrix, limestone and dolomite have the higher average velocity and clay minerals are lowest in sonic velocity compared to carbonate groups and quartz. Therefore it is obvious that the rock strength of carbonates is higher than quartz and the clay minerals are at the end. Calcareous intervals usually consider as fracture energy attenuators in the identification of preferred zones for hydraulic fracturing because of high compressive strength and Young's modulus (Jacobi et al., 2008). Jarvie et al. (2007) and Rickman et al. (2008) review the mineralogical relationships of the brittleness measured within the Barnett shales. The results of their studies confirm the mentioned point related to brittleness of different lithologies. Based on these studies the most brittle section of the Barnett shale has abundant quartz, the least brittle has abundant clay, and those with abundant carbonates are moderate.

Table 5.4: Some typical matrix velocities of common components in the gas shale matrix (from Picket(1963), Rider (1996)and Mondol et al.(2008)).

Name	**V_p(m/s)**	**V_s(m/s)**	**Density(gr/cc)**
Quartz	5530	3455	2.65
Limestone	5800-7000	3050-3684	2.71
Dolomite	6770-7925	3760-4402	2.87
Smectite	2780-6072	1300-3134	2-2.7
Kaolinite	1440-6230	930-3550	2.60
Methane	550	---	0.00717
Brine (120Kppm)	1740-1840	---	1.0686

Fig. 5.12 and Fig. 5.13 show the crossplot of Young's modulus vs. Poisson's ratio for the gas shale data points with compositional data from three different wells in the Perth Basin. It is worth mentioning that while the compositional data in wells AS2 and RB2 are coming from

the XRD analysis, the compositional data from well WD1 are coming from the mineralogical logging tool. As it was expected increasing the quartz content would be resulted in increasing Young's modulus and decreasing Poisson's ratio which can be interpreted as enhancing the brittleness of the rock (Fig. 5.12a and Fig. 5.13a). On the other hand the clay content weakens the rock strength by decreasing Young's modulus (Fig. 5.12b and Fig. 5.13b).

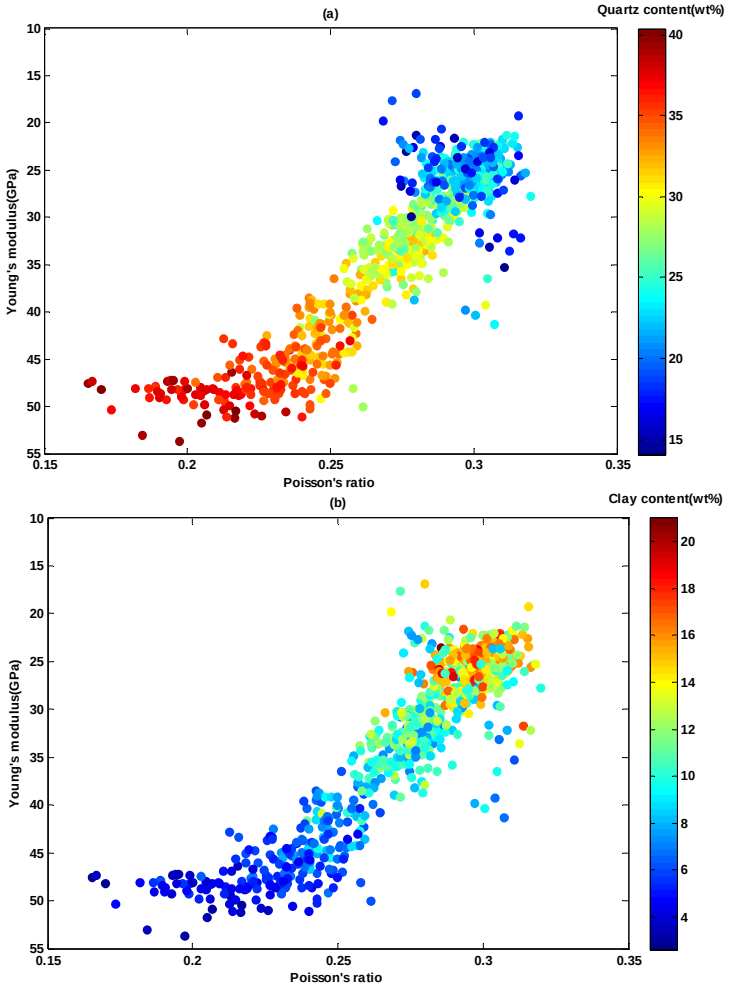

Fig. 5.12: Crossplot of Young's modulus vs. Poisson's ratio color coded with (a) quartz and (b) clay content for well WD1 from the Perth Basin.

5.5 Discussion and conclusions

Every parameter which can affect on the matrix of the gas shale layers could be effective on its rock mechanical properties as well. Considering the results of this study it could be concluded that both of the organic matter quantity (TOC) and maturity can decrease the potential of the rock for hydraulic fracturing. On the other hand quartz content can increase the brittleness and clay content will decrease the rock strength and brittleness of the shale layers. However effect of these parameters depends on their effect on the shale matrix. For example while the maximum amount of TOC content for the studied gas shale data points is

around 5 wt%, the quartz content of these rocks could be reached up to 65 wt% (Fig. 5.13a). Therefore it is clear that a component with the higher weight contribution (i.e. mineralogical composition) will have the higher effect on sonic velocity and bulk density of the rock and as a result on the extracted dynamic Young's modulus and Poisson's ratio. As well as, geochemical parameters and compositional parameters of the shale matrix are not dependent to each other. For example while TOC content of the rock increases; the quartz content of the shale layers can change in such a way to increase sonic velocity. Therefore the authors recognized that it would be possible to extract a qualitative trend between geochemical parameters and rock mechanical properties of the shale layers if it is assumed that the other parameters related to shale matrix does not change significantly which cannot occur in most of the cases. This justification becomes more important for analysing thermal maturity effect on the rock mechanical properties of the shale layers. Effect of thermal maturity on the matrix properties is dependent to the organic matter content itself thus obviously with a low TOC content thermal maturity has not a prominent effect on the shale matrix and consequently on the brittleness as well.

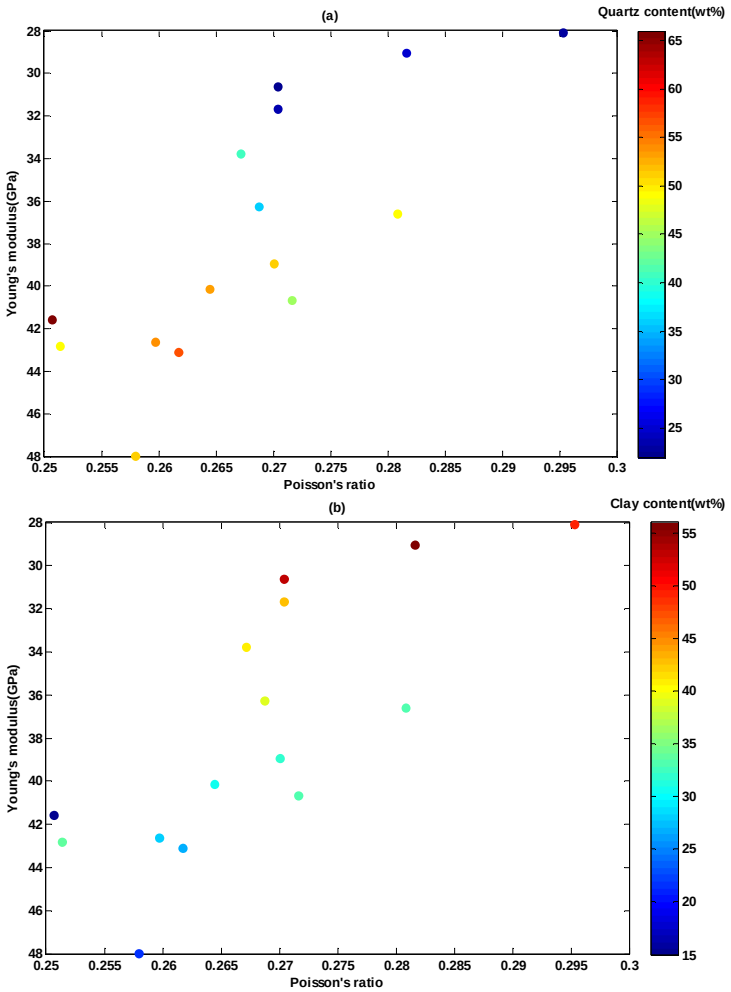

Fig. 5.13: Crossplot of Young's modulus vs. Poisson's ratio color coded with (a) quartz and (b) clay content for well AS2 and RB2 from the Perth Basin.

Therefore it could be concluded that while geochemical parameters are so important on some parameters like pore structure properties and adsorbed gas content of the gas shale samples (Ross and Bustin, 2009) they cannot consider as an important factor for determining the potential intervals for hydraulic fracturing. It can be assumed that geochemical parameters can affect on nano-scale properties like pore structure parameters while they cannot be effective on the rock mechanical properties which investigated at the higher scale thus locating the nano and micro issues into the macro scale for gas shale evaluation is under debate and still needs more investigation. The results of this study could be helpful as screening criteria for selecting the proper interval for doing hydraulic fracturing in gas shale layers.

5.6 References

Cadman, S.J., Pain, L., Vuckovic, V., 1994. Australian Petroleum Accumulations Report 10: Perth Basin, WesternAustralia. 116 pp.

Castagna, J.P., Batzle, M.L., Eastwood, R.L., 1985. Relationships between compressional-wave and shear-wave velocities in clastic silicate rocks. Geophysics 50, 571-581.

Castagna, J.P., Batzle, M.L., Kan, T.K., 1993. Rock-physics: The link between rock properties and AVO response, in Castagna, J.P., and Backus, M.M., Eds., Offset-dependent reflectivity – Theory and practice of AVO analysis. Investigation in Geophysics 8, 135-171.

Grieser, W.V., Bray, J.M., 2007. Identification of production potential in unconventional reservoirs. Production and Operations Symposium, Oklahoma City, Oklahoma, USA. SPE106623.

Hornby, B.E., Schwartz, L.M., Hudson, J.A., 1994. Anisotropic effective-medium modeling of the elastic properties of shales. Geophysics 59, 1570-1583.

Jacobi, D.J., Gladkikh, M., LeCompte, B., Hursan, G., Mendez, F., Longo, J., Ong, S., Bratovich, M., Patton, G.L., Shoemaker, P., 2008. Integrated petrophysical evaluation of shale gas reservoirs. CIPC/SPE Gas Technology Symposium - Joint Conference, Calgary, Alberta, Canada. SPE114925.

Jarvie, D.M., Hill, R.J., Ruble, T.E., Pollastro, R.M., 2007. Unconventional shale-gas systems: The Mississippian Barnett Shale of north-central Texas as one model for thermogenic shale-gas assessment. AAPG Bulletin 91, 475-499.

Josh, M., Esteban, L., Piane, C.D., Sarout, J., Dewhurst, D.N., Clennell, M.B., 2012. Laboratory characterisation of shale properties. Journal of Petroleum Science and Engineering 88-89, 107-124.

Labani, M.M., Rezaee, R., 2012. Thermal maturity estimation of gas shale layers from conventional well log data: A case study from Kockatea Shale and Carynginia Formation of Perth Basin, Australia. SPE Asia Pacific Oil and Gas Conference and Exhibition, Perth, Australia. SPE158864.

Mondol, N.H., Jahren, J., Bjørlykke, K., Brevik, I., 2008. Elastic properties of clay minerals. The Leading Edge 27, 758-770.

Passey, Q.R., Bohacs, K., Esch, W.L., Klimentidis, R., Sinha, S., 2010. From oil-prone source rock to gas-producing shale reservoir - geologic and petrophysical characterization of unconventional shale gas reservoirs. International Oil and Gas Conference and Exhibition in China, Beijing, China. SPE131350.

Passey, Q.R., Creaney, S., Kulla, J.B., Moretti, F.J., Stroud, J.D., 1990. A practical model for organic richness from porosity and resistivity logs. AAPG Bulletin 74, 1777-1794.

Pickett, G.R., 1963. Acoustic character logs and their applications in formation evaluation. Journal of Petroleum Technology 15, 650-667.

Rickman, R., Mullen, M.J., Petre, J.E., Grieser, W.V., Kundert, D., 2008. A practical use of shale petrophysics for stimulation design optimization: all shale plays are not clones of the Barnett Shale. SPE Annual Technical Conference and Exhibition, Denver, Colorado, USA. SPE115258.

Rider, M.H., 1996.The geological interpretation of well logs. Whittles Publishing, 280 pp.

Ross, D.J.K., Bustin, R.M., 2009. The importance of shale composition and pore structure upon gas storage potential of shale gas reservoirs. Marine and Petroleum Geology 26, 916-927.

Slatt, R.M., Abousleiman, 2011. Merging sequence stratigraphy and geomechanics for unconventional gas shales. The Leading Edge 30, 274-282.

Thomas, B. M., 1979. Geochemical analysis of hydrocarbon occurrences in northern Perth Basin, Australia. AAPG Bulletin 63,1092-1107.

Vanorio, T., Mukerji, T., Mavko, G., 2008. Emerging methodologies to characterize the rock physics properties of organic-rich shales. The Leading Edge 27, 780-787.

Vernik, L., Fisher, D., Bahret, S., 2002, Estimation of net-to-gross from P and S impedance in deepwaterturbidites. The Leading Edge 21, 380-387.

Vernik, L., Liu, X., 1997. Velocity anisotropy in shales: A petrophyscial study. Geophysics 62, 521-532.

Vernik, L., Milovac, J., 2011. Rock physics of organic shales. Leading Edge 30, 318-323.

Vernik, L., Nur, A., 1992. Ultrasonic velocity and anisotropy of hydrocarbon source rocks. Geophysics 57, 727-735.

Wang, Z., 2001. Fundamentals of seismic rock physics. Geophysics 66, 398-412.

Wang, F.P., Gale, J.F., 2009. Screening criteria for shale-gas systems. Gulf Coast Association of Geological Societies Transactions 59, 779-793.

Zhu, Y., Liu, E., Martinez, A., Payne, M.A., Harris, C.E., 2011. Understanding geophysical responses of shale-gas plays. The Leading Edge 30, 332-338.

CHAPTER 6

CONCLUSIONS

CHAPTER 6

Conclusions

6.1 Introduction: challenges and limitations

Determining the petrophysical parameters of the shale layers are required for locating the sweet spot of gas shales. However there are some challenges in petrophysical evaluation of gas shales:

- There are not any standard analytical protocols or procedures for gas shales characterization therefore there would be a degree of uncertainty comparing the gas shale properties measured in different laboratories,
- Considering the high degree of heterogeneity in the gas shales up scaling the measured values from nano-scale to macro-scale (core scale) and finally mega scale (reservoir scale) is complex. Therefore, it is difficult to develop a global model for predicting the controlling parameters on the gas storage capacity,
- The main objective of this study is to determine the interrelationship between physical properties of the potential gas shales from the Perth and Canning Basins, Western Australia. As it is clear the case study of this project is so widespread but the problem is the required data for evaluation of the shale layers are so limited. Most of the wells which have been drilled in these two basins do not have any cores in the shale layers or if they have any core data they do not have the core analysis for the shale layers. As well as the number of geochemical data points are so limited and most of the geochemical data are the vitrinite reflectance, and
- Last but not the least converse to the conventional reservoirs herein conventional well log data like neutron porosity, resistivity and density could not get much more information about the reservoir and the parameters which are required for gas shale evaluation like micropore volume. Advanced well log data like pulsed neutron mineralogy and nuclear magnetic resonance log are useful for evaluation of these reservoirs but in most of the cases they are not available for the old wells.

6.2 Concluding remarks

The detailed conclusion and discussion were provided in each chapter therefore they are not mentioned here in detail. The following points are the highlighted conclusions which can be drawn based on the obtained results from petrophysical measurements and well log analysis on the potential gas shales from the Perth and Canning Basins:

- The results of pore structure evaluation techniques show that among the studied formations samples from the Goldwyer Formation have the higher specific surface area and micropore volume and the samples from the Carynginia Formation have the lower of these values,
- The results of adsorbed gas measurement on the collected shale samples approximately show the similar finding with pore structure evaluation results. The Carynginia Formation has the lowest adsorbed gas capacity while approximately the adsorbed gas capacity for the Goldwyer Formation and the Hovea member of the Kockatea Shale are the same,
- The specific surface area and micropore volume are the most effective factors on the adsorbed gas capacity of the shale layers. The geochemical and compositional parameters can affect on the adsorbed gas capacity as long as they have a strong effect on the pore structural properties; i.e. specific surface area and micropore volume,
- Adsorption capacity of the analysed samples is not so high and they show a significant decrease with increasing temperature. Therefore it can be proposed that at the reservoir temperature, the role of the free gas is so prominent for gas production from these shales, and
- As it was expected calibrating some physical properties which are influencing the nano-scale properties with the log data is difficult. It is due to this fact that the parameters like organic matter quantity and organic matter maturity have a low impact on the matrix of the studied gas shales. Therefore to be able to predict geochemical parameters directly from conventional well log data it is required to have a high percentage of organic content.

It should be mentioned again due to the high degree of heterogeneity of the shale layers the results of this study may not be representative of the mentioned geological formations.

6.3 Recommendations and future researches

This study is the first comprehensive study which investigating the importance of geochemical and compositional parameters on the gas storage capacity and well log responses of the potential gas shales from Western Australia. Regarding the challenges, limitations and results of this research the followings points can be recommended for future studies:

- Investigations on more shale samples with different physical properties to expand the findings of this study and determine the required parameters needed to produce gas economically from the potential gas shales of Western Australia.
- Although effect of temperature on the adsorption phenomena is an indirect relationship; increasing temperature decreasing the adsorption affinity, more investigations are required on the adsorbed gas capacity of the shale samples at different temperatures to develop a model for estimating the adsorbed gas capacities at different burial depths and temperatures.
- As it was discussed the adsorption affinity has an important role for desorbing the gas and gas production rate from the shale layers. Regarding the importance of this parameter on gas production from shale layers more investigations are required at different temperatures to determine the effective parameters on heat of adsorption.
- Different techniques have been employed in this study for pore structure evaluation of the gas shale layers. It seems that by overlaying pore size distribution from mercury and nitrogen it would be possible to extract some information related to pore aspect ratio and pore geometry of the shales considering this fact that the mercury determines the pore throat size and nitrogen measures the pore body size. However more investigations are required on the shale samples to establish an accurate model for extracting the pore aspect ratio of the shale layers based on the overlaying pore size distribution of nitrogen adsorption and mercury porosimetry. The nuclear magnetic resonance spectroscopy can be used accompanied with the other data to help out in solving this issue.
- Although the author believes that accurate scaling of laboratory data to in-situ reservoir conditions is difficult it would be useful to investigate the calibration between the log data with measured physical properties to develop a methodology for estimating these parameters directly from log data.

'Every reasonable effort has been made to acknowledge the owners of copyright material. I would be pleased to hear from any copyright owner who has been omitted or incorrectly acknowledged.'